

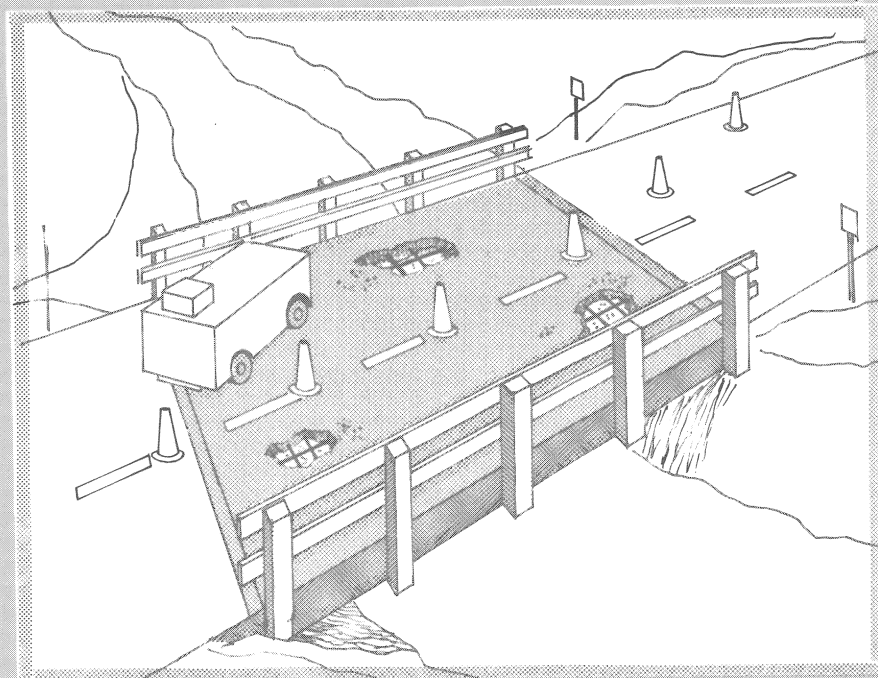
Report No. FHWA-RD-77-26

IN SITU DETERMINATION OF THE CHLORIDE CONTENT OF PORTLAND CEMENT CONCRETE IN BRIDGE DECKS

Feasibility Study



February 1977
Interim Report



Document is available to the public through
the National Technical Information Service,
Springfield, Virginia 22161

Prepared for
FEDERAL HIGHWAY ADMINISTRATION
Offices of Research & Development
Washington, D. C. 20590

NPR-2(115)
Idaho Research Proj. 74

NOTICE

This document is disseminated under the sponsorship of the Department of Transportation in the interest of information exchange. The United States Government assumes no liability for its contents or use thereof.

The contents of this report reflect the views of the Office of Research of the Federal Highway Administration, which is responsible for the facts and the accuracy of the data presented herein. The contents do not necessarily reflect the official views or policy of the Department of Transportation.

This report does not constitute a standard, specification, or regulation.

UNITED STATES GOVERNMENT

Memorandum

DEPARTMENT OF TRANSPORTATION
FEDERAL HIGHWAY ADMINISTRATION

Transmittal of Research Report No. FHWA-RD-77-26,
"In Situ Determination of the Chloride Content
of Portland Cement Concrete in Bridge Decks -
Feasibility Study" - Output from Pooled Fund
Project HPR-2(115)

DATE: **SEP 28 1977**
In reply refer to: HRS-21

SUBJECT :

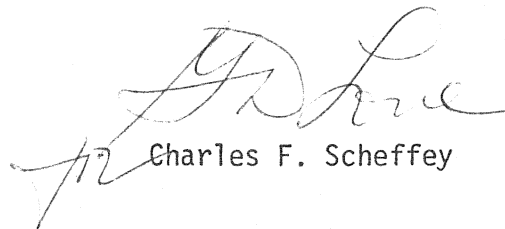
FROM : Director, Office of Research

TO : Individual Researchers and
Participating State Highway and Transportation Departments

Distributed with this memorandum is the subject report intended primarily for research and development audiences. This report is the first output from Project HPR-2(115), which is being funded by 23 participating State highway and transportation departments. The report will be of interest to researchers involved in the assessment of the condition of bridge decks and other reinforced structural concrete.

This research was initiated to develop a gage and corresponding test method for rapid, in situ, and, if possible, nondestructive determinations of the total chloride ion concentration in PCC bridge decks or other reinforced concrete members at the level of the outermost mat of reinforcing steel. This report presents the results of the first phase of the research, the feasibility study. The contractor found that a dual measurement method, employing a pair of nuclear techniques, was feasible for nondestructive measurements at a specified depth. He is currently working on the second phase of the study, the development of a prototype field instrument using the dual measurement method.

Additional copies of the report are available from the National Technical Information Service (NTIS), U.S. Department of Commerce, 5285 Port Royal Road, Springfield, Virginia 22161. A small charge is imposed for copies provided by NTIS.


Charles F. Scheffey

Attachment

Technical Report Documentation Page

| | | | |
|---|--|--|-----------|
| 1. Report No. FHWA-RD-77-26 | 2. Government Accession No. | 3. Recipient's Catalog No. | |
| 4. Title and Subtitle In Situ Determination of the Chloride Content of Portland Cement Concrete in Bridge Decks - Feasibility Study | | 5. Report Date February 1977 | |
| | | 6. Performing Organization Code | |
| 7. Author(s) J. R. Rhodes, N. C. Carino, R. D. Sieberg J. Stout, M. C. Taylor | | 8. Performing Organization Report No. | |
| 9. Performing Organization Name and Address Columbia Scientific Industries P. O. Box 9908 Austin, Texas 78766 | | 10. Work Unit No. (TRAIS) FCP 44B2-193 | |
| | | 11. Contract or Grant No. DOT-FH-11-8901 | |
| 12. Sponsoring Agency Name and Address U. S. Department of Transportation Federal Highway Administration Offices of Research and Development Washington, D. C. 20590 | | 13. Type of Report and Period Covered Interim Report - Phase I | |
| | | 14. Sponsoring Agency Code M/0390 | |
| 15. Supplementary Notes Pooled Fund Project HPR-2(115) FHWA Contract Manager: T. M. Mitchell (HRS-21) Advisory Panel Chairman: G. Morrison | | | |
| 16. Abstract The objective of this two-phase program is to develop a gauge and corresponding test method for rapid, local, in situ determinations of the total chloride ion concentration in P.C.C. bridge decks or other reinforced concrete members at the level of the outermost mat of reinforcing steel, with a sensitivity of 100 ppm Cl or better. In Phase I a literature search and paper study confirmed that X-ray fluorescence, thermal neutron activation and thermal neutron-prompt gamma analysis were the only promising techniques. Experimental investigations showed that the following methods were feasible for analysis of samples taken from drill holes; energy dispersive XRF with Si(Li) spectrometer and ⁵⁵ Fe source; non-dispersive XRF with proportional counter, balanced filters and ⁵⁵ Fe source; thermal neutron activation with NaI(Tl) spectrometer and ²⁵² Cf source. A dual measurement method, employing both the prompt gamma and activation techniques, was shown to be feasible for nondestructive monitoring of chloride content at a specified depth or depth region below the surface with a sensitivity of 100 ppm or better, independently of the chloride content in the surface layers. With a properly designed gauge and test method several such measurements per hour would be feasible, on bridge decks. The same instrumentation could be used for rapid in-situ sample analysis. Design and performance data were obtained to facilitate the development of field instruments of each type. | | | |
| 17. Key Words chlorides, concrete, bridge decks, nondestructive testing, field instrumentation, concentration gradient, thermal neutron activation, thermal neutron-prompt gammas, Californium-252, X-ray fluorescence | | 18. Distribution Statement No restrictions. This document is available to the public through the National Technical Information Service, Springfield, Va. 22161 | |
| 19. Security Classif. (of this report) Unclassified | 20. Security Classif. (of this page) Unclassified | 21. No. of Pages 114 | 22. Price |

TABLE OF CONTENTS

| | <u>PAGE</u> |
|---|-------------|
| 1. INTRODUCTION. | 1 |
| 1.1 Bridge Deck Deterioration and Corrosion. | 2 |
| 1.2 Repair and Prevention. | 2 |
| 1.3 Requirements of the Method and Instrumentation | 3 |
| 2. PAPER STUDY | 5 |
| 2.1 Literature Search. | 5 |
| 2.1.1 Methods for Determination of Chlorides in Concrete. | 5 |
| 2.1.2 Corrosion of Concrete and Bridge Decks. | 6 |
| 2.1.3 Analytical Techniques for Chlorine and Chlorides in Bulk Materials and Nondestructive Analysis of Concrete. | 6 |
| 2.1.4 Analysis of Chlorine and Chlorine Compounds | 8 |
| 2.1.5 Other Related References. | 8 |
| 2.2 Evaluation of Candidate Methods. | 8 |
| 2.2.1 X-Ray and Gamma-Ray Methods | 8 |
| 2.2.2 Neutron-Gamma Methods | 9 |
| 2.2.3 Laser Pyrolysis Methods | 11 |
| 2.2.4 Acoustic Methods. | 11 |
| 2.2.5 Electromagnetic Methods | 12 |
| 2.3 Selection of Methods for Further Study | 12 |
| 3. SAMPLE PREPARATION. | 13 |
| 3.1 Chloride-Doped Concrete Specimens. | 13 |
| 3.2 Chloride-Impregnation Procedure. | 16 |
| 4. X-RAY FLUORESCENCE METHODS. | 24 |
| 4.1 General Principles | 24 |
| 4.2 Sample Preparation and X-Ray Instrumentation | 25 |
| 4.3 Sampling and Sample Preparation. | 27 |
| 4.4 Feasibility of the EDX Method. | 29 |
| 4.5 Feasibility of the NDX Method. | 34 |

TABLE OF CONTENTS CONT.

| | <u>PAGE</u> |
|---|-------------|
| 5. NEUTRON-GAMMA TECHNIQUES. | 44 |
| 5.1 General Principles | 44 |
| 5.2 Choice of Source and Detector. | 46 |
| 5.2.1 Available Sources | 46 |
| 5.2.2 Gamma-Ray Spectrometers | 48 |
| 5.2.3 Spectra and Preliminary Sensitivity Comparisons | 50 |
| 5.3 Total Chloride Determination | 64 |
| 5.3.1 Analysis of Pulverized Drill Hole Samples | 64 |
| 5.3.2 Analysis of Stacks of Test Plates | 66 |
| 5.4 Chloride Gradient in a Single Measurement. | 70 |
| 5.4.1 Neutron Spectrum Tailoring. | 70 |
| 5.4.2 Detector Collimation. | 73 |
| 5.4.3 Detector Collimation with Coincidence Counting. | 76 |
| 5.5 Chloride Gradient in a Dual Measurement. | 80 |
| 5.5.1 Calculations of Depth Response. | 82 |
| 5.5.2 Neutron Activation Experiments. | 84 |
| 5.5.3 Prompt-Gamma Experiments. | 89 |
| 5.5.4 Combined Neutron Activation-Prompt Gamma Measurements. | 92 |
| 5.5.5 Discussion of Dual Measurement Technique. | 95 |
| 6. CONCLUSIONS AND RECOMMENDATIONS | 99 |
| 6.1 Recommendations. | 99 |
| 7. BIBLIOGRAPHY. | 102 |

LIST OF FIGURES

| | | <u>PAGE</u> |
|-----------|---|-------------|
| FIGURE 1 | Wet Chemistry Analysis of Samples from Concrete Plates | 15 |
| FIGURE 2 | Vacuum Impregnation Process. | 19 |
| FIGURE 3 | Chlorine Concentration vs Depth for Small Specimens. . | 20 |
| FIGURE 4 | Vacuum Chamber for Impregnation of Larger Slabs. . . . | 21 |
| FIGURE 5 | Chloride Content vs Depth for Vacuum Impregnated Concrete Test Slabs. | 23 |
| FIGURE 6 | Calibration for Pressed Briquettes Using Si(Li) Spec- trometer and ^{55}Fe Source | 30 |
| FIGURE 7 | X-Ray Spectrum from Concrete Sample Using Fe^{55} Source and Si(Li) Spectrometer, Showing X-Ray Lines and Energies in keV. | 31 |
| FIGURE 8 | Calculated Transmission Curves for Cl/S Balanced Filters. | 35 |
| FIGURE 9 | Arrangement of Source, Sample, Filters and Detector for Transmission Filter Experiments. | 37 |
| FIGURE 10 | Arrangement of Source, Sample, Filters and Detector for Secondary (Reflection) Target Experiments. | 38 |
| FIGURE 11 | Block Diagram of Electronics Used for Proportional Counter Experiments. | 39 |
| FIGURE 12 | Proportional Counter Spectra Through Balanced Filters, from Briquette Containing 3830 ppm Cl. | 41 |
| FIGURE 13 | Calibration Curve for Pressed Briquettes Using Propor- tional Counter and Balanced Filters. | 42 |
| FIGURE 14 | Schematic of Gamma-Ray Spectrometers | 49 |
| FIGURE 15 | Activation Spectrum Using Ge(Li) Spectrometer. | 51 |
| FIGURE 16 | Thermal Neutron Activation Spectrum From Chloride-Doped Concrete Test Plate Using the Ge(Li) Gamma-Ray Spec- trometer | 52 |
| FIGURE 17 | Irradiation and Counting Configurations (Schematic) for Preliminary Ge(Li) and NaI(Tl) Activation Experi- ments. | 53 |

LIST OF FIGURES CONT.

| | <u>PAGE</u> |
|---|-------------|
| FIGURE 18 Thermal Neutron Activation Spectra from Concrete Test Plates Using the NaI(Tl) Gamma-Ray Spectrometer. . . . | 55 |
| FIGURE 19 Thermal Neutron-Prompt Gamma Spectrum from Chlorine Sample (PVC Tile) Using the Ge(Li) Spectrometer. . . . | 56 |
| FIGURE 20 Thermal Neutron-Prompt Gamma Spectrum from Pair of Concrete Test Plates Containing 3830 ppm Chloride Using the Ge(Li) Spectrometer. | 57 |
| FIGURE 21 Thermal Neutron-Prompt Gamma Spectrum from Pair of Concrete Test Plates Containing Zero Chloride Using the Ge(Li) Spectrometer. | 58 |
| FIGURE 22 Source-Sample-Detector Configuration for Preliminary Thermal Neutron-Prompt Gamma Experiments | 59 |
| FIGURE 23 Thermal Neutron-Prompt Gamma Spectrum from Concrete Test Plates Containing 3830 ppm Chloride Using the NaI(Tl) Detector | 60 |
| FIGURE 24 Thermal Neutron-Prompt Gamma Spectrum from Concrete Test Plates Containing Zero Chloride Using the NaI(Tl) Detector | 61 |
| FIGURE 25 Calibration Curve for Thermal Neutron Activation Analysis of Pressed Powder Briquettes. | 65 |
| FIGURE 26 Calibration Curve for Thermal Neutron-Prompt Gamma Analysis of a Stack of Concrete Test Plates. | 67 |
| FIGURE 27 Calibration Curve for Thermal Neutron Activation Analysis of a Stack of Concrete Test Plates. | 69 |
| FIGURE 28 Thermal Neutron Flux Gradient in Concrete as a Function of Moderator Thickness for ^{252}Cf Source. | 72 |
| FIGURE 29 Sketch of Irradiation and Counting Geometries Used for Detector Collimation Studies | 75 |
| FIGURE 30 Sketch of Two-Detector Geometry Used for Coincidence Counting Measurements. | 77 |
| FIGURE 31 Coincidence Counting System - Electronic Schematic . . | 78 |

LIST OF FIGURES CONT.

| | | <u>PAGE</u> |
|-----------|---|-------------|
| FIGURE 32 | Coincidence Spectra from a Single Plate, Gated on 2.17 MeV. | 79 |
| FIGURE 33 | Schematic of Model for Depth Response Calculations . . | 83 |
| FIGURE 34 | Calculated Response Functions $R(Z)$ | 85 |
| FIGURE 35 | Calculated Curves of $\frac{dI}{dZ}$ vs Depth (Z), for an Exponential Concentration Gradient $C(Z)$ | 86 |
| FIGURE 36 | Depth Response Curves, Neutron Activation Method . . . | 88 |
| FIGURE 37 | Source-Shield-Detector-Sample Configuration Used for Prompt Gamma-Ray Measurements. | 93 |
| FIGURE 38 | Depth Response Curves, Prompt Gamma Method | 94 |
| FIGURE 39 | Schematic of Combination Neutron Activation-Prompt Gamma Chloride Analyzer. | 100 |

LIST OF TABLES

| | | |
|---------|--|----|
| TABLE 1 | Chloride-Doped Plates Prepared for Feasibility Studies | 14 |
| TABLE 2 | Wet Chemistry Results. | 17 |
| TABLE 3 | Candidate XRF Techniques | 26 |
| TABLE 4 | Comparison of Sensitivities Obtained Using NaI(Tl) and Ge(Li) Spectrometers for Prompt and Activation Gamma Methods. | 63 |
| TABLE 5 | Concentration Distribution of the Concrete Test Specimens Used for Total Chloride Sensitivity Tests | 68 |
| TABLE 6 | Calibration Data for Dual Neutron Activation Chloride Concentration Gradient Measurements. | 90 |
| TABLE 7 | Results of Dual Neutron Activation Measurements of Chloride Concentration Gradient. | 91 |
| TABLE 8 | Calibration Data for Combined Neutron Activation-Prompt Gamma Measurements | 96 |
| TABLE 9 | Results of Combined Neutron Activation-Prompt Gamma Measurements of Chloride Concentration Gradient. . . . | 97 |

1. INTRODUCTION

The deterioration of portland cement concrete (PCC) due to corrosion of reinforcing steel in bridge decks caused by deicing salts, and in decks, caps, piles and piers caused by sea salts, has established the need for a rapid, nondestructive, in situ test for the chloride content of concrete. The present test method is to remove pulverized core samples from the bridge deck by means of a rotary hammer and analyze the powder using a wet chemistry-potentiometric technique.^(1,2) This method is not satisfactory for rapid field testing because it is too slow, destructive and traffic-disrupting. Another possible method is being evaluated in a parallel study⁽³⁾ and is accordingly disqualified from this investigation. It comprises drilling a clean, 3/4 in. (2 cm) dia. hole in the deck, partially filling it with a predetermined volume of solution, inserting a chloride ion specific electrode and comparing the reading after a fixed time with a calibration curve.

The objective of the current two-phase project is to develop a field instrument and corresponding test procedure for rapid, in situ, preferably nondestructive determination of chloride ion concentration in PCC bridge decks and other reinforced concrete members at the level of the outermost mat of reinforcing steel. Phase I, the feasibility study, is the subject of this report. Recommendations for Phase II, prototype instrument development and field testing, are made herein.

The feasibility study was divided into the following logical segments: a broad-based literature search designed to find all possible methods, however unlikely; a paper study aimed at eliminating all but the best candidate techniques; experiments and calculations aimed at defining and optimizing the best nondestructive and destructive methods and instruments; preparation of chloride-impregnated PCC calibration samples for the Phase I experiments, and development of rapid salt impregnation methods for use in preparation of larger test samples for Phase II.

In order to more fully understand the requirements of the gauge the rest of this section briefly discusses relevant aspects of the bridge deck deterioration problem.

1.1 Bridge Deck Deterioration and Corrosion

Deterioration of reinforced concrete takes the form of cracking, spalling and eventual failure of components. A major cause and accelerating factor is corrosion of the reinforcing steel.⁽⁴⁻⁶⁾ Chlorides diffuse into the concrete at a rate determined primarily by concrete permeability, moisture content and rate of surface salt application. Electrochemical corrosion cells are set up at concrete-steel interfaces and corrosion activity is a function of local pH and dissolved oxygen. The normal pH of concrete is very high (12 to 14) but as little as 300 parts per million* of chloride can reduce the pH to 10, at which threshold value the passivity of the steel is counteracted and electrochemical corrosion can begin to proceed rapidly.⁽¹⁾ Since the depth distribution of chloride concentration can vary due to surface washout or accumulation of salt, or to differing concrete permeabilities,⁽⁷⁾ and since the concrete surface may have been covered by a protective overlay (e.g., a 1/8 in. (3 mm) thick 15% PVC-loaded bitumen-based sheet and 1 to 6 in. (2.5 to 15 cm) of asphalt), the onset of rapid corrosion is very difficult to detect.

Corrosion of the reinforcing bars expands them, so causing cracking and spalling of the surface layers of concrete. Deterioration is accelerated by water ingress, by freezing and thawing and by the repeated load fluctuations due to traffic.

1.2 Repair and Prevention

Repair and maintenance of bridges is a continuing program. Repair of minor deterioration is relatively rapid and inexpensive compared to major jobs whose cost can be comparable with that of rebuilding the bridge. The earlier that chloride penetration to the reinforcing bars can be detected the better.

In many states protective membranes and overlays are placed either during construction or at any time afterwards. In the latter case

*300 ppm \approx 1.2 lb Cl^- /yd.³

tests are desirable to determine whether chloride penetration has already taken place before the overlay is placed. Thereafter, tests are desirable for chloride that may have leaked under the overlays.

Repair by removal of deteriorated areas and patching is not permanent if all the chloride-contaminated concrete is not removed. Rapid monitoring is needed at such repair sites.

Many materials impermeable to chloride are being tested both at repair sites and in new construction. They include low water-cement ratio, dense concrete; latex modified concrete;(7,8) surface polymer impregnated concrete;(7-9) internally sealed (wax-bead) concrete;(10) and polymer concrete.(11) The selected test method should be capable of monitoring chloride in or near all these new materials. Also electrochemical methods for driving chloride out of contaminated concrete are being investigated.(12)

1.3 Requirements of the Method and Instrumentation

The method must be specific to chloride or total elemental chlorine. The sensitivity and accuracy should be such that chloride contents from 10^2 to 10^4 ppm can be measured with 10% accuracy. Less accuracy is tolerable in the lower concentration ranges as long as the corrosion threshold (~ 300 ppm) can be monitored.

Bound chlorine atoms (which do not, of course, initiate corrosion) can be present in some components of, or additives to, PCC, but the frequency of occurrence and chlorine concentration are low enough that the errors inherent in a total chlorine measurement are tolerable. PVC-loaded membranes are another matter, however, and could cause severe interferences.

The method must be capable of making the above measurements with the required sensitivity at the level of the outermost mat of reinforcing bars, which is usually about 2 in. (5 cm) below the concrete surface. Protective overlays and asphalt coverings can vary from 1/8 in. (3 mm) to several inches (~ 20 cm) thick, resulting in the reinforcing mat layer being that much further below the surface.

The measurement should be nondestructive, if possible. If not, drilling holes, or coring, is an acceptable way of obtaining depth information.

The instrumentation should be transportable and fieldworthy. Since it is also necessary to make measurements on vertical surfaces (e.g., pilings), on the underside of decks and near drainage culverts, it must be possible either to make direct measurements in these circumstances or take samples.

The analysis cost and time, and potential traffic disruption should be minimized. Several measurements per hour are desired together with the lowest possible labor costs.

2. PAPER STUDY

In order to give consideration to every potential analytical technique yet limit detailed experimental investigation to only those techniques which exhibit a high probability of success, a comprehensive search of published literature and other sources was conducted for candidate techniques. Each technique was then evaluated on paper based upon the requirements set forth in Section 1.3. Those techniques found to exhibit a high probability for success were selected for further investigation by detailed calculations and experimentation.

2.1 Literature Search

The literature review was divided into five categories. References in each category were compiled from sources known to the investigators, information received from other investigators involved in related work and a computerized search provided by the NASA Technical Applications Center in Albuquerque, New Mexico. The computer search proved to be by far the most productive source of references, yielding some 700 articles. The following data sources were used in the computer search:

- (1) Chemical Abstracts (1972-present)
- (2) Government Reports Announcements (1964-present)
- (3) Engineering Index (1970-present)

The search references were reviewed and a bibliography of materials relevant to the chloride problem was assembled. Copies of the most relevant articles were obtained from either the University of Texas library or the National Technical Information Service (NTIS). This section presents brief summaries of the findings and lists some of the more significant articles by category.

2.1.1 Methods for Determination of Chlorides in Concrete (31 references)

The first search category was specific analytical methods for chlorides in concrete. This category produced a relatively small number of references, but a very high percentage of these were relevant to the

problem. However, the material found under this category yielded little new knowledge beyond what was known at the beginning of the project.

Most of this literature discusses destructive methods of analysis, especially wet chemistry. (1,2,17,20,22,23) A comprehensive review of the status of chloride determinations prior to 1974 is given by Clear. (1) This review includes a discussion of the techniques used in, and materials required for, the wet chemistry methods of Berman. (2) The status of recent FHWA investigations of radiation methods for analysis of powdered core samples are also presented. Among these are reactor neutron activation analysis and X-ray fluorescence analysis. A review of nondestructive techniques that have potential for field use is presented by Li et al. (13) These include ultrasonic, radioactive and electrical methods. Electrical potential methods, which are ruled out of this study, are also discussed by Spellman and Stratfull (16) and by Stratfull et al. (18)

Works on other non-destructive methods (X-ray, thermal neutron capture, neutron activation and electron microprobe), each of which involves some sample preparation, are also included. (14,15,19,24).

The procedures described by Berman (2) form the basis for the wet chemistry used as a primary standard for all experimental investigations performed under this project.

Two of the articles (16,21) provide useful information on the depth distribution of chlorides.

2.1.2 Corrosion of Concrete and Bridge Decks (174 references)

A search category closely related to chloride determination is corrosion. A large number of references turned up in this category. These papers are primarily concerned with the mechanism for corrosion of the reinforcing steel, corrosion prevention, and methods for repair of bridge decks, and few are directly applicable to the problem. A representative sample of these articles is found in references 4, 5, 25-29.

2.1.3 Analytical Techniques for Chlorine and Chlorides in Bulk Materials and Nondestructive Analysis of Concrete (226 references)

This search category was expanded to include bulk materials other than concrete which may present similar analysis problems, as well

as to analysis of elements other than chlorine in concrete. The references are sorted by analytical technique into six (6) subcategories.

X-Ray Fluorescence (53 references)

XRF analysis is a very active field with a wealth of information on analysis of elements with medium to high atomic number in prepared samples. The list included here(30-38) is limited primarily to the search parameters of "chlorine" and "concrete." However, references 37 and 38 are included as examples of work performed at CSI that is relevant to the problem.

Gas Chromatography (15 references)

There were few articles relevant to the project in this category. The two references listed(39,40) describe the principles used and apparatus required for sniffing the chloride compounds evolving from a solid sample.

Neutron Activation Analysis (55 references)

Much of the literature found in this category deals with radiation shielding because concrete is commonly used for this purpose. Some of the papers on neutron albedos were useful for analytical paper studies of different irradiation and detection configurations.

Activation analysis has been employed as a tool for elemental analysis of bulk materials for many years and a number of references on chloride and concrete analysis were found. A representative sample of these references is 41-49. Included are two references to work performed at CSI.(41,49)

Gamma-Ray Analysis (58 references)

Most of the gamma-ray references found in the search are concerned with albedo calculations in concrete shielding materials. However, there are also several articles on gamma-ray backscatter(50,51,53) and thermal neutron capture gamma-ray analysis.(14,52,54-56) Gamma-ray backscatter is not applicable to the present problem, but capture gamma-ray analysis is one of the potentially useful techniques.

Electromagnetic Radiations (13 references)

None of the references found under this category were considered relevant to direct measurement of the chloride content of concrete.

Acoustic Analysis (32 references)

References 57-60 are representative. While the presence of salts in concrete and other materials may alter their acoustic properties, no evidence was found in the references to support the use of this technique for a unique determination of chlorides.

2.1.4 Analysis of Chlorine and Chlorine Compounds (78 references)

There is a large body of information on the analysis of chlorine compounds, especially pesticides, by gas chromatography. Some typical examples are given in references 61-63. There are also a number of articles on X-ray fluorescence analysis and neutron activation analysis. These are primarily related to environmental monitoring, as illustrated by reference 64. None of the articles found under this category contributed to the understanding of the problem.

2.1.5 Other Related References (138 references)

This is a list of references that could not be categorized. Most of the articles are not relevant to this project. A few are of passing interest as illustrated by the sampling given. (65-70)

2.2 Evaluation of Candidate Methods

2.2.1 X-Ray and Gamma-Ray Methods

All methods that involve the detection of X-rays or low energy gamma rays are grouped into this classification. These radiations are characterized by their low penetrating power.

X-Ray Fluorescence. XRF is a well-established technique for elemental analysis of solids down to ppm levels. There is extensive literature on the general application of this technique as well as several key publications dealing with the detection of chlorine in concrete. Many types of XRF instrument have been built. They range from expensive, high resolution laboratory systems with computer interfacing to simple hand-held portable analyzers capable of single-element determination.

There are several instrument configurations which potentially could be employed for chlorine analysis of prepared samples (destructive analysis). Total nondestructive analysis by XRF is not possible because the radiation will penetrate only a very short distance into concrete. Moreover, XRF is not as good for light element analysis as it is for heavier elements, because of such problems as particle size effects, self-absorption in the sample and low signal-to-noise ratio. The severity of these problems increases rapidly as atomic number (Z) decreases below about 20 (calcium). In fact, it is no longer practical to do field analysis below $Z = 14$ (silicon), because the absorption effects become so pronounced that vacuum or helium paths and thin-windowed or windowless detectors become essential. Chlorine ($Z = 17$) is in the marginal region between silicon and calcium, where the degree to which portable instrumentation will work is not known. Sensitivity for chlorine, particle size effects and matrix effects can be evaluated only by extensive and careful experimentation.

Electron Microprobe. While this technique has been employed for laboratory analysis of prepared concrete specimens,⁽¹⁵⁾ it is not considered to be fieldworthy in comparison with XRF because the apparatus required is complex, bulky and expensive. In addition, the size of the area sampled is much too small to give a representative measurement on a heterogeneous material such as concrete. Therefore, no advantage is seen for this method over less sophisticated XRF apparatus.

Gamma-Ray Backscatter. This technique suffers from the disadvantage of not being elementally specific for chlorine. It is instead sensitive to the average atomic number of the sample and has proven useful for determining the cement content of fresh concrete.⁽⁵¹⁾

2.2.2 Neutron-Gamma Methods

The use of neutron excitation for quantitative elemental analysis offers advantages not found in other analytical techniques. The high penetration of the incident and emitted radiation minimizes heterogeneity effects, permitting the analysis of a volume of sufficient size to be representative of the entire sample, even with heterogeneous substances such as concrete. Neutron methods were the only ones

found in this study which are potentially capable of nondestructive measurement of elemental chlorine concentrations below the concrete surface.

Thermal Neutron Activation. Because of the availability of thermal neutrons from nuclear reactors, neutron generators and isotopic sources, there is considerable literature on the subject of thermal neutron activation analysis.

There is evidence in the literature, and simple calculations confirm, that sufficient sensitivity can be obtained with several combinations of source and detector to determine the average chlorine content of concrete either in situ or by core analysis, with a sensitivity of the order of 100 ppm. (41,46,47) However, measurement of concentration gradient has not been done previously. It is anticipated that tailoring of the neutron energy spectrum or some technique employing combinations of sources and detectors will be required to achieve depth discrimination. Detailed calculations and experimentation will be required to assess the potential of this technique.

Thermal Neutron Capture. Energy released in the neutron capture process appears in the form of prompt gamma rays. In the case of chlorine, the reaction $^{35}\text{Cl}(n,\gamma)^{36}\text{Cl}$, which results in the stable isotope ^{36}Cl , produces a large number of intense gamma rays which are potentially useful for capture, or prompt gamma, analysis⁽⁵⁶⁾ (in fact, only Cd, Hg and a few of the rare earths have greater capture gamma-ray yields). Unlike activation gamma rays which are present after the irradiating neutron source has been removed, capture gamma rays are produced during irradiation and are accompanied by a high intensity of background radiation such as source neutrons, scattered neutrons, and other gamma rays. Detection of capture gamma rays in the presence of this large background requires judicious use of shielding materials, large sample-to-detector distances and high resolution detection apparatus. These factors tend to offset the advantage of the high gamma-ray yield, but this technique still offers the greatest promise of those considered for measurements at depth.

Fast Neutron Activation. There are no fast neutron reactions with chlorine which produce gamma-rays of sufficient intensity to be useful for quantitative analysis. However, fast neutron sources may be useful for thermal neutron measurements at depth after thermalization in the concrete.

Neutron Inelastic Scattering. Inelastic scattering of fast neutrons is a key technique for measurement of certain elements such as carbon, nitrogen and oxygen. However, for chlorine determination, the inelastic gamma rays and excitation sources are not intense enough to give sensitivities comparable to those obtainable with thermal neutron capture and activation measurements.

2.2.3. Laser Pyrolysis Methods

Laser pyrolysis is currently being investigated as a method for producing an analyzable gas from certain solid or liquid materials.^(71,72) These gases can be analyzed by gas chromatography or mass spectrometry.

Most applications of these techniques have been concerned with detection of organic compounds. Pyrolysis gas chromatography is generally limited to the analysis of low boiling point (less than 400°C) organic and some inorganic compounds.⁽⁷³⁾ NaCl, with a boiling point of 1413°C, and other chloride ion compounds would require an exchange process before analysis. Mass spectrometry techniques are less developed but may be more suitable for chloride analysis because of the high temperature ionization involved.

Both gas chromatographs and mass spectrometers can be used in a field environment, but these techniques would require considerably more development effort for field use than the neutron-gamma and X-ray methods described earlier, and even then would not guarantee a practicable instrument.

2.2.4 Acoustic Methods

It is possible by acoustic techniques to measure certain properties of concrete, including quality, and the acoustic characteristics may be influenced by the presence of chlorides. However, this technique is

not elementally specific for chlorine and no evidence was found in the literature to support it for unique determination of chlorides.

2.2.5 Electromagnetic Methods

Microwaves can be used in either reflection or transmission measurements to determine moisture content and changes in the refractive index of the material. These measurements are not elementally specific for chlorine, and successful use of microwaves would require close correlation of the response with the physical and chemical properties of the concrete.

2.3 Selection of Methods for Further Study

The literature survey produced no clear cut technique for non-destructive in situ measurement of the chloride depth profile. Therefore, it was concluded that both destructive and nondestructive techniques should be included in the feasibility study phase. The following techniques were selected for the feasibility study:

Nondestructive (no sample removed from deck):

- 1) Thermal neutron activation analysis
- 2) Thermal neutron capture gamma-ray analysis
- 3) A combination of 1) and 2)

Destructive (sample by rotary hammer):

- 1) Portable XRF with balanced filters
- 2) Energy dispersive XRF with Si(Li) detector
- 3) Thermal neutron activation analysis

3. SAMPLE PREPARATION

There were two objectives in the sample preparation work:

1) to provide chloride-doped concrete specimens for use in the evaluation of possible test methods, and 2) to develop a procedure for producing concrete slabs with controlled chloride concentration gradients for use in Phase II (development and testing of prototype test instrument).

3.1 Chloride-Doped Concrete Specimens

For the evaluations described in this report, concrete specimens were required having a variety of chloride concentrations and various chloride concentration gradients. It was decided that the simplest approach would be to prepare concrete plates 12 in. x 12 in. x 1 in. (1 in. = 2.54 cm) having different chloride concentrations. The plates could then be stacked one above the other to produce thick specimens with various chloride concentration profiles.

The plates were prepared by dissolving an appropriate amount of NaCl in the mixing water before adding it to the dry ingredients. This resulted in a uniform distribution of chloride in each specimen. The plates were made with Type III cement, 0.5 in. (1.3 cm) maximum size coarse aggregate and natural river sand. The water-cement ratio was 0.58 and the cement factor was 6.5 sacks/yd.³ (360 kg/m³). The plates were cured for seven days by placing them in polyethylene bags to prevent water evaporation. A total of 64 plates were produced, some of which contained a 12 in. (30.5 cm) long, #3 rebar at the center of the plate. Table 1 shows the chloride concentrations and quantities of concrete plates that were prepared.

Once the plates had acquired sufficient strength, some of them were analyzed for chloride content using Berman's wet chemistry method.⁽²⁾ Powder samples were taken from the plates using a rotary-hammer with a 1-1/2 in. (3.8 cm) core drill with a starter bit. Each powder sample taken from the 1-1/2 in. holes was divided into eight sub-samples; four sub-samples were randomly chosen for chlorine analysis (two for wet chemistry and two for X-ray fluorescence) and the remainder were saved for future use. Figure 1 is a plot of measured chloride concentration

TABLE 1. CHLORIDE-DOPED PLATES PREPARED FOR FEASIBILITY STUDIES

| PPM Cl^- | Cl^- Content* lb/cu. yd. | Number of Samples With Rebars | Number of Samples Without Rebars |
|-------------------|--------------------------------------|-------------------------------------|--|
| 128 | 0.5 | 2 | 4 |
| 255 | 1.0 | 2 | 4 |
| 383 | 1.5 | 2 | 4 |
| 510 | 2.0 | 2 | 4 |
| 638 | 2.5 | 2 | 4 |
| 765 | 3.0 | 2 | 4 |
| 893 | 3.5 | 2 | 4 |
| 1280 | 5.0 | | 4 |
| 1910 | 7.5 | | 4 |
| 2550 | 10.0 | | 4 |
| 3830 | 15.0 | | 4 |
| 0 | 0.0 | 4 | 6 |

*Assuming a unit weight of 145 lbs/ft.³ (2.32 g/cm³) for fresh concrete.

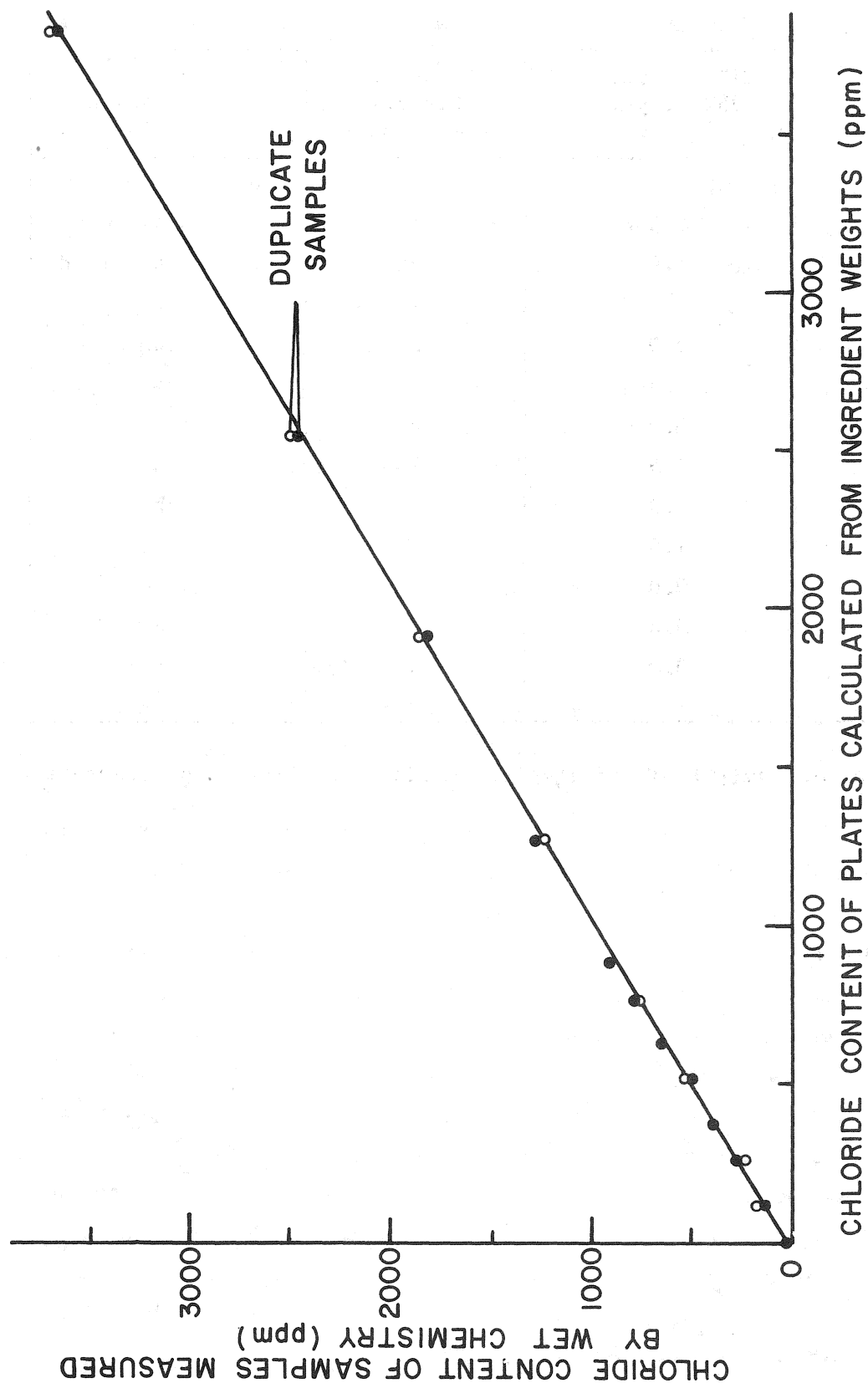


FIGURE 1. WET CHEMISTRY ANALYSIS OF SAMPLES FROM CONCRETE PLATES

against amount of chloride added during the mixing process. The results plotted were for the samples "as received" and the slope of the curve is 0.95. When the chloride contents are referred to a zero free moisture basis (the average free moisture was found to be 4 percent) and replotted, the slope of the best fit straight line was found to be 0.99. The standard deviation for the wet chemistry method was found to be 24 ppm chloride. Thus, it was confirmed that actual chloride contents of the plates were very close to the calculated values shown in Table 1. The data obtained from wet chemistry analyses of the subsamples is shown in Table 2. An initial 35 ppm of chloride was added for each analysis to facilitate end-point determination at low chloride concentrations. Since the subsamples analyzed from the same plate had approximately equal chloride concentrations, it was concluded that the sampling procedure produced a homogeneous sample. In addition, the close agreement between measured and theoretical chloride concentrations of the samples assured us that we were prepared to use wet chemistry as a reference standard for the remainder of the study.

3.2 Chloride-Impregnation Procedure

Phase II of the study is to involve testing of the prototype instrument on test slabs that simulate the chloride concentrations and gradients to be expected in actual reinforced concrete members. Anticipating that production of the necessary slab specimens would require a large amount of time and would possibly delay the completion of Phase II, it was decided to develop the procedures to be used for preparing the required test slabs during Phase I of the study.

The usual procedure for introducing chloride into hardened concrete is by soaking specimens in aqueous solutions or by ponding^(7-9,21,74) an aqueous solution on the surface of slabs. When concrete is initially saturated, it takes a long period of time for chloride penetration to take place. The length of time can be reduced if the concrete specimens are oven-dried before soaking or ponding with salt solutions.

A preliminary study was conducted to determine rate of penetration of ponded water on oven-dried concrete specimens. The specimens, which were 12 in. x 12 in. x 6 in. (1 in. = 2.54 cm), were made with a water-cement ratio of 0.5, a cement factor of 7.3 sks/yd.³ (408 kg/m³) and 3/4 in. (1.9 cm) maximum aggregate size.

TABLE 2. WET CHEMISTRY RESULTS

| Sample No. | % Free Moisture | ppm Chloride (y) | |
|-------------------------|-----------------|--------------------|-----------------------|
| | | y (as received) | y (dry) ^{a)} |
| 0*-0-1-a-i ⁺ | 3.6 (ii) | 56, 39, 22 | 36 |
| " -v | | 33 } 35 ± 12 | |
| " -vi | | 24, 34 | |
| 128-0-1-a-i | 6.43 | 134, 144 | 145 |
| -ii | | 149 } 139 | 155 |
| 255-0-1-a-i | 3.60 | 247, 233 | 250 |
| " -ii | | 251 } 240 | 261 |
| 383-0-1-a-i | 3.3 | 423, 418, 414 | 435 |
| -ii | | 418 } 418 | 435 |
| 510-0-1-a-i | 3.4 | 489, 509, 502, 489 | 517 |
| " -ii | 3.2 | 515 } 497 ± 10 | 535 |
| 638-0-1-a-i | 4.07 | 650 | 676 |
| " -ii | | 655 | 681 |
| 765-0-1-a-i | 3.82 | 766 | 796 |
| " -ii | | 778 | 809 |
| 893-0-1-a-i | 4.15 | 912 | 948 |
| " -ii | | 905 | 941 |
| 1280-0-1-a-i | 3.60 | 1248 | 1297 |
| " -ii | | 1262 | 1312 |
| 1910-0-1-a-i | 3.93 | 1835 | 1908 |
| " -ii | | 1829 | 1901 |
| 2550-0-1-a-i | 3.88 | 2462 | 2557 |
| " -ii | 4.14 | 2481 | 2579 |
| 3830-0-1-a-i | 4.27 | 3693 | 3839 |
| " -ii | | 3679 | 3825 |
| Avg. | 3.96% | | |

Note a) $y \text{ (dry)} = y \text{ (as received)} \times (1.0396)$

*First number is ppm Cl⁻ added to plate during preparation.

⁺Last number indicates sub-sample number.

The results of the ponding procedure were very discouraging. For a soak period of up to 4 days, very little penetration was attained. It was therefore concluded that another approach would be required for rapid penetration. A possible procedure that we felt would be successful is the method employed for rapid impregnation of concrete with monomer systems in the production of polymer-impregnated concrete samples.⁽⁷⁵⁾ The method involves oven-drying hardened concrete, placing specimens in a chamber and evacuating, introducing the monomer liquid into the chamber, releasing the vacuum and allowing the liquid to penetrate into the concrete.

To determine whether the vacuum method would work with a solution of NaCl, several small scale experiments were performed with a vacuum desiccator and 2 in. x 2 in. x 6 in. (5 x 5 x 15 cm) concrete specimens having a water-cement ratio of 0.5. The specimens were coated with a clear epoxy on all sides except the bottom face, which would be in contact with the salt solution. After coating, the specimens were placed in the vacuum desiccator, a pump was attached and the desiccator was evacuated. Evacuation took place overnight. The following day a 6% NaCl solution was introduced into the desiccator and the vacuum was released. Figure 2 shows schematically the steps of the procedure. One specimen was allowed to soak for 8.5 hours and another for 25 hours. After soaking, the specimens were oven dried and powder core samples were taken at 1/2 in. (1.3 cm) intervals. The powder samples were prepared and analyzed by the X-ray fluorescence method described in Section 4.4 of this report. Figure 3 shows the results of chloride analysis of the powder samples. We concluded that the vacuum-impregnation method can be used to rapidly introduce significant amounts of chloride to depths corresponding to rebar levels in actual reinforced concrete bridge decks.

Next, a large steel vacuum chamber was fabricated that could be used for vacuum-impregnation of large concrete slabs. The chamber was made from standard rolled channel sections with 1/4 in. (0.64 cm) plate for the top and bottom (Figure 4).

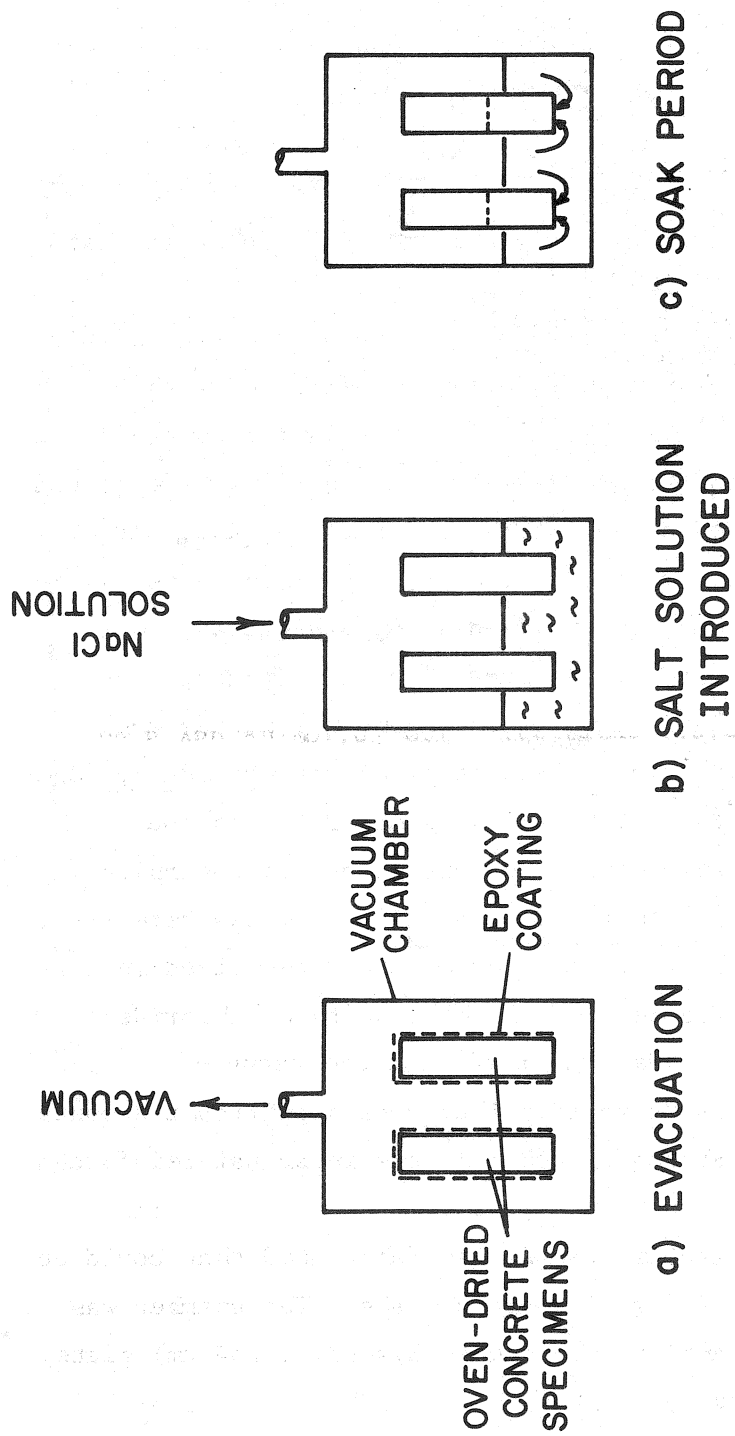


FIGURE 2. VACUUM IMPREGNATION PROCESS

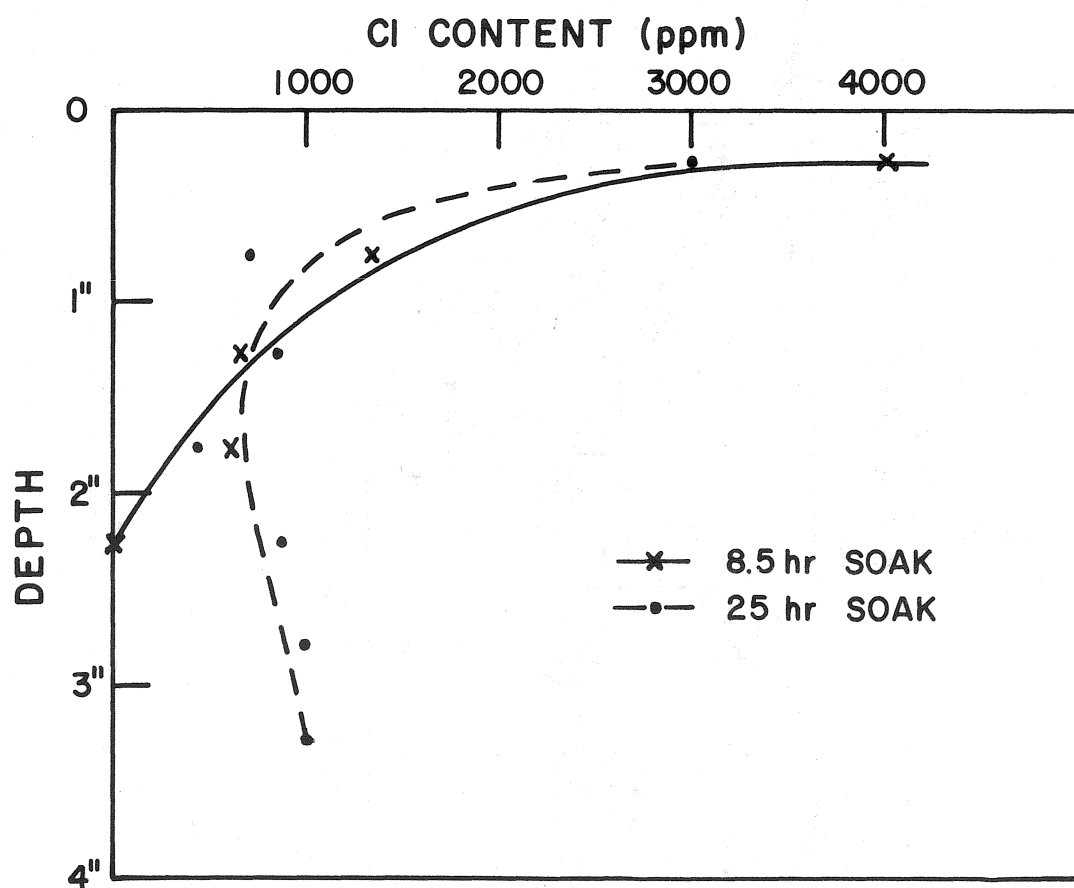


FIGURE 3. CHLORINE CONCENTRATION VS DEPTH FOR SMALL SPECIMENS
(1" = 2.54 cm)

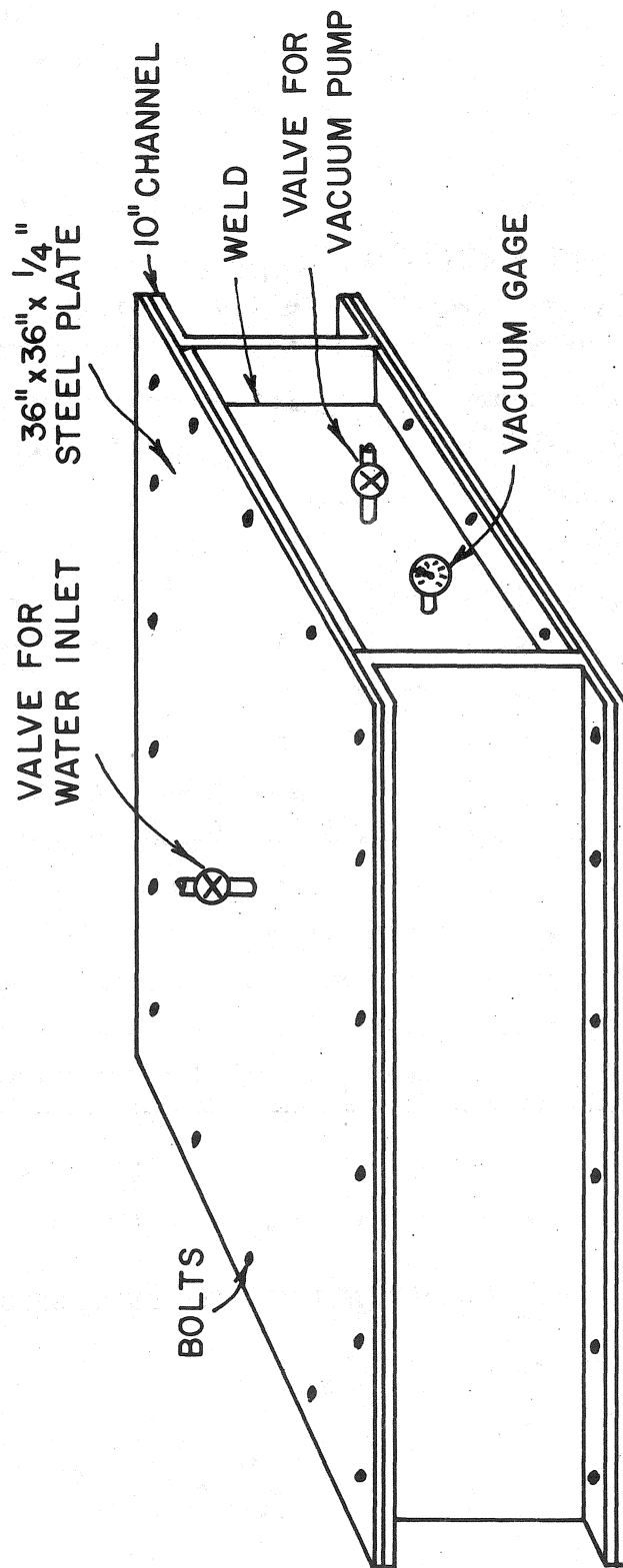


FIGURE 4.. VACUUM CHAMBER FOR IMPREGNATION OF LARGER SLABS
(1" = 2.54 cm)

Two 12 in. x 12 in. x 6 in. (1 in. = 2.54 cm) slabs were impregnated with a 6% NaCl solution, using the same techniques as were used in the vacuum desiccator experiments. One slab soaked for 26 hours, the other for 50 hours. After soaking, the slabs were broken in half and it was observed that 3-1/2 in. (9 cm) and 5-1/2 in. (14 cm) penetration depths were achieved for the respective soak periods. One-half of each slab was oven dried and the other half was allowed to stand in the laboratory; this was to determine the effect on chloride concentration if oven drying is not carried out after soaking.

Powder samples were taken at 1/2 in. (1.3 cm) intervals using the rotary hammer with 1-1/2 in. (3.8 cm) drill, and these were analyzed by X-ray fluorescence. Figure 5 shows the chloride content as a function of depth for the slabs oven dried after soaking. Also shown is the chloride concentration gradient obtained by Clear⁽⁷⁾ after 330 daily applications of 3% NaCl to concrete slabs having a water-cement ratio of 0.5.

The halves of the slabs that were not oven dried were cored after 14 days of air drying. The results of X-ray fluorescence analysis of the powder samples indicate that, if chloride-impregnated slabs are allowed to air dry, there will be a redistribution of chloride. The resultant concentration gradient will become erratic; that is, there is not a gradual decrease in chloride content from the surface to the inside of the slab. It thus appears that slabs should be oven dried after chloride impregnation to "freeze" the desired concentration gradient.

From these studies, we have concluded our method can be used to rapidly impregnate hardened concrete with chloride to any desired depth. By adjusting the concentration of the salt solution and soaking times, we hope to be able to produce chloride concentration gradients that are similar to those measured in actual concrete bridge decks exposed to deicing salts.

The next series of tests using this method will be to study the effects of different concentrations of salt solutions and concrete water-cement ratios on the chloride concentration gradients. The final goal is to develop procedures for producing any desired gradient.

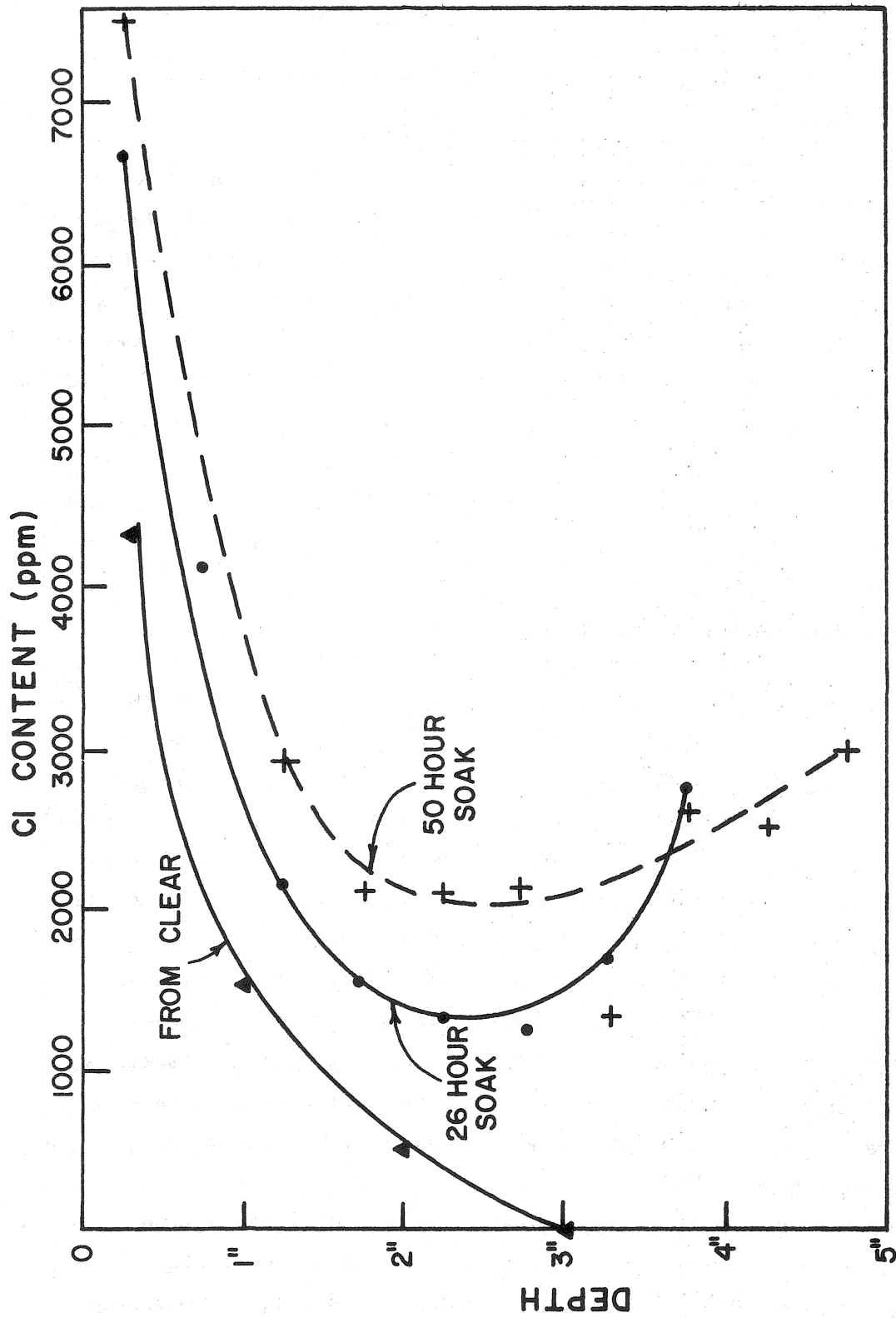


FIGURE 5. CHLORIDE CONTENT VS DEPTH FOR VACUUM IMPREGNATED CONCRETE TEST SLABS
(1" = 2.54 cm)

4. X-RAY FLUORESCENCE METHODS

4.1 General Principles

X-ray fluorescence analysis consists in, principle, of irradiating a sample with X-rays from a suitable source such as an X-ray tube or radioisotope source, and measuring the intensity of characteristic X-rays of the elements excited in the sample using an X-ray spectrometer to discriminate between wanted and unwanted X-rays. The highest energy characteristic X-rays (the K X-rays) emitted by each element are the only useful ones for the present study and consist of a pair of lines K_{α} and K_{β} with an intensity ratio of about 7 to 1. The K_{α} energies of the most important elements are: Si, 1.74 keV; Cl, 2.61 keV; K, 3.31 keV; Ca, 3.69 keV; and Ti, 4.51 keV. In order to excite a given X-ray, the source energy must be greater than the K electron binding energy for that element. For the above elements the K electron binding energies are 1.84, 2.82, 3.61, 4.04 and 4.96 keV, respectively.

Three types of X-ray spectrometer are used, wavelength dispersive (WDX), energy dispersive (EDX) and non-dispersive (NDX). The wavelength dispersive spectrometer is like an optical spectrometer. It employs a single crystal of a suitable salt (e.g., LiF) whose ionic lattice acts as a diffraction grating, and uses highly collimated beams and a goniometer to achieve high resolution. The energy dispersive spectrometer relies on the ability of the X-ray detector to resolve the spectral lines. The detector produces output pulses whose size (charge) is proportional to the incident X-ray energy. A lithium-drifted silicon diode (Si(Li)), operated at liquid nitrogen temperature in a vacuum cryostat, provides sufficiently good X-ray energy resolution to resolve the abovementioned characteristic K X-rays from concrete. Other energy dispersive detectors, gas-filled proportional counters and sodium iodide (thallium-doped) scintillation counters, operate at room temperature and pressure but do not provide sufficient X-ray energy resolution. In order for these detectors to be useful, they must be augmented by X-ray absorption edge filters (see Section 4.5). The use of filters in this way is called the nondispersive (NDX) method.

4.2 Sample Preparation and X-Ray Instrumentation

The objective of the study of XRF methods was to find the simplest and most portable instrument configuration that, coupled with the simplest and most rapid field sampling and sample preparation procedure, will achieve the required sensitivity and accuracy.

Table 3 lists each X-ray instrument configuration considered, together with the four relevant sample preparation methods. The instrument configurations are in order of increasing portability from left to right. The sample preparation methods are in order of increasing simplicity for field use from top to bottom. Entries in the table are coded F = feasible, NT = not tested, T = tested, NF = not feasible; NP = not portable, TP = transportable (e.g., in a light van), P = hand-portable.

The candidate instruments are coded as follows. WDX is the conventional wavelength dispersive method with high power X-ray tube and high resolution crystal spectrometer. EDX is energy dispersive using a Si(Li) spectrometer. Excitation can be by X-ray tube (low or high powered) or radioisotope X-ray source. NDX is nondispersive, relying on absorption edge filters for selection of the required characteristic X-rays and either a proportional counter or NaI(Tl) scintillation counter for low resolution energy spectrometry. The usual excitation method is with a radioisotope source, but a portable low-power X-ray tube is also available.*

We already know that the wavelength dispersive method is feasible but instruments are not portable, and nondispersive instrumentation using a scintillation counter (i.e., sodium iodide scintillation crystal coupled to a photomultiplier) is hand-portable but not sensitive enough, partly because the energy of the Cl K X-rays (2.61 keV) is too near the photomultiplier noise threshold.

The proportional counter has approximately 30% resolution in the 2 to 3 keV range, which, coupled with a very low noise level at room temperature, makes it quite suitable for a hand-portable field instrument.

*Model NUTMAQ 8000, Nuclear Enterprises Ltd.

TABLE 3. CANDIDATE XRF TECHNIQUES

| Method Sample Prep | WDX | EDX Si(Li) with X-Ray Tube | NDX Prop. Ctr. with X-Ray Tube | EDX Si(Li) with Source | NDX Prop. Ctr. with Source | NDX Scint. Ctr. with Source |
|---|-----|-------------------------------------|---|---------------------------------|-------------------------------------|--------------------------------------|
| Fused Pellet | F | NT | NT | NT | NT | NF(NT) |
| Pressed Powder Briquette | F | F | NT | F? / / / / / TP | F? / / / / / P | NF(NT) |
| Loose Powder in Holder | F | F | NT | F | NT | NF(NT) |
| Deposit on Filter Paper (Thin Specimen) | NT | NT | NT | NF(T) | NT | NT |
| | | NP | TP | TP | TP | P |
| | | NP | TP | TP | TP | P |
| | | NP | TP | TP | TP | P |
| | | NP | TP | TP | TP | P |

It would, however, require balanced filters for selection of the Cl K characteristic X-rays, whatever the excitation method. The use of balanced filters (thin foils) for energy discrimination makes for portability, but the reduced energy selection capabilities compared with WDX or EDX spectrometers can cause considerable loss of sensitivity. On the other hand, the geometrical efficiency is one to two orders of magnitude greater than that of an EDX spectrometer and four to six orders greater than that of a WDX spectrometer. As a result, a small radioisotope X-ray source can excite a suitably large signal. At the beginning of this study, a nondispersive instrument using a proportional counter, balanced filters and a radioisotope source was considered to be the most suitable candidate for X-ray fluorescence, but its feasibility needed to be verified experimentally. EDX instruments using Si(Li) spectrometers are readily truck-mountable, and hand-portable vacuum cryostats are available. However, we feel that hand-portable instruments with Si(Li) spectrometers have very marginal practicability because of the sensitivity of the detector to vibration and the fragility of the 0.001 inch (25 micron) thick x 0.5 inch (1.27 cm) diameter beryllium window on the vacuum cryostat. If that window breaks, the Si(Li) detector and cryogenically cooled preamplifier usually have to be replaced. For Cl K X-rays, the energy resolution of a Si(Li) spectrometer is approximately 7 percent, which is adequate to resolve the Cl K peak from even a hundred-times more intense X-ray peak from a neighboring element (such as Ca). Either a radioisotope source or an X-ray tube can be used for excitation, both being truck-mountable; the source however, is the more portable and the less expensive. Most of our experimental studies were performed with a Si(Li) spectrometer and source because suitable instrumentation was available,⁽⁷⁶⁾ and represented a feasible and practicable approach.

4.3 Sampling and Sample Preparation

Any XRF method selected would employ the following sampling procedure: drill a hole to a predetermined depth; discard unwanted drillings from, e.g., overlays; collect drillings from the depth increment required to be analyzed; prepare the sample as discussed below and analyze it for chlorine content. The hole diameter should be at least 1 in. (2.5 cm) to provide enough sample from a 0.5 in. (1.3 cm) depth

increment to analyze and to be representative. The powdered sample can be conveniently collected during drilling using a vacuum chuck already developed elsewhere.⁽⁷⁷⁾

The idea of sampling by depositing some of the concrete powder from air suspension onto a filter paper,⁽⁷⁸⁾ and thus obtaining a "thin specimen" for XRF analysis, was considered first. It has the merits of speed and simplicity. Also, XRF analysis of "thin specimens" avoids errors due to matrix absorption and enhancement effects^(37,76) and simplifies any necessary corrections for particle size effects. Finally, the calculated sensitivity of the EDX method using a radioisotope source was better than 100 ppm Cl. Experiments showed, however, that this approach was not feasible. Samples of concrete powder from holes drilled in the concrete test plates prepared for the Phase I studies (see Section 3.1) were deposited from air suspension onto filter paper discs and analyzed by our Si(Li) XRF spectrometer.⁽⁷⁶⁾ The measured Cl K X-ray intensity was found to be very poorly correlated with the known chlorine content of the concrete slabs. The reasons for this are thought to be: 1) the 10 mg deposit weight was not representative of the slab even though the powder sample had been well mixed and reground; 2) practical deposits are neither ideally "thin" nor "infinitely thick" for Cl K X-rays, resulting in the X-ray intensity being a nonlinear function of both sample weight and chlorine content. For the above reasons, the thin specimen approach was abandoned.

At the other extreme, fused pellets are ideal specimens for XRF analysis because the heterogeneity has been removed. Sample fusion is barely practicable as a field method; however, it is the method that we would have to fall back on if heterogeneity effects in powder or briquetted samples cause unacceptable errors.

Experiments showed that powder samples briquetted without binder using a hand-operated hydraulic press* gave satisfactory results, whereas loose powder samples were significantly inferior. Powder samples were obtained by drilling 1-1/2 in. (4 cm) dia. holes in

*Carver, Model C.

the 1 in. (2.5 cm) thick test plates using a rotary hammer* (this yielded 70 to 80 g. of powder), crushing any large pieces, mixing, coning and quartering. Briquettes were made by pressing about 15 g. (for 1-1/8 in. (2.9 cm) dia. specimens) or about 40 g. (for 2-1/4 in. (5.7 cm) dia. specimens) under a load of about 3×10^4 lb (1.5×10^4 kg). The briquettes were sprayed, on their back sides only, with acrylic lacquer to prevent fragmentation during repeated handling. Both loose powders and 1-1/8 in. (2.9 cm) dia. briquettes covering the chlorine range 0 to 3830 ppm were analyzed using the Si(Li) spectrometer with radioisotope source (^{55}Fe) excitation (see Section 4.4). The overall standard deviation of the linear regression of Cl K intensity vs chlorine content of each slab was 141 ppm Cl for loose powders and 110 ppm for pressed briquettes. It was decided, therefore, to use the pressed briquette method for all XRF analyses. It was also decided to postpone further refinement of the sample preparation method until a practical field instrument configuration had been worked out and had been shown sensitive enough to warrant further work on sample preparation. Note that the absence of severe heterogeneity effects on the chloride measurement is probably due to a relatively homogeneous dispersion of chloride in the concrete by virtue of its addition as aqueous solution.

4.4 Feasibility of the EDX Method

Figure 6 shows a calibration curve obtained using the CSI Si(Li) spectrometer with a 40 mCi Fe-55 source. Fe^{55} emits Mn K X-rays, 5.90 keV, with a half-life of 2.6 years, and is readily available in encapsulations suitable for X-ray fluorescence, in the activity range 1 to 1000 mCi. Its emission efficiency is approximately 5×10^6 Mn K X-rays per second per mCi (over 4π steradians). It is the only radioisotope X-ray source suitable for excitation of Cl K X-rays. The standard deviation due to counting statistics was 36 ppm Cl in a count time of 8000 seconds. The method of data analysis used was simply to integrate a spectral region about the Cl K X-ray peak plus two immediately adjacent regions, above and below, for background (see Figure 7). A more sophisticated

*Milwaukee, Cat. No. 5300, with 1-1/2 in. (3.8 cm) bit.

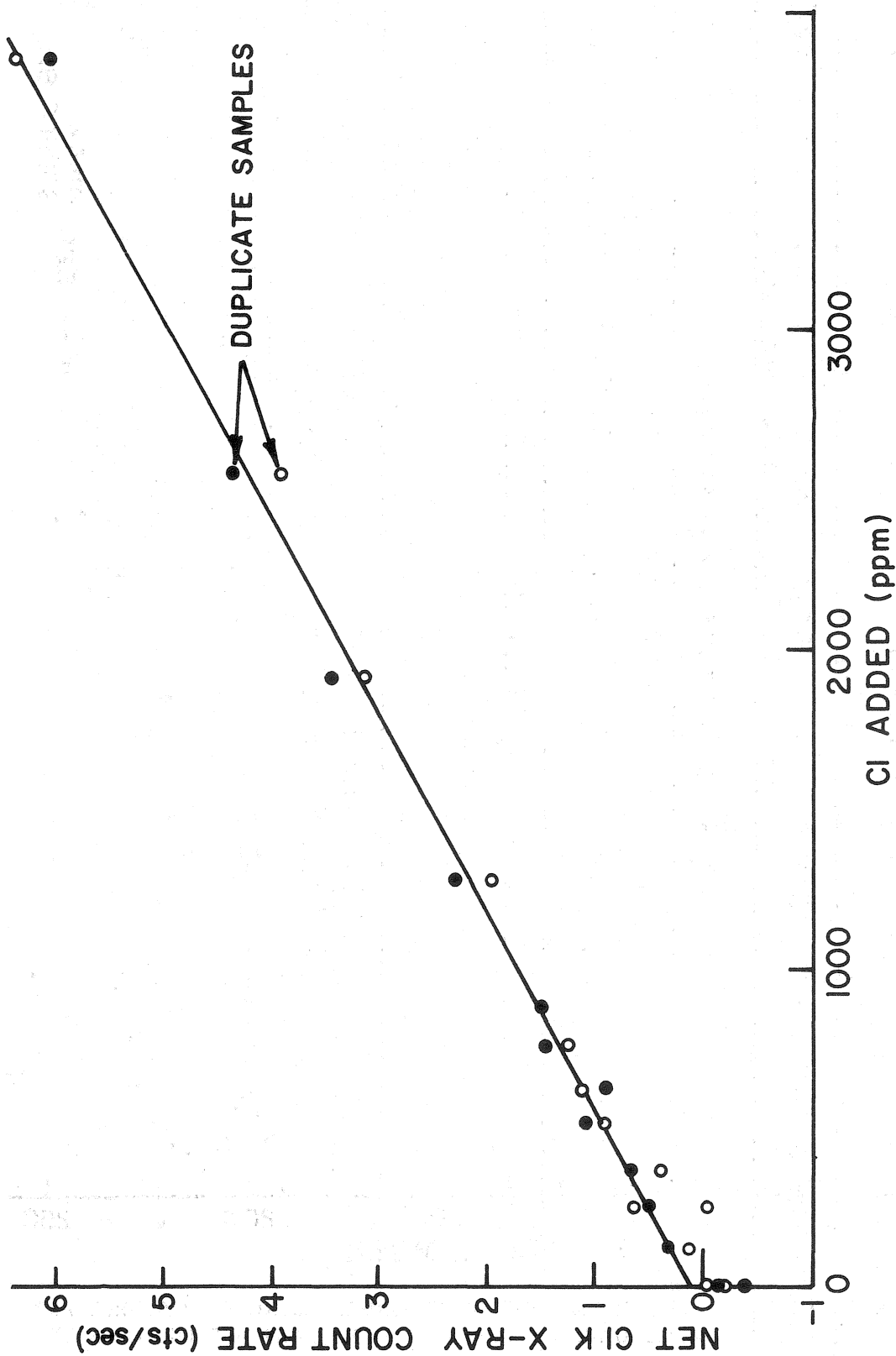


FIGURE 6. CALIBRATION FOR PRESSED BRIQUETTES USING Si(Li) SPECTROMETER AND ^{55}Fe SOURCE

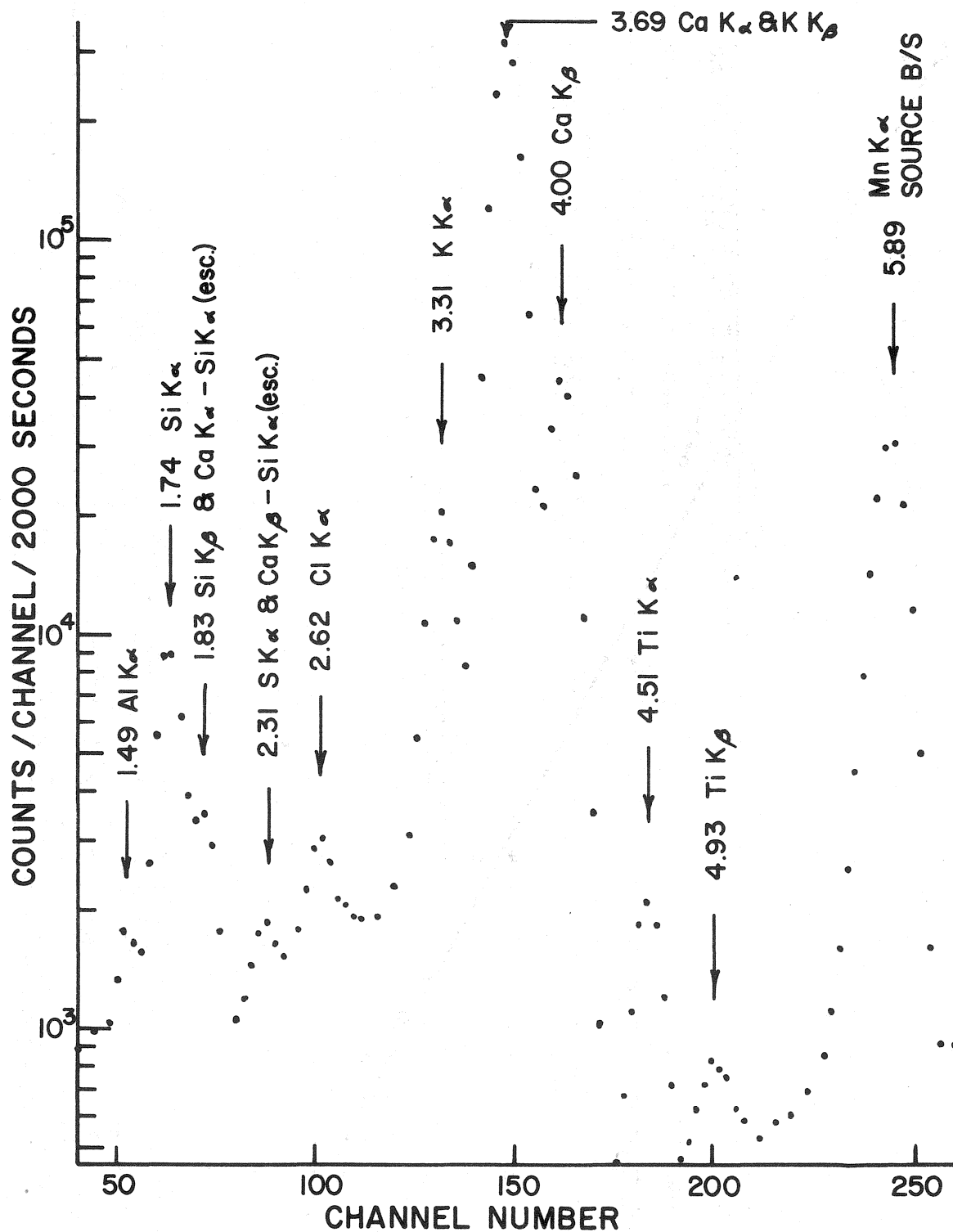


FIGURE 7. X-RAY SPECTRUM FROM CONCRETE SAMPLE USING Fe^{55} SOURCE AND Si(Li) SPECTROMETER, SHOWING X-RAY LINES AND ENERGIES IN keV

method would not gain anything, because there are no spectral interferences and no significant matrix effects.

The standard deviation (σ) due to counting statistics is given by the formula

$$\sigma = \frac{1}{St} \sqrt{N_p + N_b} \quad \text{ppm} \quad (1)$$

where S is the slope of the calibration curve in counts/sec. of Cl K X-rays per ppm Cl;

N_p is the count in the Cl peak (total area under the peak);

N_b is the sum of the areas of the adjacent background windows;

and t is the count time corrected for dead time; i.e., the "live time" (see below).

Using this formula, the experimental standard deviation obtained for a given source strength and count time can be calculated from the measured "signal" and "background" counts. Since the count rate is proportional to source strength, values of σ for other count times and source strengths can also be calculated.

The total count rate was 2250 cts/sec., of which 1500 cts/sec. was due to Ca K X-rays and the remainder was due to backscattered source X-rays. Figure 7 shows a typical spectrum which includes the intense Ca K X-ray peak. Si(Li) spectrometers have a pulse processing time of about 100 microseconds, during which period (called the "dead time") incident X-rays are not counted and a fraction of the signal is lost. In order to keep dead time losses tolerable, the total count rate should not exceed about 5000 cts/sec. At this count rate, dead time losses are 50 percent; a 1000-second "live time" count* thus would take 2000 seconds of "clock time" to complete. The pulse processing time cannot be reduced much below 100 microseconds, otherwise the energy resolution of the spectrometer suffers. It is clear from the spectrum of Figure 7 that any degradation of resolution would seriously reduce the signal-to-background ratio for the Cl K X-rays.

*That is, a count during which automatic correction is made for dead time losses.

The EDX method is therefore limited by the high intensity of Ca K X-rays excited. The best way to avoid this problem is to use a source energy in the range 2.82 to 4.03 keV so as to excite Cl K X-rays but not Ca K X-rays. Backscattered source X-rays must still be resolved from the Cl K X-rays, and this increases the practical lower limit of the source energy to at least 3 keV. The following possibilities exist: 1) X-ray tube operated at a high voltage, not exceeding 4.0 kV, with a Ag anode; 2) X-ray tube operated at low voltage (< 10 kV) with an external Ca, K, Ag, Cd or In reflection target or transmission filter (see, for example, Section 4.5); 3) Fe-55 source with a similar reflection target or transmission filter (Ca K, K K, Ag L, Cd L and In L X-rays all lie within the permitted energy region, with Ca theoretically the preferred element).

Calculations showed that using an Fe-55 source and a reflection target ("source-target assembly") was not feasible with a Si(Li) spectrometer because of geometrical losses, but this could be a satisfactory arrangement for a portable proportional counter-based instrument. A 100 mCi Fe⁵⁵-Ca source-target assembly* was ordered for the proportional counter studies (Section 4.5). Further calculations showed that a Ca transmission filter (see below) was a feasible approach for both detectors; however, the optimum filter thickness must be determined experimentally in each case.

As a parallel backup effort, a telephone survey was made of all known XRF equipment manufacturers to solicit their views on the feasibility of a field instrument using an X-ray tube with one of the above-mentioned targets. Of the 13 firms contacted, four expressed interest and willingness to run a few test samples. Four sets of powdered concrete samples taken from the test slabs, as per Section 4.2, were sent out. Three sets of results were eventually turned in, none of which were any better than the in-house results obtained with a radioisotope source.

*Amersham Searle Model IEC in X203/1 capsule.

Calcium filters containing up to 15 mg/cm^2 Ca were made by: mixing finely ground calcium carbonate in equal proportions with polyethylene powder; heating to 200°C to melt the polyethylene; mixing while melted; allowing to solidify; hot pressing into a sheet with predetermined thickness, and cutting out. This is a standard procedure used at CSI for making X-ray filters. Using the Si(Li) X-ray spectrometer and a 380 mCi Fe-55 source covered with filters of varying thicknesses, calibration curves such as Figure 6 were obtained. From each set of data, the limiting standard deviation due to counting statistics at zero chlorine was calculated for a count time of 1000 seconds (live time), with the total count rate not allowed to exceed 5000 counts/sec., and the total activity not allowed to exceed 1000 mCi (see Equation 1).

A curve of limiting standard deviation vs filter thickness was obtained and showed a minimum value, at 4.4 mg/cm^2 Ca, of 56 ppm for a 1000 mCi source and 5000 counts/sec. Associated experiments using Cl and K detector filters to try to further improve the "signal-to-background" ratio did not succeed.

The optimized Si(Li) EDX system, with the available 380 mCi Fe-55 source, a 4.4 mg/cm^2 Ca source filter, and a 2000 second (live) count time, was used in all subsequent concrete analyses attendant to the development of the chloride impregnation method (see Section 3.2). Some 200 determinations were made and the method was found to be fast and reliable, taking about 2 man-hours and 15 instrument-hours per batch of 30 samples. Each batch of 30 samples was run overnight in the spectrometer.

4.5 Feasibility of the NDX Method

The proportional counter (NDX) method depends on balanced filters⁽³⁷⁾ for energy selection of the Cl K X-rays. The proper filter elements are Cl and S, and Saran* wrap makes an ideal Cl X-ray filter. Figure 8 shows the calculated transmission curves for two suitable filter thicknesses. The theoretical Cl content of Saran is 73 percent but X-ray transmission measurements showed that the actual content of the batch used here was 60 percent. The total mass per unit area was 2.23 mg/cm^2 .

*Polyvinylidene chloride film available at grocery stores.

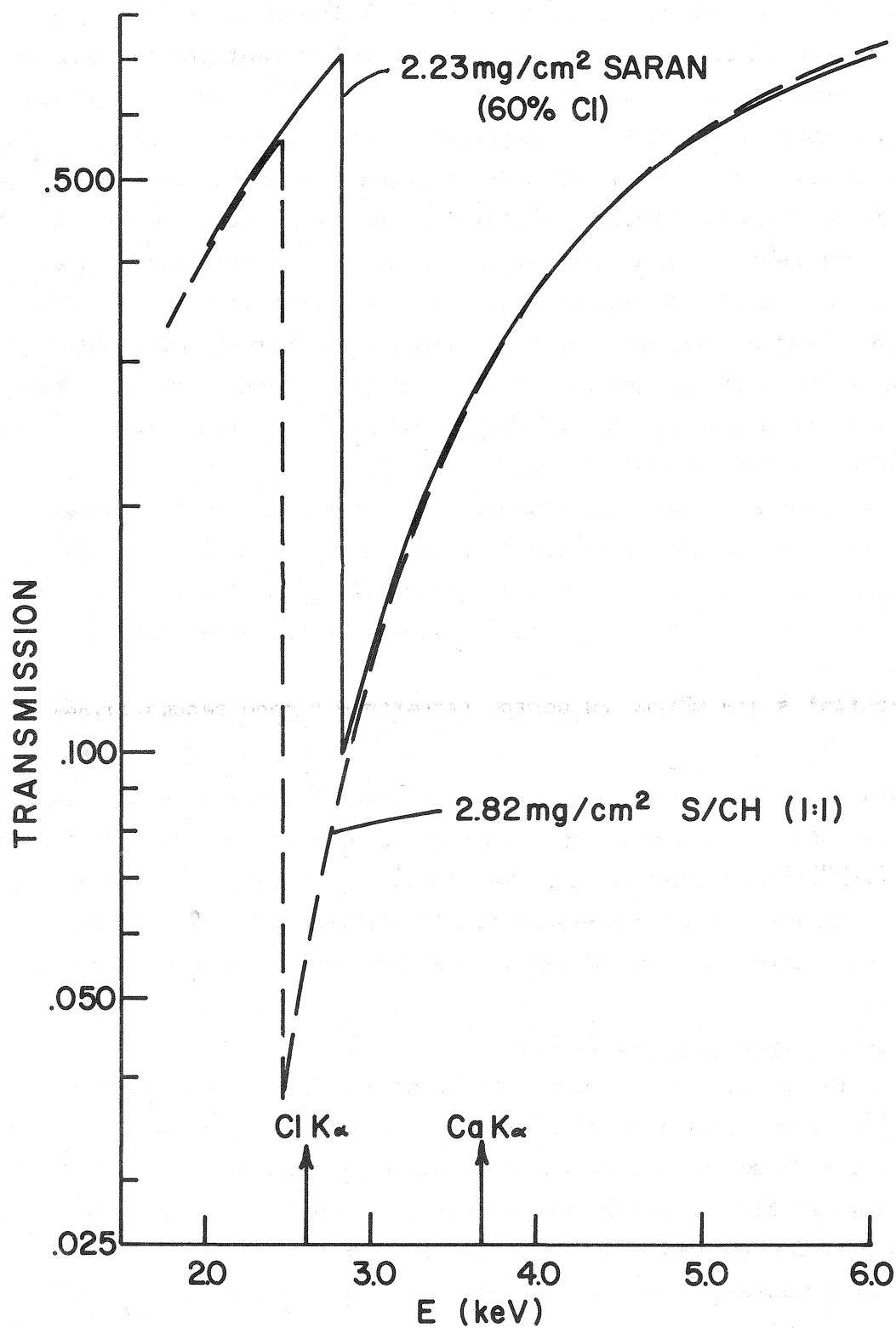


FIGURE 8. CALCULATED TRANSMISSION CURVES FOR Cl/S BALANCED FILTERS

The sulfur filter is a 1:1 mixture of sulfur and a hydrocarbon polymer. The method of mixing the filter element with molten polyethylene and pressing out cannot be used to make filters this thin. An alternative method is to thoroughly mix the element with a solution of a polymer⁽⁷⁹⁾ and spread a film of a predetermined thickness using a film casting knife.* Experiments were performed to perfect this approach. A 25 percent solution of polystyrene in xylene was ball milled for 48 hours with a weight of sublimed sulfur equal to the weight of polystyrene. The ratio of wet film thickness to dry film thickness was found to be 5:1. Films of predetermined thicknesses varying about the theoretical thickness were prepared by spreading, with the film casting knife, aliquots of the colloidal suspension onto a glass plate coated with a silicone release compound. Several portions of sulfur film were tested for balance with a given Cl filter using equal transmission of Ca K X-rays as the criterion. An X-ray transmission gauge using the Fe⁵⁵-Ca source-target assembly was set up for this purpose. The filters were mounted in curved filter holders for use.

Figures 9 and 10 show the source-sample-filter-detector arrangements used to investigate the transmission filter and secondary target methods, respectively. In each case the source angles of inclination and the sample and source distances were experimentally optimized for best "signal-to-background" ratio. The sample aperture diameter of 2 in. (5 cm) was chosen after it was verified that pressed briquettes of concrete powder could be made this size. A block diagram of the electronics used is shown in Figure 11. Artificial samples were made by mixing reground NaCl, CaCO₃ and starch, and making 2-1/4 in. (5.7 cm) dia. pressed briquettes. Chlorine contents varied from 0 to 5 percent with calcium contents of 10 and 15 percent.

Experiments were performed to find the sensitivities of the reflection target method and of the transmission filter method for a range of calcium filter thicknesses. Results were in reasonable agreement with previous calculations. The best possible sensitivity for the reflection

*Gardner Instruments.

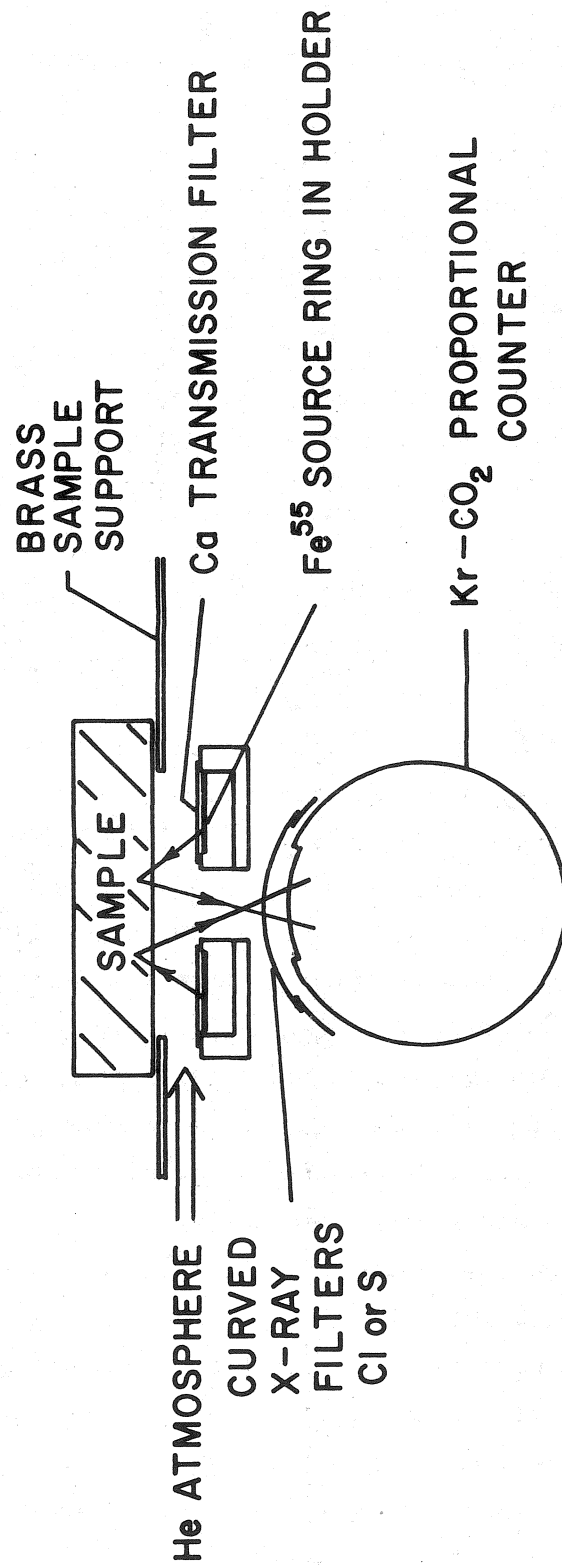


FIGURE 9. ARRANGEMENT OF SOURCE, SAMPLE, FILTERS AND DETECTOR FOR TRANSMISSION FILTER EXPERIMENTS

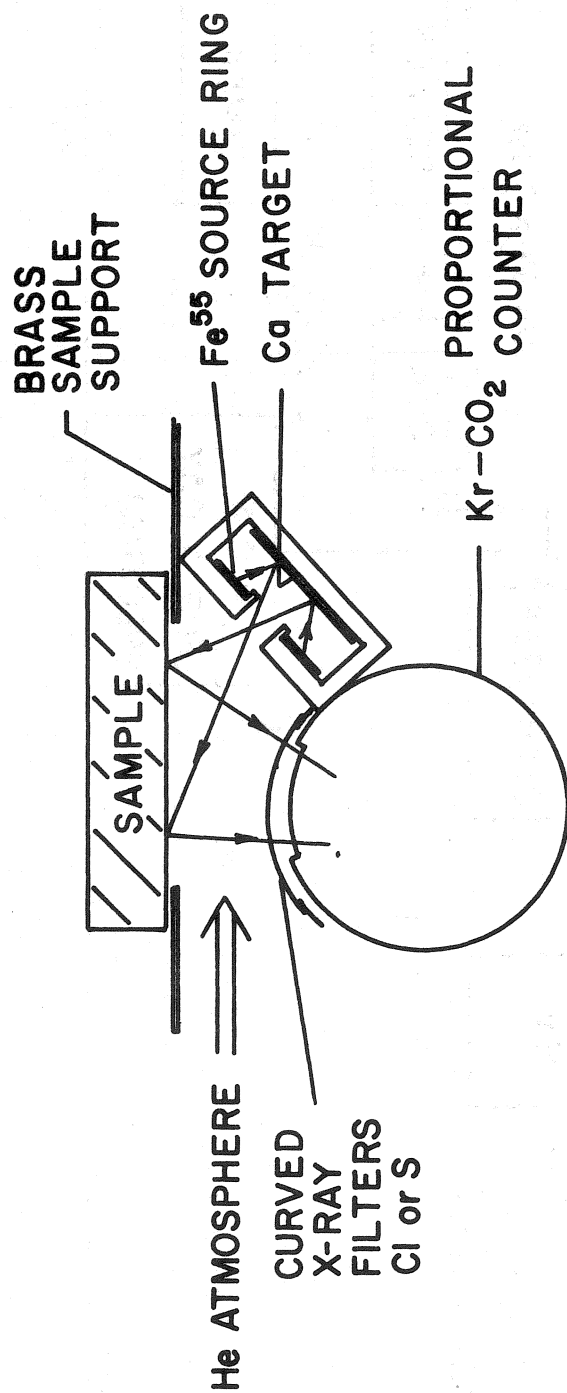


FIGURE 10. ARRANGEMENT OF SOURCE, SAMPLE, FILTERS AND DETECTOR FOR SECONDARY (REFLECTION) TARGET EXPERIMENTS

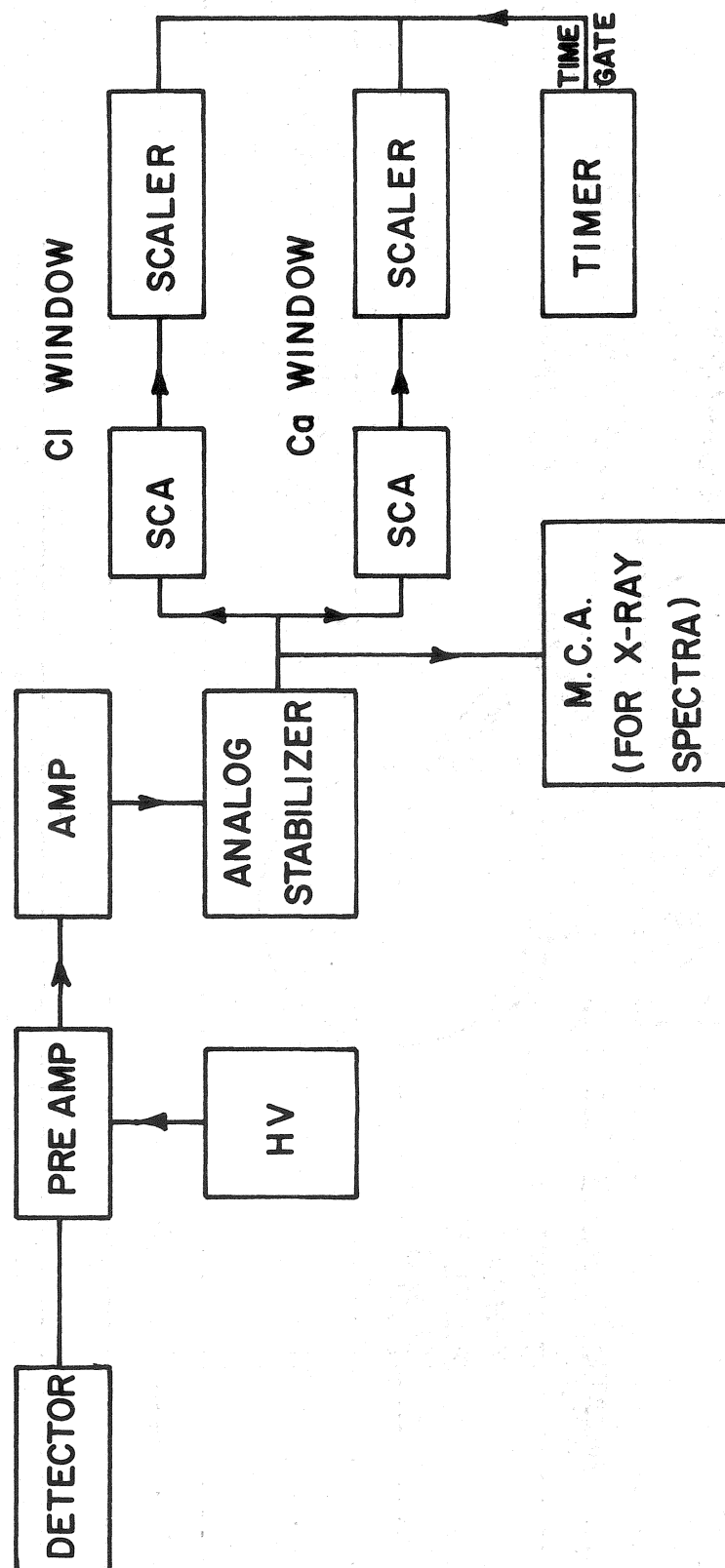


FIGURE 11. BLOCK DIAGRAM OF ELECTRONICS USED FOR PROPORTIONAL COUNTER EXPERIMENTS

target method is source-limited; a 1000 mCi source-target assembly is expected to yield a detection limit of about 150 ppm Cl in a count time of 1000 sec per filter. The transmission filter experiments yielded a curve of optimum sensitivity vs filter thickness with a minimum value at 4.4 mg/cm² Ca, a similar result to that obtained previously using the Si(Li) spectrometer. The optimum value of statistical standard deviation at zero chlorine was found to be 100 ppm using a 215 mCi Fe-55 source and a count time of 500 sec per filter. Changing the proportional counter window from 10 mil (0.025 cm) beryllium to 5 mil (0.013 cm) would double the signal without changing the background and thus improve the sensitivity by a factor of 2. This sensitivity is limited by count rate effects and by electronic system stability. The total count rate would be 10⁴ cts/sec., a rate which can be exceeded by a factor of four before serious resolution degradation is apparent (dead time losses are negligible with a proportional counter). However, the gas gain changes significantly with count rate at count rates above about 10³ cts/sec. because of space charge effects. This, coupled with the fact that a count rate stability of better than 0.15 percent would be required to achieve the above sensitivity in practice, means that even with an electronic gain stabilizer it would be difficult to attain a better sensitivity by using a stronger source.

To finally confirm the feasibility of the proportional counter method, the 380 mCi source was set up with a 4.4 mg/cm² Ca source filter, and the 2-1/4 in. (5.7 cm) dia. pressed briquettes of concrete powder were measured. Figure 12 shows spectra obtained through each balanced filter from the 3830 ppm Cl specimen. The positions of the Cl K signal, the Ca K combined backscattered-fluorescent peak and their respective single channel analyzer (SCA) windows are shown. Figure 13 shows the calibration curve obtained for count times of 1000 sec. per filter. The (Cl-S) balanced filter difference count in the chlorine window was corrected as follows for Ca K interference caused by slight imbalance of the filters used. For each filter count in the chlorine SCA window, an amount proportional to the Ca K intensity (recorded simultaneously in the Ca K SCA window) was subtracted. The proportionality constants were determined empirically to be 0.060 for the Cl filter and 0.044 for the

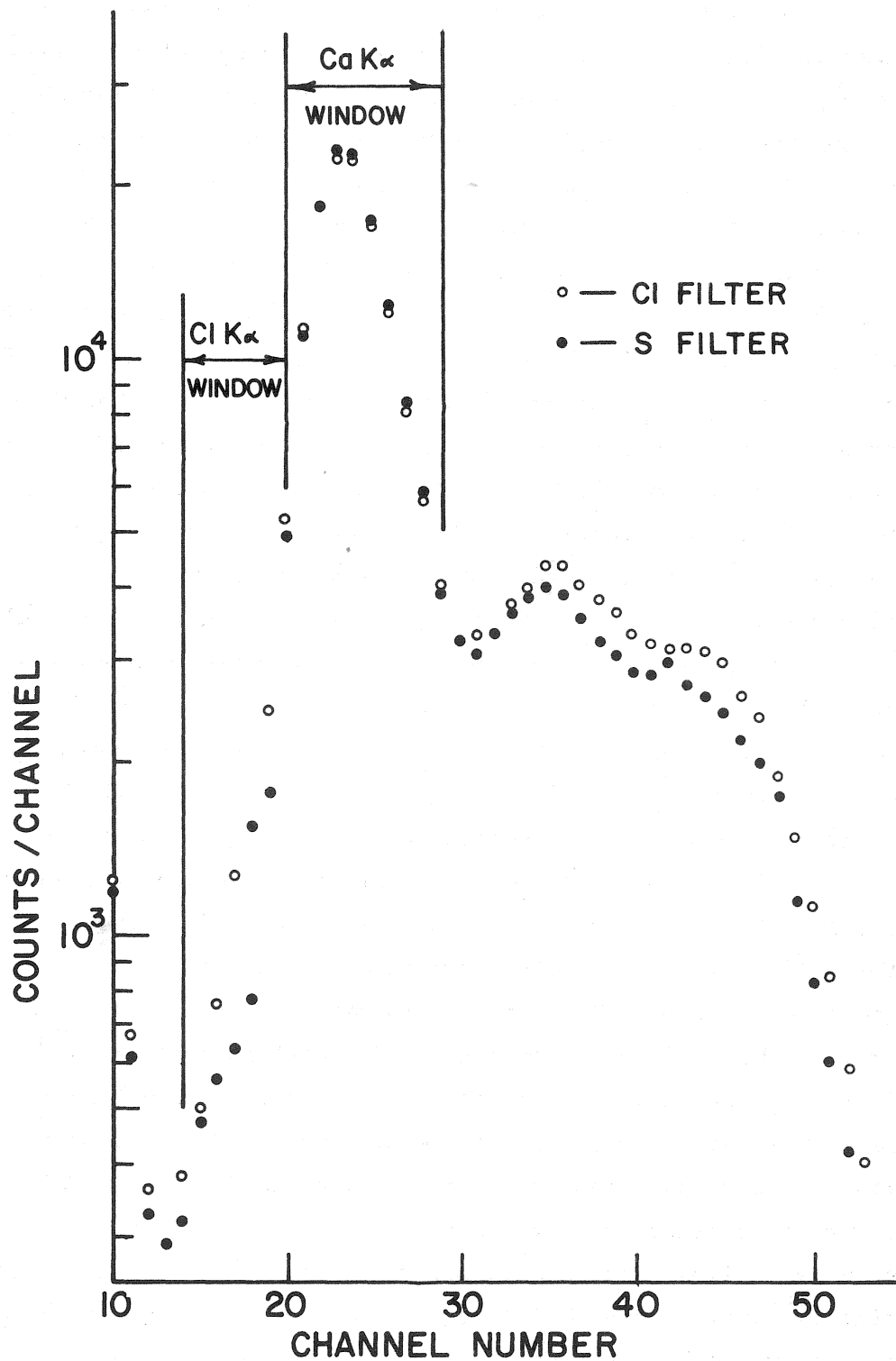


FIGURE 12. PROPORTIONAL COUNTER SPECTRA THROUGH BALANCED FILTERS, FROM BRIQUETTE CONTAINING 3830 PPM Cl

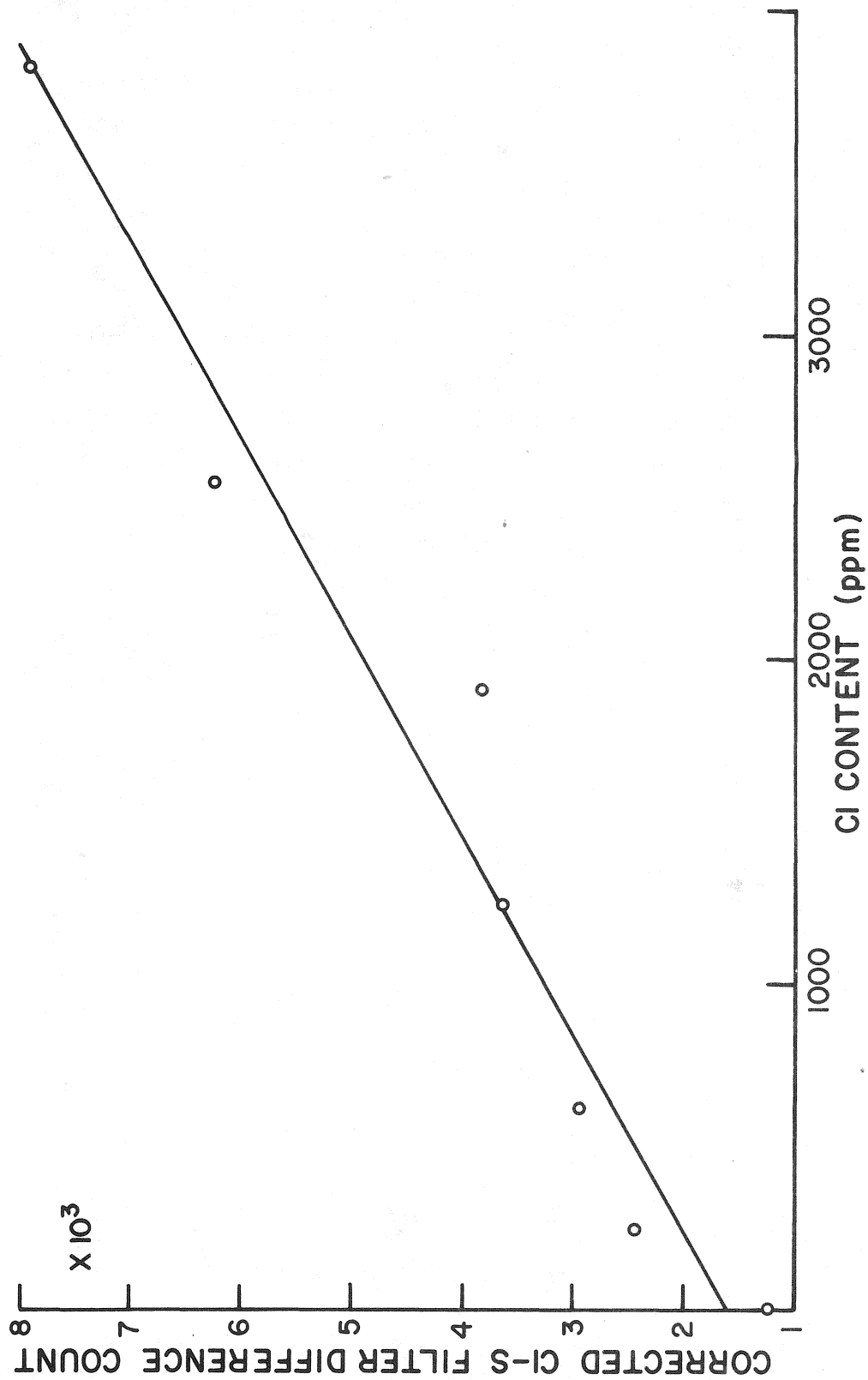


FIGURE 13. CALIBRATION CURVE FOR PRESSED BRIQUETTES USING PROPORTIONAL COUNTER AND BALANCED FILTERS

S filter. Such correction factors are instrumental constants and could be reduced to zero by very careful filter balancing.

The standard deviation of the linear regression of corrected net Cl K X-ray count vs chloride content was found to be 330 ppm Cl, whereas the calculated standard deviation due to counting statistics is only 96 ppm Cl, as expected from the earlier results. Repeated readings taken with one sample, changing filters and removing and replacing the sample between readings, gave a standard deviation of 280 ppm Cl. The error component due to electronic drift was shown in a separate experiment to be less than 0.1 percent of the count rate, which is negligible compared to the error due to counting statistics. Thus the difference between the statistical and the overall error was shown to be due mainly to errors of filter changing and sample repositioning which would be eliminated in a well-engineered instrument.

5. NEUTRON-GAMMA TECHNIQUES

5.1 General Principles

Neutrons of all energies from thermal (0.02 eV) to fast (keV to MeV range) are penetrating, available and potentially useful for exciting characteristic gamma rays. Prompt gamma rays are emitted during neutron irradiation mainly from fast neutron inelastic scattering or thermal neutron capture. The intensity, I_p (counts/sec.), of prompt gamma rays is proportional to the neutron flux, ϕ (n/cm²/sec.), from the source, the prompt gamma excitation cross section, σ_p (barns)*, for the reaction and the concentration, C , of the element:

$$I_p = k_p \phi \sigma_p C \quad (2)$$

where k_p is an instrumental constant.

As soon as the neutron source is removed, I_p falls to zero.

The product nucleus from these interactions is usually radioactive and thus can emit characteristic gamma rays after the sample and source are separated. The intensity of activation gamma rays is built up during irradiation, and falls off thereafter, according to the half-life ($\tau_{1/2}$) of the radioactive isotope produced. The intensity, I_a , of activation gamma rays is proportional to the neutron flux, ϕ , the activation cross section, σ_a , and the element concentration, C , as above, but also varies with time:

$$I_a = k_a \phi \sigma_a C (1 - e^{-\lambda t_1}) (e^{-\lambda t_2} - e^{-\lambda t_3}) \quad (3)$$

where k_a is an instrumental constant;

λ is the decay constant = $\frac{0.693}{\tau_{1/2}}$;

t_1 is the irradiation time interval;

t_2 is the time interval between the end of the irradiation and the beginning of the measurement (the delay time); and

t_3 is the time interval between the end of the irradiation and the end of the measurement ($t_3 - t_2$ equals the measurement time).

*1 barn = 10^{-24} cm²

Four main types of neutron-gamma interaction can occur; fast neutron-prompt gamma, thermal neutron-prompt gamma, fast neutron-activation gamma and thermal neutron-activation gamma. Each of the reactions can occur in both stable isotopes of chlorine, ^{35}Cl (75.5 percent abundant) and ^{37}Cl (24.5 percent abundant).

A study was made of the cross section and nuclear data to find the most likely reactions, the neutron energies required and the gamma rays emitted. (56,80-82) Possible interferences from the other constituents of concrete, and from reinforcing bars, asphalt and membranes were also borne in mind.

The best reactions were found to be thermal neutron-prompt gamma and thermal neutron activation. The total thermal neutron cross section for chlorine is high (33 barns), and about a dozen relatively intense prompt gamma lines are emitted (mainly from $^{35}\text{Cl}(n,\gamma)^{36}\text{Cl}$, cross section 44 barns), ranging in energy from 1.16 to 8.58 MeV. (56,82) Several of these lines have relative intensities one to three orders of magnitude greater than prompt gammas emitted from the other elements possibly present, with the exception of hydrogen which emits an intense line at 2.22 MeV.

Activation gamma rays arise from the reaction $^{37}\text{Cl}(n,\gamma)^{38}\text{Cl}$, cross section 0.43 barns. The ^{38}Cl decays with a half-life of 37.3 min., emitting 1.64 and 2.17 MeV gamma rays with relative abundances of 38 and 47 percent, respectively. The $^{35}\text{Cl}(n,\gamma)^{36}\text{Cl}$ reaction does not produce significant activation gammas. The most likely spectral interferences could arise from thermal neutron activation of manganese (associated with iron), sodium and aluminum. Calcium is activated significantly ($^{48}\text{Ca}(n,\gamma)^{49}\text{Ca}$; $\tau_{1/2} = 8.8$ mins, $E_{\gamma} = 3.09$ MeV) but would not interfere. Manganese is activated by $^{55}\text{Mn}(n,\gamma)^{56}\text{Mn}$ ($\tau_{1/2} = 2.58$ hrs; $E_{\gamma} = 0.847$ MeV (99%), 1.81 MeV (29%) and 2.12 MeV (15%)). Sodium is activated by $^{23}\text{Na}(n,\gamma)^{24}\text{Na}$ ($\tau_{1/2} = 15.0$ hrs; $E_{\gamma} = 1.37$ MeV (100%) and 2.75 MeV (100%)). Aluminum is activated by $^{27}\text{Al}(n,\gamma)^{28}\text{Al}$ ($\tau_{1/2} = 2.31$ mins; $E_{\gamma} = 1.78$ MeV (100%)). Possible fast neutron reactions are much less favorable and were ruled out in the paper study (Section 2.2.2).

5.2 Choice of Source and Detector

5.2.1 Available Sources

Available neutron sources are nuclear reactors, neutron generators and sealed radioisotope sources. Nuclear reactors are strictly non-portable.

Neutron generators produce fast neutrons by accelerating deuterium ions through ~ 150 kV onto a tritium target (e.g., titanium tritide on a copper foil) in a sealed or pumped vacuum tube. Fourteen MeV neutrons are produced by the reaction $d + T = {}^4\text{He} + {}^1_0\text{n}$. Two MeV neutrons can be produced from the (d,d) reaction by using a deuterated target, but their intensity is an order of magnitude lower. Neutron generators have the advantage that they can be switched off when not in use. They also have an advantage over other neutron sources in that the neutrons can be rapidly pulsed on and off. Such pulsing can be advantageous in prompt-gamma analysis, if rapid enough. Transportable sealed tube neutron generators are available and have found wide use in the field, especially in oil well logging. However, the pulse characteristics and repetition rate of these tubes is not satisfactory for prompt-gamma analysis. Also the total neutron output (about $10^8/\text{sec.}$, yielding $\sim 10^5/\text{cm}^2/\text{sec}$ thermal fluxes) is too low for either the activation or the prompt-gamma analyses under investigation here. Pumped tube neutron generators can have suitable pulsing characteristics and can yield 14 MeV neutron outputs of more than 10^{11} n/sec. However, these machines are much more expensive, nonportable, laboratory based installations. Another problem is that the 14 MeV neutrons require a relatively large volume of moderator to thermalize them. This diffuses the neutrons and reduces the flux by two to three orders of magnitude compared to the fast neutron flux near the target. Our recent studies on a similar problem (field analysis of fresh concrete)⁽⁴¹⁾ have shown that neutron generators offer no advantages over radioisotope sources for thermal neutron analysis methods in the field.

Radioisotope neutron sources are small, portable and self-contained, and need no supplies of power, cooling water, vacuum or special gases. Their output is quite reliable and the rate of radioactive

decay accurately predictable. However, the weight of shielding required both in use and for safe transportation (the sources cannot be "switched off") limits their portability. An isotope neutron source emitting about 10^9 n/sec (over 4π) represents the practical limit for convenient portability in this application. The closest safe distance of approach on a regular basis to such a source, when unshielded, is about 10 feet (3 meters) and the shielding weight required for storage and transportation is several hundred kilograms.

Three main types of radioisotope neutron source are available: (α ,n), (γ ,n) and spontaneous fission. An α -emitter such as ^{238}Pu , ^{241}Am or ^{226}Ra is mixed with beryllium and encapsulated to give an (α ,n) source which emits fast neutrons in the energy range 3 to 8 MeV by virtue of the reaction $^9\text{Be}(\alpha, n)^{12}\text{C}$. Available sources have outputs up to about 10^8 n/sec. Other (α ,n) sources use B, Li or F target materials for special applications, but their neutron outputs are lower. The (γ ,n) reaction on beryllium is used to produce low energy (25 keV) fast neutrons from ^{124}Sb . However, the half-life of ^{124}Sb is only 60 days, the neutron output per curie of ^{124}Sb is only 1.3×10^6 /sec., and strong sources are very expensive.

The preferred source for this application is ^{252}Cf . (83,84) It is primarily a spontaneous fission source with a half-life of 2.65 yrs and a neutron output of 2.3×10^9 n/sec (over 4π) per milligram ^{252}Cf ; this output is at least three orders of magnitude greater than that of other radioisotope neutron sources. The fission neutron spectrum has a low mean energy and so is relatively easily thermalized; thermal fluxes in the sample as high as several percent of the fast neutron output can be achieved. The lower energy neutrons are also somewhat more easily shielded than (α ,n) and 14 MeV neutrons. The isotope is readily available in suitable encapsulations. A loan program exists through which sources of any suitable strength can be obtained for evaluation purposes. (84)

Up to six ^{252}Cf sources were employed in the present investigations, one containing 108 μg and 5 containing 14 μg each, as of January 1, 1977.

5.2.2 Gamma-Ray Spectrometers

A gamma-ray spectrometer is required for discrimination and measurement of the prompt or activation gamma-ray signals. Figure 14 shows the electronic schematic of the spectrometer used in this investigation. The detector gives one output pulse per gamma ray detected, with an amplitude proportional to the gamma-ray energy. The pulses are amplified and the system gain is stabilized (if necessary) by standard NIM* modules, unless the count rate is very high ($> 10^5/\text{sec.}$). In the latter case, special electronics are required. The analog-to-digital converter (ADC) digitizes the pulse height and the multichannel analyzer (MCA) produces a histogram of number of pulses per channel vs channel position. This is the gamma-ray spectrum. Data collection and spectrum processing comprise, at a minimum, accumulation of the spectrum for a time sufficient to provide adequate statistics, integration of regions containing peaks and backgrounds, and subtraction of the relevant backgrounds to yield net peak intensities. Multichannel analyzers are available having various degrees of data analysis capability, including spectrum stripping and least squares fitting. Very simple spectrum processing involving only a few integration regions can be handled with NIM modular single channel analyzers and scalers.

Two types of detector are in use, the NaI(Tl)** scintillation counter and the Ge(Li)⁺ solid state detector. A large (e.g., 5 in. (12.7 cm) dia. x 5 in. (12.7 cm) thick) crystal of NaI(Tl) absorbs gamma rays efficiently (10-100%), yielding bursts of light at ~ 400 nm which are converted to electrical charge and amplified ($\times \sim 10^5$) by an optically coupled photomultiplier tube. The detector operates at room temperature, requires a photomultiplier HV supply of 1000 V and is temperature-sensitive (gain coefficient ~ 1 percent $^{\circ}\text{C}$). The energy resolution is about 5 percent in the gamma-ray region of interest, which is sufficient to resolve the simpler gamma spectra.

*Nuclear Instrumentation Modules.

**Sodium iodide, thallium-doped.

⁺Germanium, lithium-drifted.

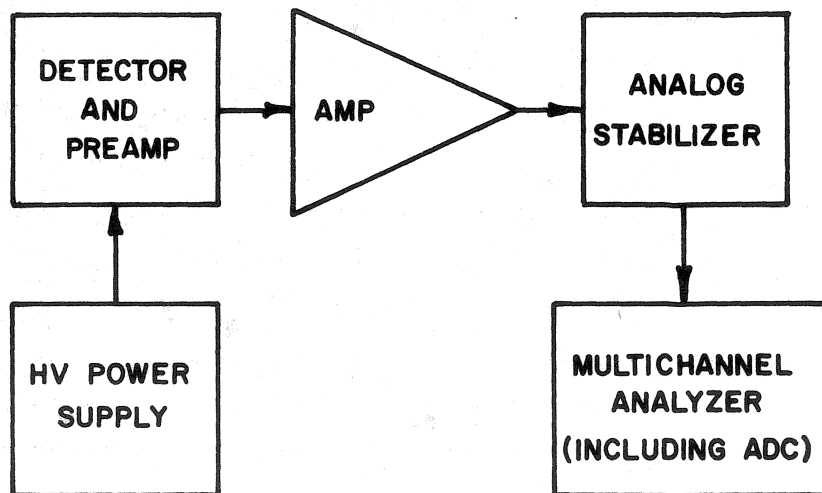


FIGURE 14. SCHEMATIC OF GAMMA-RAY SPECTROMETERS

A Ge(Li) detector is housed in a vacuum cryostat and must be kept at liquid nitrogen temperature at all times; otherwise, irreparable damage would occur to the Ge(Li) diode. Gamma rays absorbed in the germanium create electron-hole pairs which are separated by the applied bias (2-3 kV) and whose charge is proportional to the gamma energy. The gamma absorption efficiency of available Ge(Li) detectors is in the range 1 to 10 percent of that of NaI(Tl) crystals, but the energy resolution is 0.1 percent, which is sufficient to resolve the gamma rays in even the most complex spectra. This higher resolution requires the use of a more sophisticated amplifier, ADC and MCA, to exploit it. Temperature stability is good, since the detector is at constant temperature, but Ge(Li) detectors are significantly less fieldworthy than NaI(Tl) scintillation counters. Also, they can suffer permanent radiation damage on exposure to neutrons. On balance, we believe that the NaI(Tl) scintillation counter is the preferred detector, unless a Ge(Li) spectrometer is necessary for feasibility.

5.2.3 Spectra and Preliminary Sensitivity Comparisons

Experiments were performed using both types of detector with the objectives of 1) measuring typical prompt and activation gamma-ray spectra from chloride-spiked concrete, 2) assessing the magnitude of spectral interference problems, and 3) comparing the sensitivities of the two detectors for chloride determination.

Figures 15 and 16 show two neutron activation spectra obtained from a 3830 ppm, 1 in. (2.5 cm) thick test specimen using the Ge(Li) spectrometer, five 14 μ g thermalized ^{252}Cf sources, and irradiation times of 30 min. and counting times of 1000 sec. The delay time for spectrum A was 1 min. and that for spectrum B, 30 min. The irradiation and counting configurations are shown in Figure 17. It is seen that the 1.64 MeV chlorine peak is swamped by the Compton background from the intense ^{28}Al peak unless the latter is allowed to decay by at least an order of magnitude. The Compton background occurs in the detector and is due to absorption of Compton electrons (which have a continuum of energies) left behind in the detector when the incident gamma ray is scattered and the scattered gamma ray escapes from the detector, carrying with it some of the incident energy. Spectrum B shows important peaks from ^{24}Na , ^{56}Mn , ^{49}Ca , ^{42}K and ^{40}K . Note that

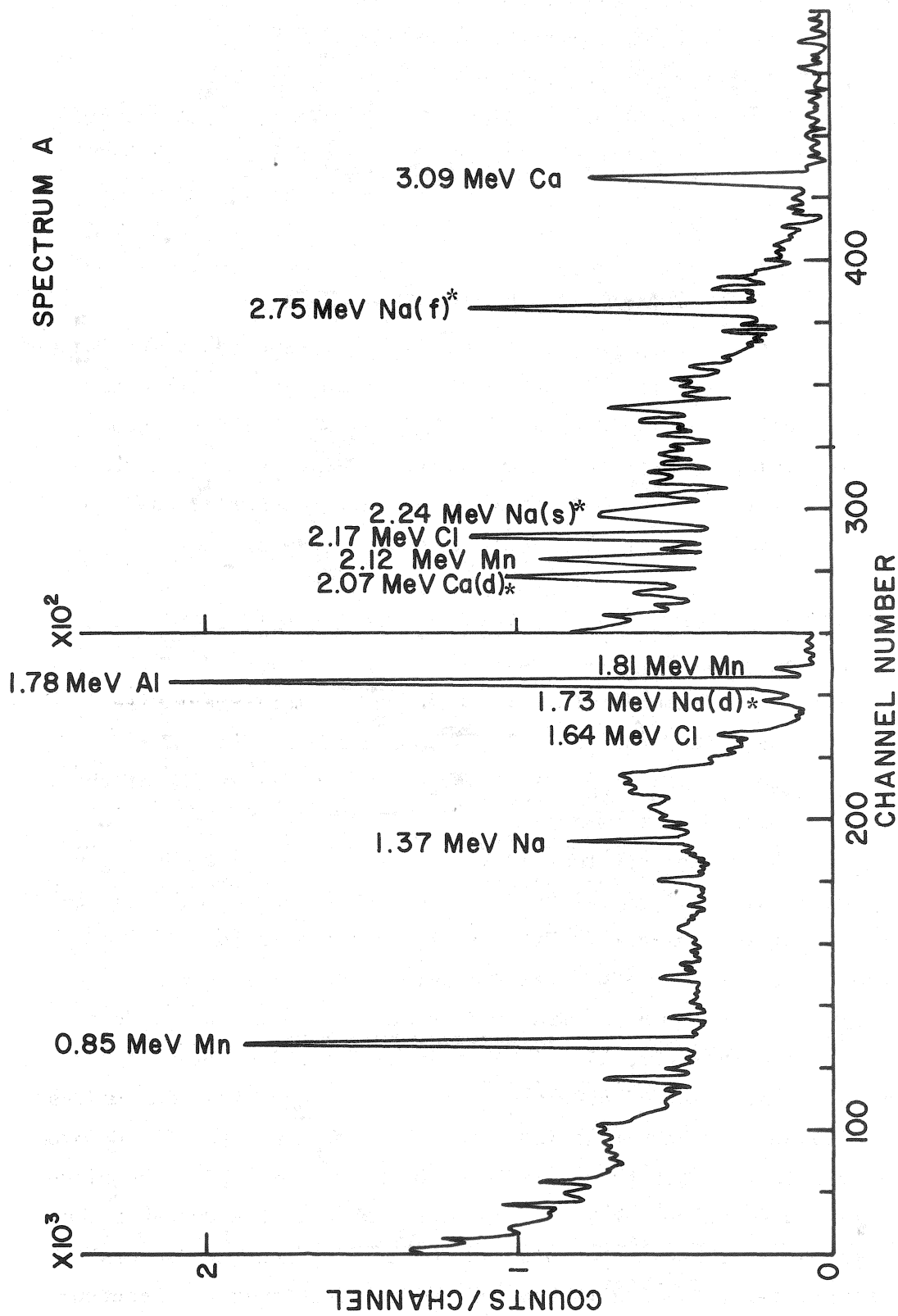


FIGURE 15. THERMAL NEUTRON ACTIVATION SPECTRUM FROM CHLORIDE-DOPED CONCRETE TEST PLATE USING Ge(Li) GAMMA-RAY SPECTROMETER - 1 MINUTE DELAY

*Note: f, s and d denote full energy, single escape and double escape peak, respectively, in this and subsequent figures.

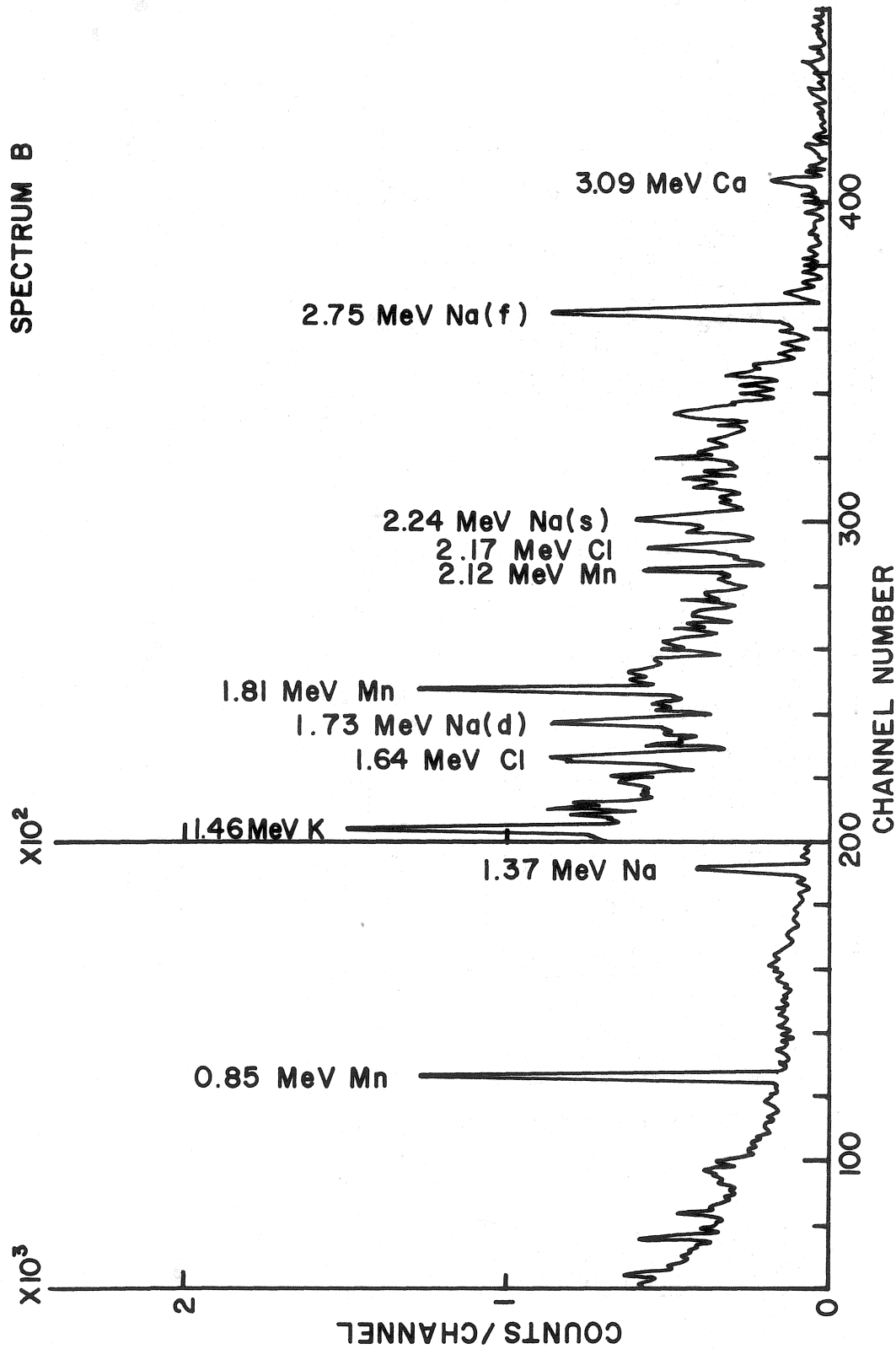
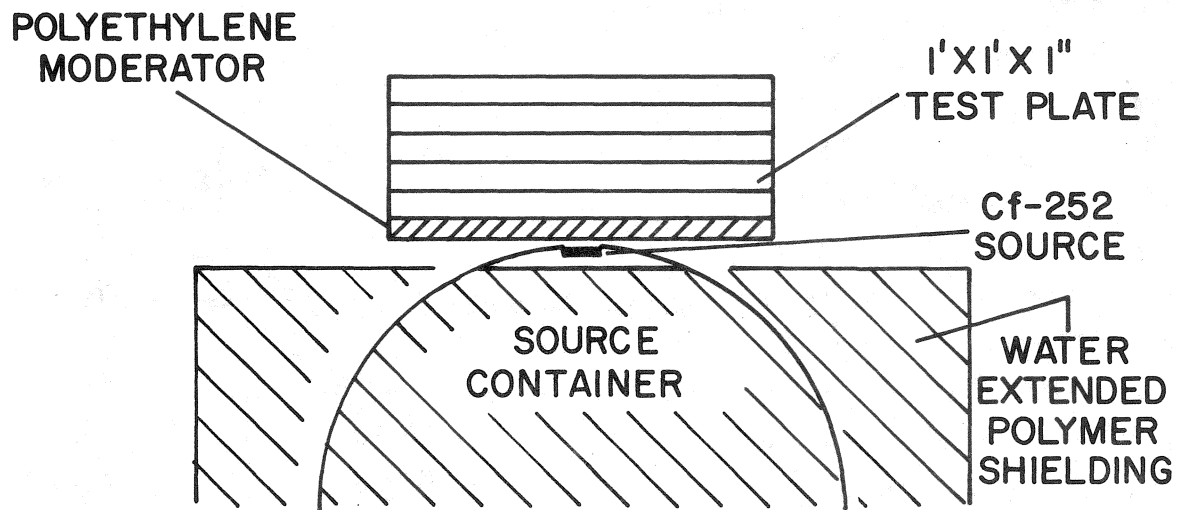
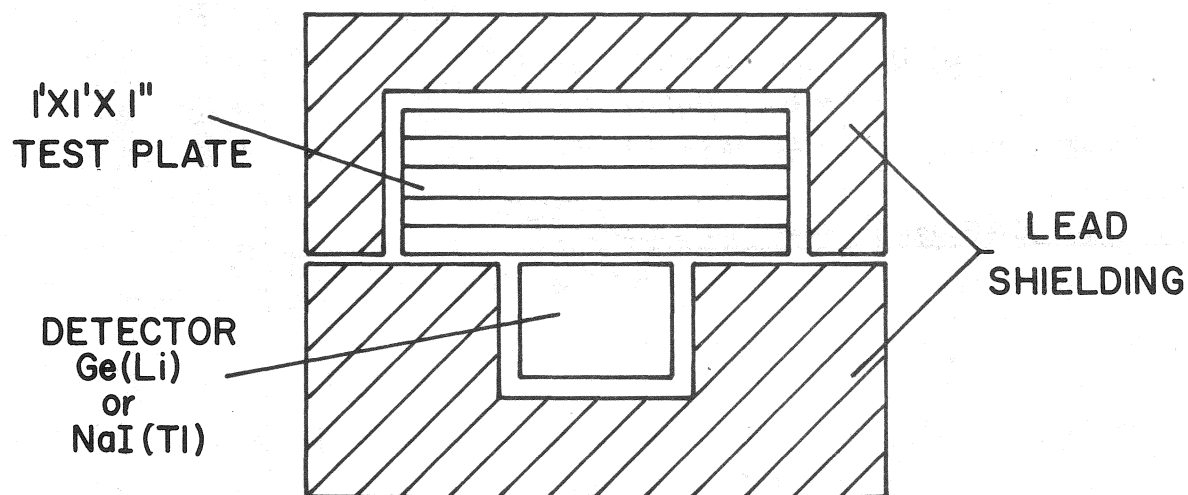


FIGURE 16. THERMAL NEUTRON ACTIVATION SPECTRUM FROM CHLORIDE-DOPED CONCRETE TEST PLATE USING Ge(Li) GAMMA-RAY SPECTROMETER - 30 MINUTE DELAY



a) IRRADIATION GEOMETRY



b) COUNTING GEOMETRY

FIGURE 17. IRRADIATION AND COUNTING CONFIGURATIONS (SCHEMATIC) FOR PRELIMINARY Ge(Li) AND NaI(Tl) ACTIVATION EXPERIMENTS (1" = 2.54 cm, 1' = 30.5 cm)

the natural gamma line from ^{40}K has the same order of intensity as the induced gamma lines. The single and double escape peaks from the 2.75 MeV ^{24}Na line arise in the detector when the incident gamma ray causes pair production followed by escape of either one or both of the pair of 0.51 MeV gamma rays formed. The threshold for this effect is 2.04 MeV.

Figure 18 shows spectra obtained from 3830 ppm Cl and 0 ppm Cl concrete plates, using the NaI(Tl) spectrometer after a 30 min. irradiation, 10 min. delay and 30 min. count. In this case the 2.12, 2.17 and 2.24 MeV lines are not resolved and the 1.64 MeV line is only partially resolved from the 1.81 MeV line. Since the intensity ratio between the 2.75 MeV line and the 2.24 MeV first escape peak, and that between the 0.85 MeV and 2.12 MeV ^{56}Mn lines are both instrumental constants, it should be possible to subtract the two interferences from the combined 2.12, 2.17 and 2.24 MeV peak. Subsequent experiments proved this to be the case. It should also be possible to extract useful data from the 1.64 MeV line by stripping off the 1.81 line and its Compton continuum.

Figures 19-21 show prompt gamma spectra from a chlorine sample (PVC) and from pairs of 3830 ppm Cl and 0 ppm Cl test plates, using the Ge(Li) spectrometer, the 108 μg thermalized Cf^{252} source and the source-sample-detector configuration* shown in Figure 22. The large number of prompt gamma lines from chlorine is evident. The lead and hydrogen lines are in the background (excited in the shielding) and the iron lines arise from both the sample and the instrument structure. Although many spectral lines are present, only six components of the sample are excited significantly. In the energy region containing most chlorine lines (5.35 to 8.90 MeV), the only other contributions are from calcium (2 lines), iron (3 lines), possibly manganese (2 lines), and the background.

Figure 23 and 24 show corresponding prompt gamma spectra obtained with the NaI(Tl) spectrometer. The two most intense lines are at 5.60 MeV and 6.11 MeV, and these are resolved from other prompt gammas. However, much more chlorine signal is not resolved but could be utilized if a

*CSI Model 115 Neutron-Gamma Sample Analysis System,⁽⁴¹⁾ on loan from the U. S. Army Construction Engineering Research Lab.

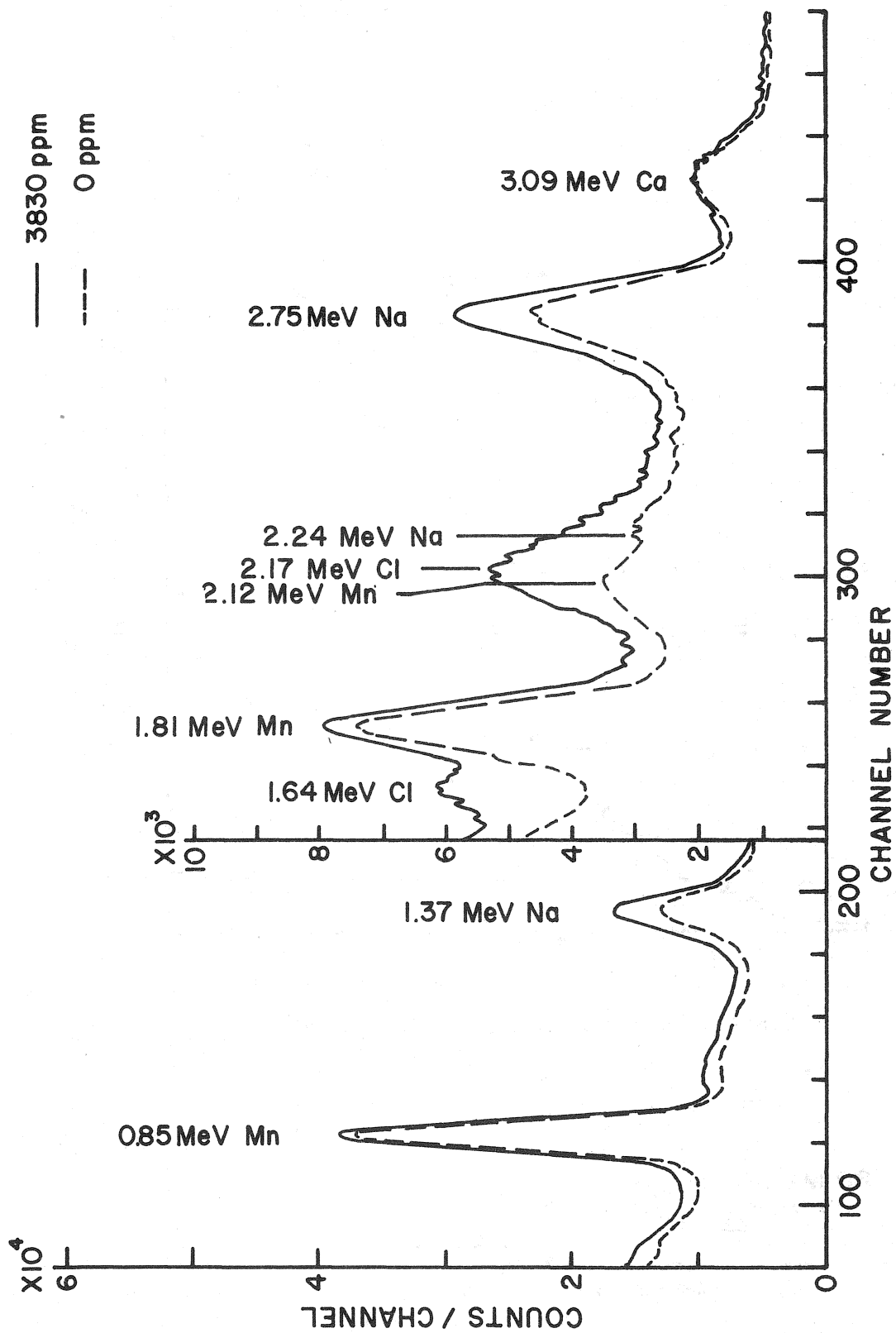


FIGURE 18. THERMAL NEUTRON ACTIVATION SPECTRA FROM CONCRETE TEST PLATES USING THE NaI(Tl) GAMMA-RAY SPECTROMETER

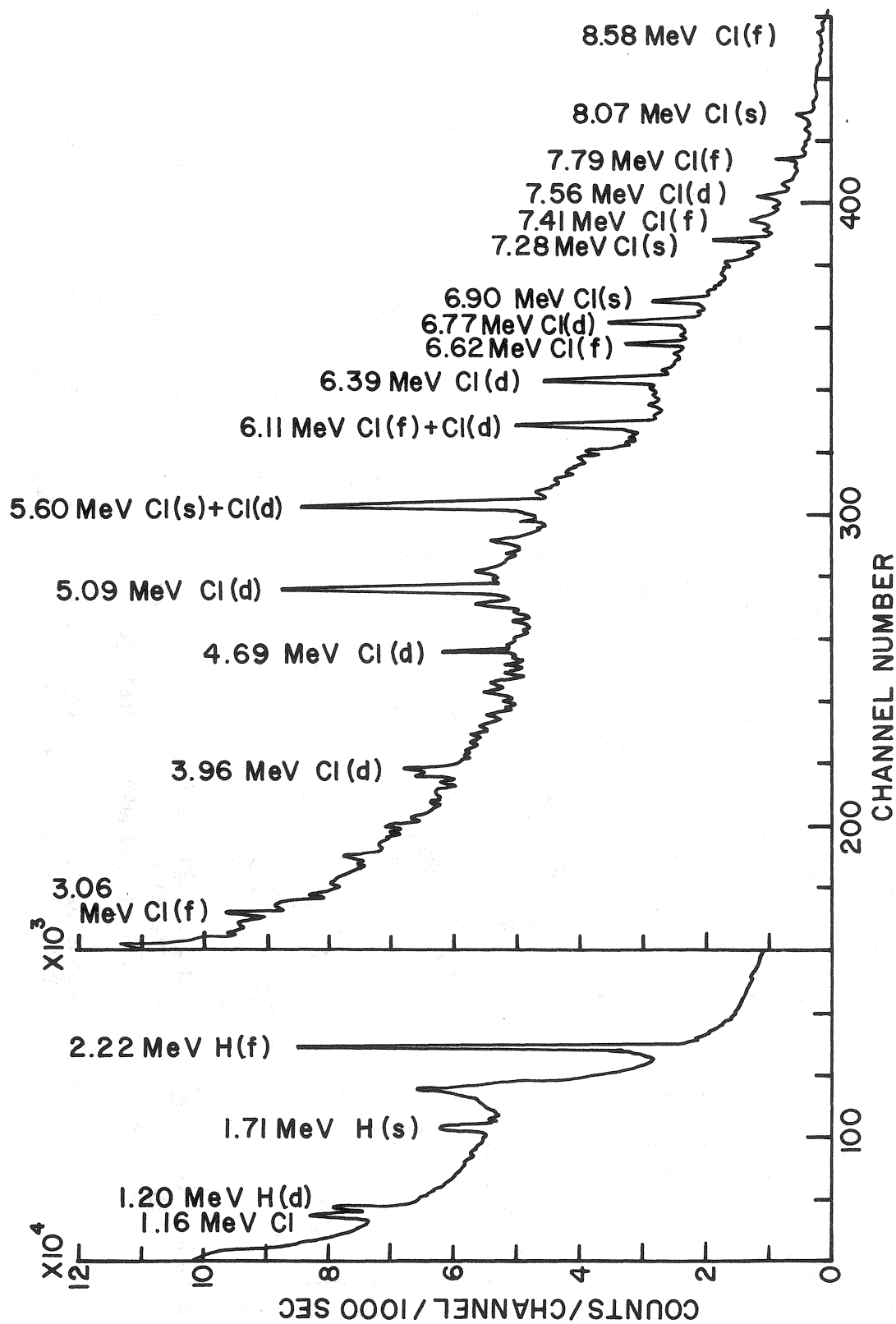


FIGURE 19. THERMAL NEUTRON-PROMPT GAMMA SPECTRUM FROM CHLORINE SAMPLE (PVC TILE) USING THE Ge(Li) SPECTROMETER

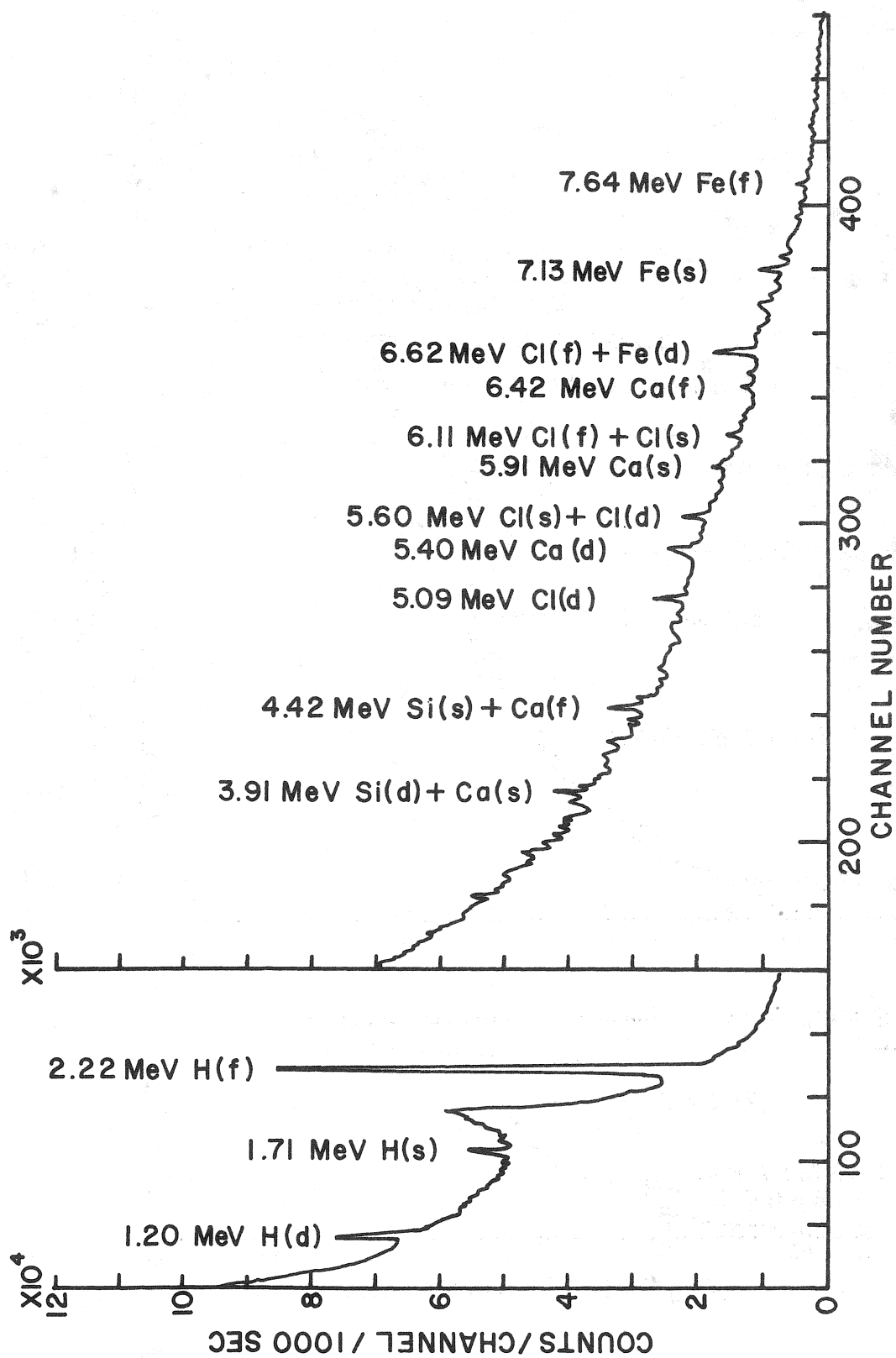


FIGURE 20. THERMAL NEUTRON-PROMPT GAMMA SPECTRUM FROM PAIR OF CONCRETE TEST PLATES CONTAINING 3830 PPM CHLORIDE USING THE Ge(11) SPECTROMETER

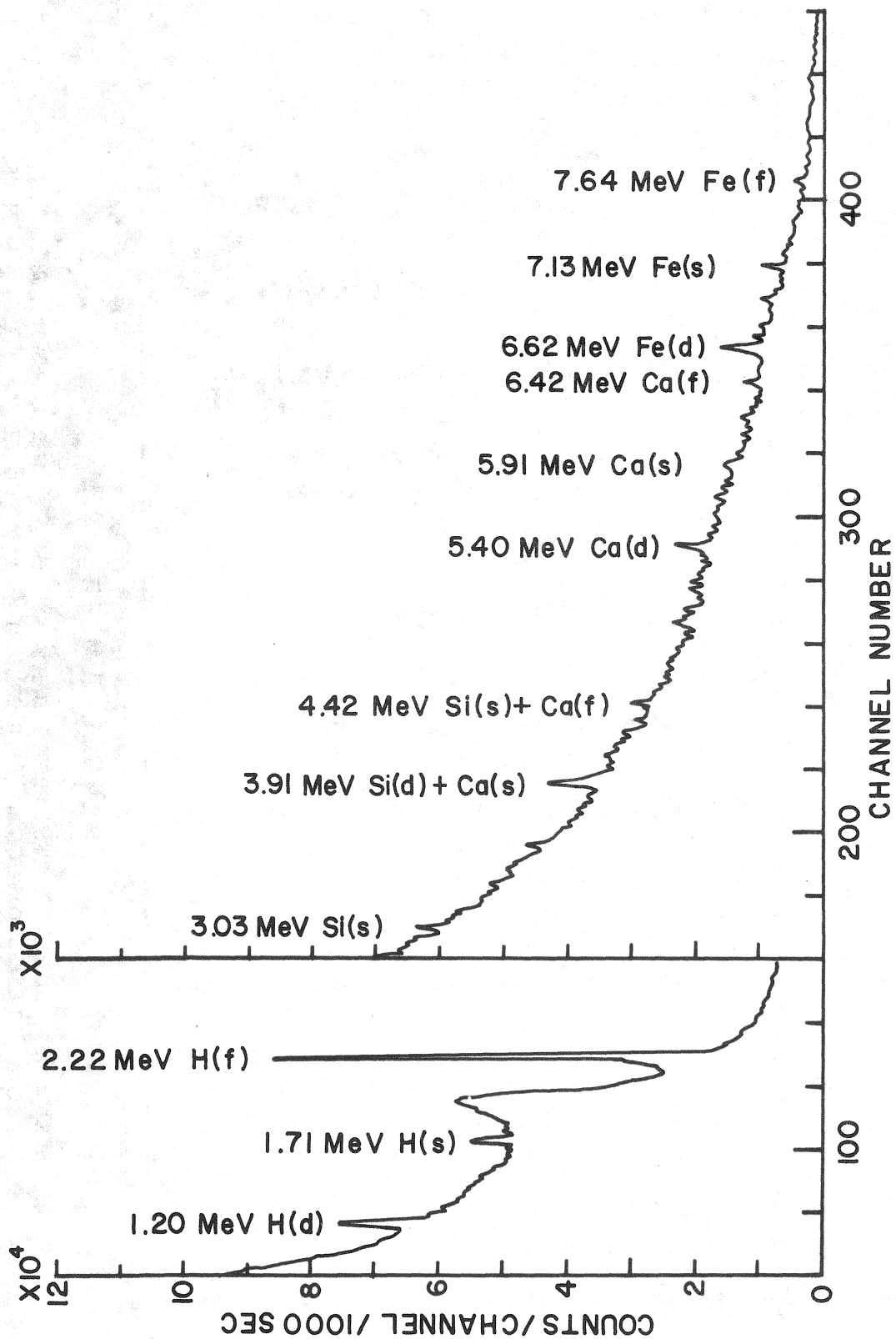


FIGURE 21. THERMAL NEUTRON-PROMPT GAMMA SPECTRUM FROM PAIR OF CONCRETE TEST PLATES CONTAINING ZERO CHLORIDE USING THE Ge(Li) SPECTROMETER

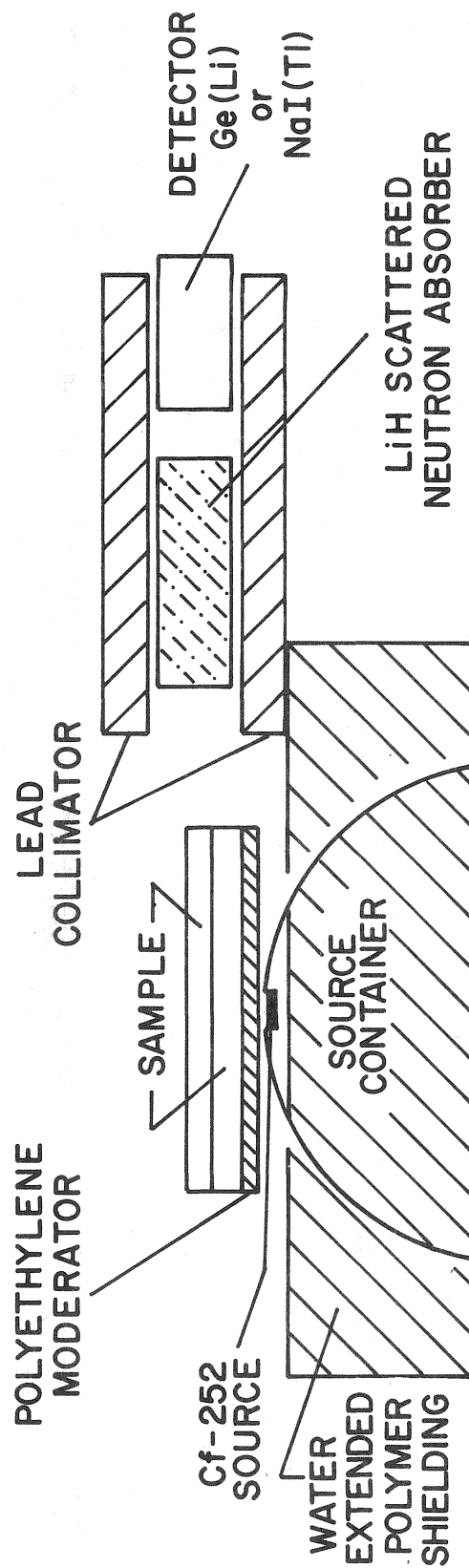


FIGURE 22. SOURCE-SAMPLE-DETECTOR CONFIGURATION FOR PRELIMINARY THERMAL NEUTRON-PROMPT GAMMA EXPERIMENTS

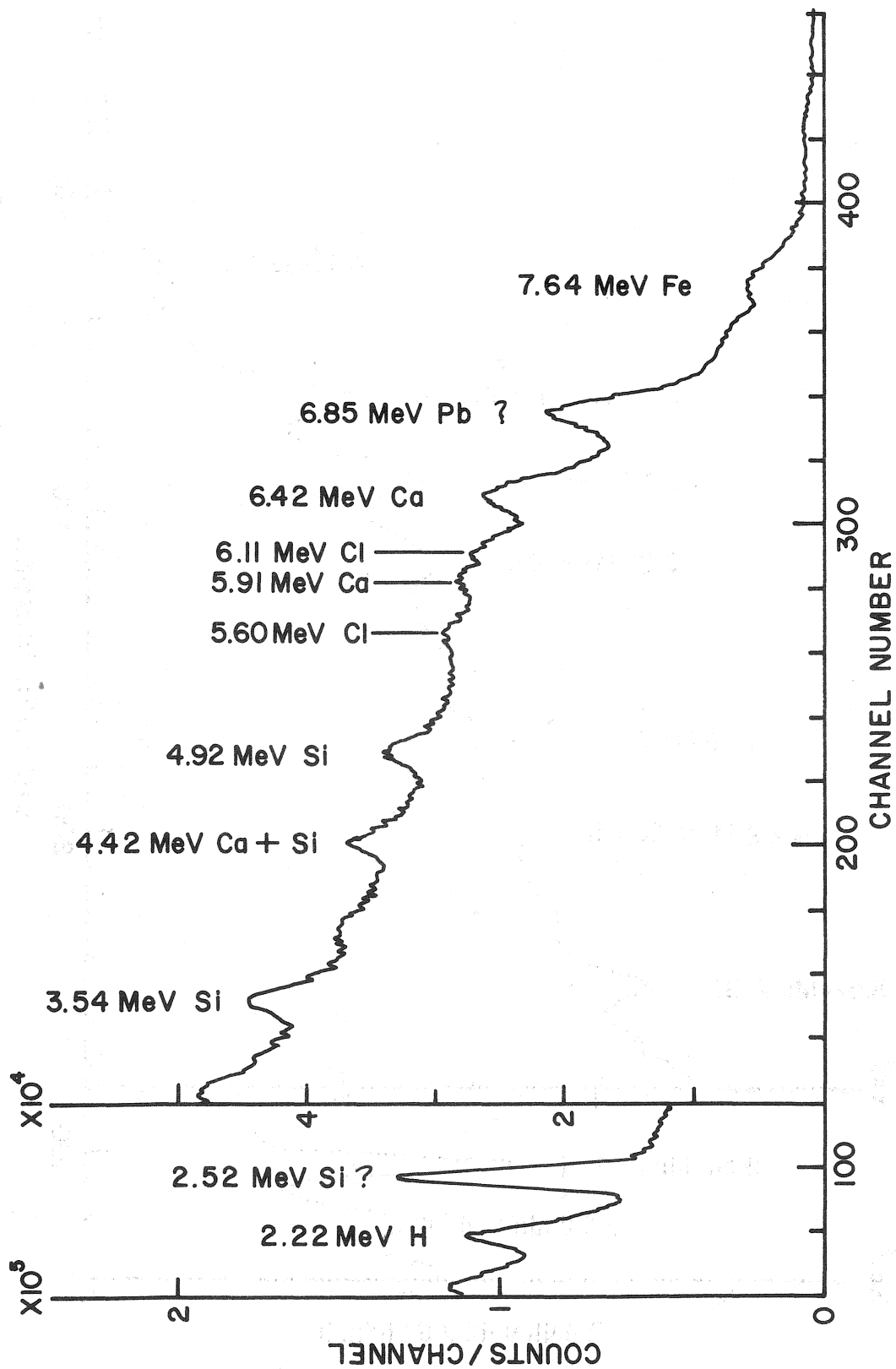


FIGURE 23. THERMAL NEUTRON-PROMPT GAMMA SPECTRUM FROM CONCRETE TEST PLATES CONTAINING 3830 PPM CHLORIDE USING THE NaI(Tl) DETECTOR

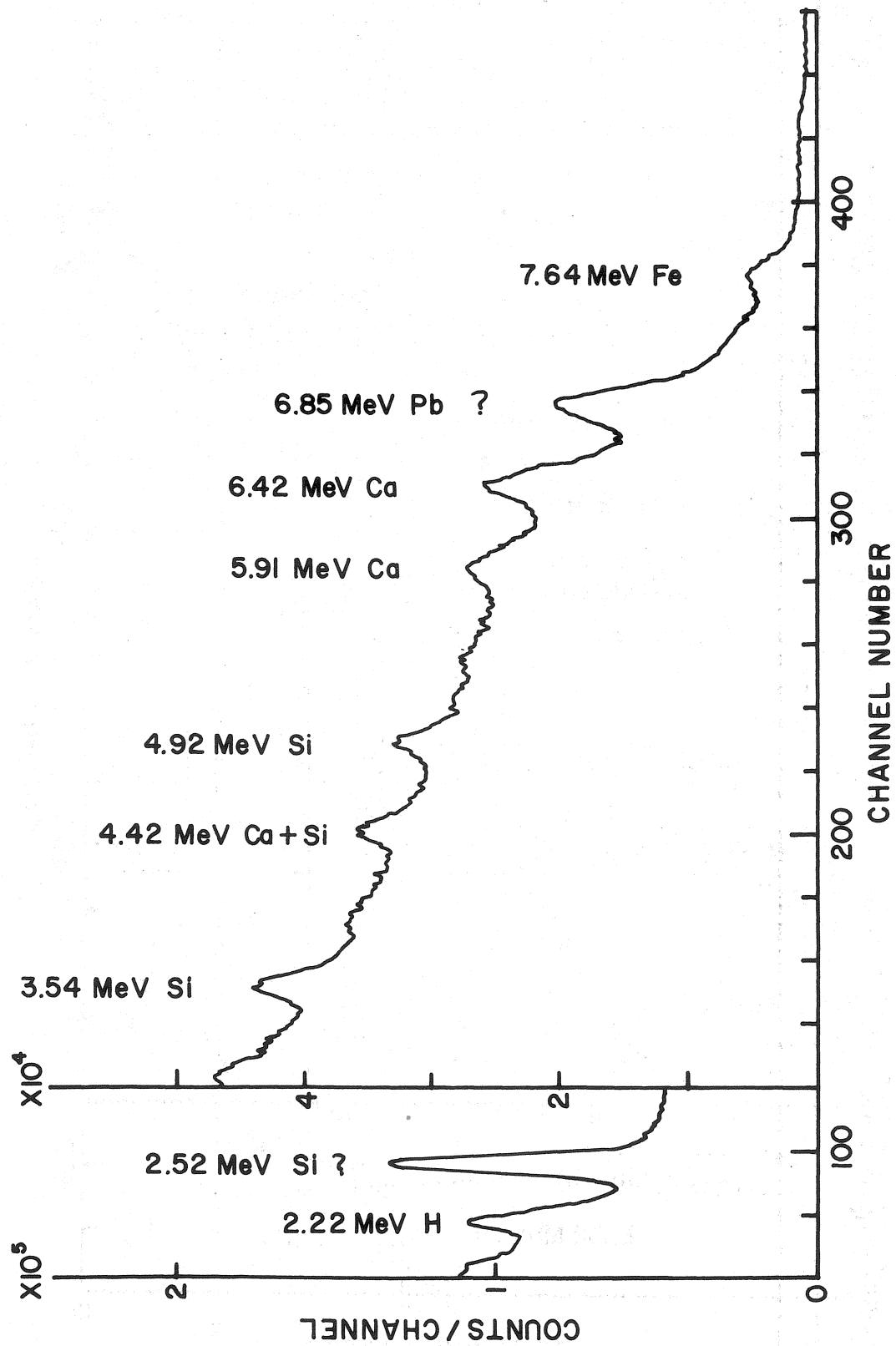


FIGURE 24. THERMAL NEUTRON-PROMPT GAMMA SPECTRUM FROM CONCRETE TEST PLATES CONTAINING ZERO CHLORIDE USING THE NaI(Tl) DETECTOR

spectrum stripping or fitting method of data analysis were to be used. It was found, by subtracting the 0 ppm spectrum from the 3830 ppm spectrum, that the total chlorine "signal" in the energy range 5.35 to 8.90 MeV was about 10 times the combined intensity of the two main peaks. Since there are only four or five components (Cl, Ca, Fe, possibly Mn, and background) in this spectral region, a spectrum fitting procedure would involve inverting only a 4 x 4 or 5 x 5 matrix, which can be done with relatively little computer memory in portable equipment.

Table 4 shows the preliminary sensitivities obtained for the prompt and activation gamma methods under comparable conditions for both the Ge(Li) and NaI(Tl) spectrometers. In each case the 108 μg ^{252}Cf source was used in the source-sample-detector configurations shown in Figures 16 and 19. For the prompt gamma method, a measurement time of 20 min. was used and each sample was a pair of plates containing equal chlorine concentrations. For the activation method, a stack of five test plates were irradiated for 35 mins., allowed to decay for 10 mins. and counted for 35 mins. The test plate nearest the source-detector was the only one that contained chloride. The other four were blanks, but contributed to the background and interferences, of course. The contributions of the 2.24 MeV ^{24}Na escape peak and the 2.12 MeV ^{56}Mn peak were subtracted as follows. The 2.24 MeV to 2.75 MeV and 2.12 MeV to 0.84 MeV gamma-ray intensity ratios, which are instrumental constants, were measured in separate experiments. Then in the measurement proper the 2.75 and 0.84 MeV gamma-ray intensities were monitored and the interferences calculated by multiplying by the above intensity ratios. The magnitudes of the interferences are equivalent to about 3000 ppm Cl for Na and about 2500 ppm Cl for Mn. However, the Na and Mn peaks can be measured with an accuracy of a few tenths of one percent.

The main source of error is counting statistics. The standard deviation due to counting statistics was calculated from the measured counts in the signal peak and associated background using equation 1.

It is seen that the sensitivities obtained in both methods using the NaI(Tl) spectrometer are better than those using the Ge(Li) spectrometer, even though a smaller number of gamma peaks are resolved

TABLE 4. COMPARISON OF SENSITIVITIES OBTAINED USING NaI(Tl) AND Ge(Li) SPECTROMETERS FOR PROMPT AND ACTIVATION GAMMA METHODS

| Method Spectrometer | Prompt Gamma | Activation Gamma |
|------------------------|-----------------------|-----------------------|
| NaI(Tl) | 126 ppm ^{a)} | 73 ppm ^{c)} |
| Ge(Li) | 589 ppm ^{b)} | 168 ppm ^{d)} |

Sensitivity defined as 1 std. dev. on counting statistics at zero chloride.

- Notes:
- a) The two cleanly resolved gamma rays, at 5.60 and 6.11 MeV, were integrated.
 - b) The three most prominent gamma rays, at 5.09, 5.60 and 5.11 MeV, were integrated.
 - c) 2.17 MeV gamma ray used, interference due to Mn and Na taken into account.
 - d) 1.64 and 2.17 MeV gamma rays used.

and integrated in the former case. Accordingly the NaI(Tl) spectrometer is the preferred one for the candidate field instrumentation.

5.3 Total Chloride Determination

The feasibility of both the prompt and activation gamma-ray methods was investigated for total chloride determination 1) in samples taken from drillings and 2) in stacks of test plates having a constant chloride depth distribution.

5.3.1 Analysis of Pulverized Drill Hole Samples

The weight of powdered concrete from a 0.5 in. (1.3 cm) depth increment of a 1-3/4 in. (4.5 cm) dia. hole is about 45 g. The neutron and gamma absorption effects in such samples are negligible (in contrast to XRF) and each part of the sample is analyzed with equal sensitivity. Thus, as long as the sample is representative, the analysis suffers negligible error due to heterogeneity. The measured gamma-ray intensity is proportional to element weight, rather than concentration, so the samples must have known or constant weight. The physical form of the samples is not important as long as the sample shape and irradiation and counting geometries are kept constant.

Powder samples from the concrete test plates (see Section 3.1) were pressed into 2-1/4 in. (5.7 cm) dia. x 1/2 in. (1.3 cm) thick briquettes, for ease of handling, and presented either to the thermal neutron activation apparatus (Figure 17) or the thermal neutron prompt gamma apparatus (Figure 22).

The prompt-gamma method proved too insensitive for such small samples and was ruled out. In a 2000 second count it was not possible to distinguish the 3830 ppm Cl sample from the 0 ppm Cl sample.

The activation method yielded satisfactory results. Figure 25 shows a calibration curve of net 2.17 MeV Cl gamma-ray counts/g sample vs ppm Cl obtained for 40 minute irradiation, 10 minute delay and 50 minute count times. Corrections for Na and Mn interferences were made as described in Section 5.2.3. The standard deviation due to counting statistics was 186 ppm Cl.

If the sample weight were increased to 300 g (a 1 in. (2.5 cm) depth increment of a 3 in. (8 cm) dia. drill hole would yield this sample

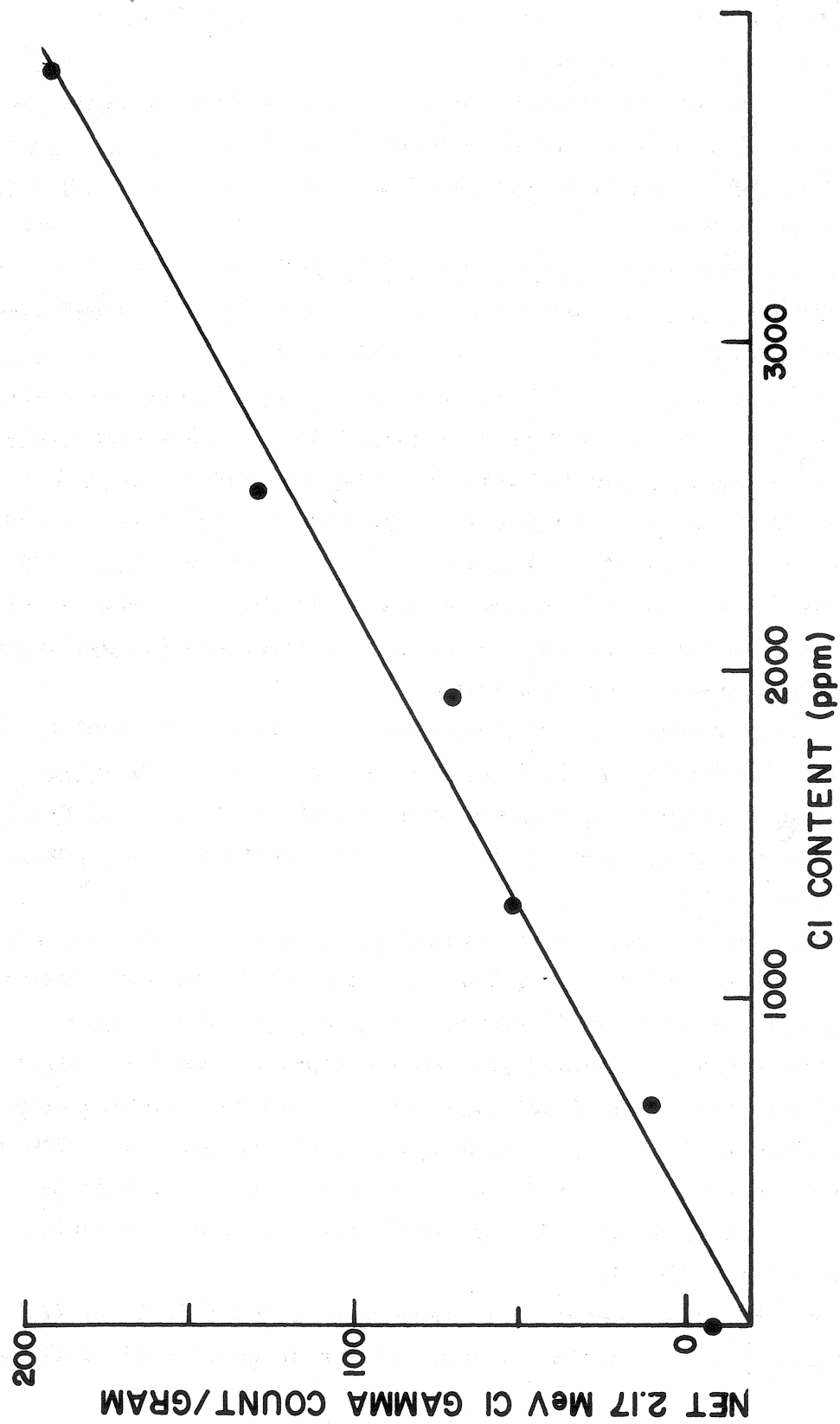


FIGURE 25. CALIBRATION CURVE FOR THERMAL NEUTRON ACTIVATION
ANALYSIS OF PRESSED POWDER BRIQUETTES

weight) and the source strength to 400 μg (from 108 μg), calculations based on Equations 1 and 3 show that the statistical error could be reduced to about 100 ppm Cl in an irradiation time of 10 mins., delay time of 5 mins., and count time of 10 mins. Inclusion of the 1.64 MeV Cl gamma ray would further improve the sensitivity by about 50 percent. Bearing in mind that one sample can be irradiated while another is being counted, it is seen that the sensitivity and measurement time of thermal neutron activation for small sample analysis can be superior to that of X-ray fluorescence. Also neutron activation analysis would not suffer from heterogeneity errors.

5.3.2 Analysis of Stacks of Test Plates

Both the prompt and activation gamma methods are feasible but have different features. Figure 26 shows the calibration curve obtained for the prompt gamma method on an array of ten plates stacked five deep and two abreast, as per the optimized prompt gamma-ray configuration shown in Figure 37 and described in Section 5.5.3. The net intensity of the 5.60 and 6.11 MeV chlorine gammas is plotted against total chloride content. The concentration distributions of the stacks were chosen to approximate the gradient measured by Clear.⁽⁷⁾ They are listed in Table 5. The sensitivity (i.e., one standard deviation due to counting statistics) obtained in a 2000 sec. count using the 108 μg ^{252}Cf source is 198 ppm. This would be improved by a factor of two by using a 400 μg source. The spectrum fitting method (Section 5.2.3) could improve the sensitivity by a further factor of three.

Placing plates containing reinforcing bars in positions 2 or 3 gave ~ 10 percent enhancement of the signal due to the increase in intensity of prompt gamma rays from iron that are unresolved from the Cl gammas. This interference can be removed by monitoring a resolved Fe prompt gamma peak (such as the 7.64 MeV peak) or by using a spectrum fitting technique.

Figure 27 shows a corresponding calibration curve obtained for thermal neutron activation using the apparatus sketched in Figure 17. The sensitivity obtained in a 30 min. activation, 10 min. delay and 30 min. count using the 108 μg source is 80 ppm Cl, based on the total chloride content of the stack. No effect was seen of placing plates

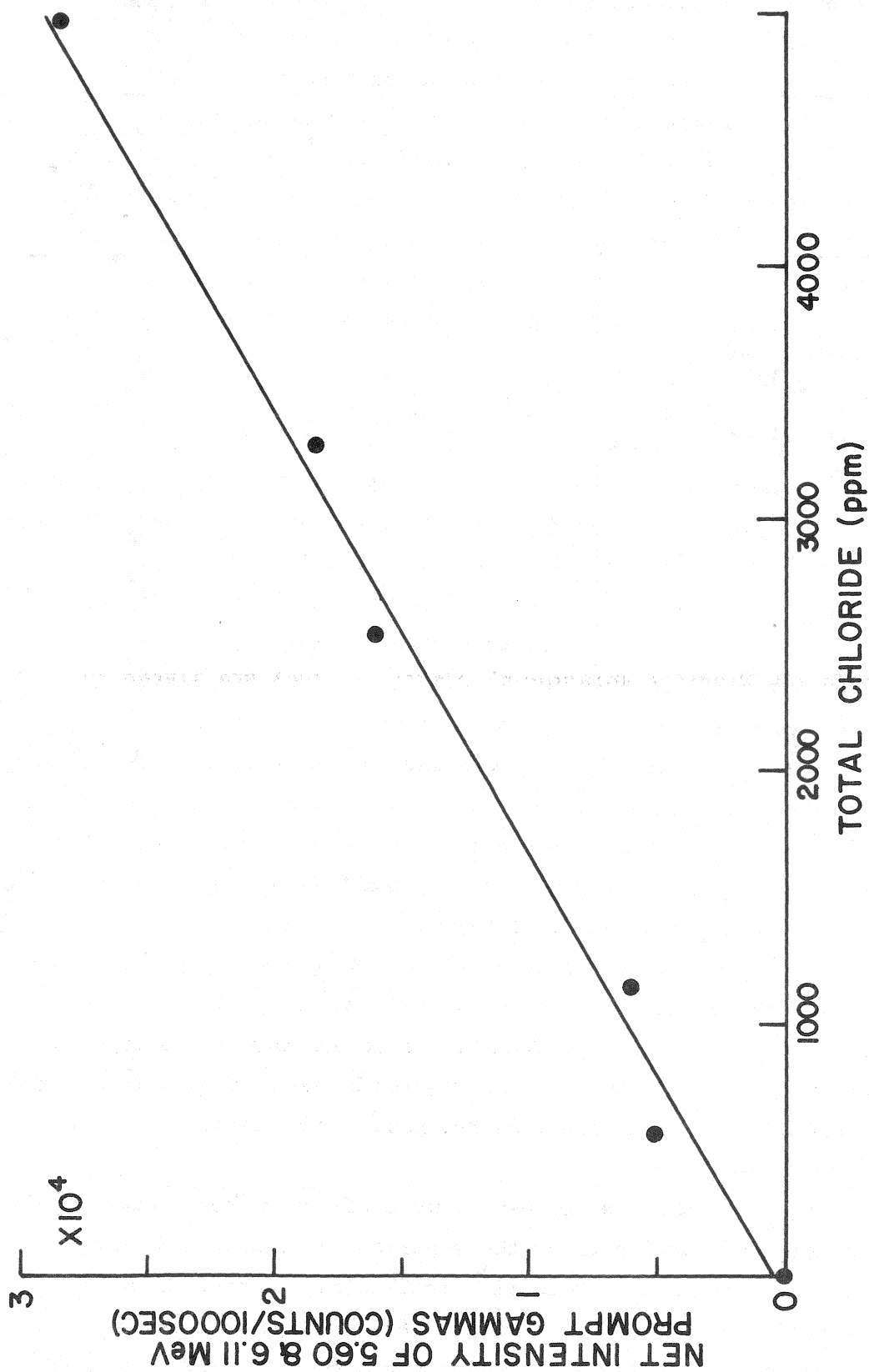


FIGURE 26. CALIBRATION CURVE FOR THERMAL NEUTRON-PROMPT GAMMA ANALYSIS OF A STACK OF CONCRETE TEST PLATES

TABLE 5. CONCENTRATION DISTRIBUTION OF THE CONCRETE TEST SPECIMENS USED FOR TOTAL CHLORIDE SENSITIVITY TESTS

| Sample No. | Plate No. Total Chloride | ppm Cl | | | | |
|------------|-----------------------------|-----------------|-----|-----|---|---|
| | | 1 ^{a)} | 2 | 3 | 4 | 5 |
| 1 | 4978 | 3830 | 893 | 255 | 0 | 0 |
| 2 | 3316 | 2550 | 638 | 128 | 0 | 0 |
| 3 | 2548 | 1910 | 510 | 128 | 0 | 0 |
| 4 | 1148 | 893 | 255 | 0 | 0 | 0 |
| 5 | 638 | 510 | 128 | 0 | 0 | 0 |
| 6 | 0 | 0 | 0 | 0 | 0 | 0 |

a) Nearest the source-detector.

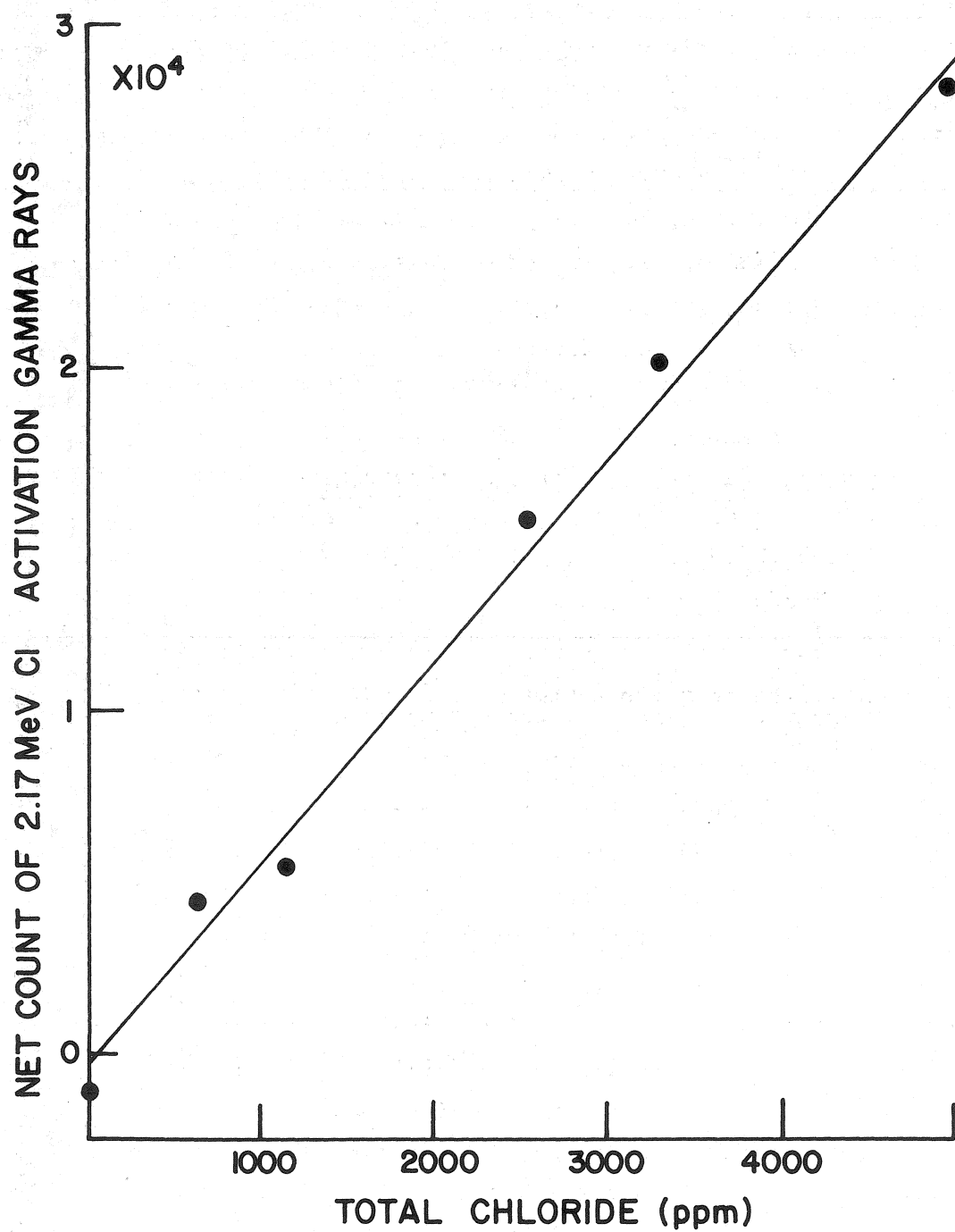


FIGURE 27. CALIBRATION CURVE FOR THERMAL NEUTRON ACTIVATION ANALYSIS OF A STACK OF CONCRETE TEST PLATES

containing reinforcing bars at the second or third position. This is not surprising since the depth response of the activation method falls off very rapidly (see Section 5.5.2, Figure 36).

If the chlorine signal is plotted against concentration of the top plate only, the calibration curve looks very similar and the sensitivity becomes 60 ppm Cl. This sensitivity compares with the data in Table 4. This is further evidence that most of the thermal neutron activation signal comes from the first inch of concrete sample.

The sensitivity of the neutron activation method can be improved by increasing the source strength (as in Section 5.3.1) and the detector area. The use of an 8 in. (20 cm) dia. x 4 in. (10 cm) thick NaI(Tl) detector would increase the signal by a factor of 2.56 and the sensitivity by $\sqrt{2.56}$ or 1.6. This could be traded for a proportionate reduction in measurement time.

5.4 Chloride Gradient in a Single Measurement

The methods investigated for monitoring chloride at the depth of the reinforcing bars were: 1) filtering or tailoring the incident neutron spectrum to change the activation or prompt gamma depth distribution; 2) collimating the detector, or using two collimated detectors, to define the volume viewed; and 3) making two measurements using methods having different depth responses and solving a pair of simultaneous equations. In this section the results of methods (1) and (2), both of which failed, are reported.

5.4.1 Neutron Spectrum Tailoring

The thermalization of fast neutrons occurs through a succession of "billiard-ball" type collisions with atoms, the neutron losing a fraction of its energy at each collision and eventually coming to thermal equilibrium with its surroundings. Since the neutron has a mass approximately equal to that of a hydrogen atom, it can lose half its energy per collision with hydrogen. Thus, approximately 27 collisions are required for a several MeV neutron to reach thermal energy (0.025 eV).

The mean free path of neutrons between collisions in a hydrogenous material, such as paraffin, polyethylene, or water, is of the order of 1 cm and, since the neutron changes its direction at each collision, a large fraction of fast neutrons incident on such a material will be thermalized in

a few cm. A maximum in the thermal neutron flux produced from incident fast neutrons can occur at some depth in the material. In non-hydrogenous material the energy loss per collision is much less, so thermalization requires greater distances. The rate of thermalization depends strongly on the hydrogen content of a given material.

Experiments were performed to measure the thermal neutron flux gradient in stacks of 1 in. (2.5 cm) thick concrete plates irradiated on one side by a fast neutron source (^{252}Cf). Weighed (~ 5 g) packs of 1 mil (25 micron) aluminum foil* were placed between each plate for 5 mins., removed, and the thermal neutron induced ^{28}Al activity measured on the NaI(Tl) spectrometer by counting the 1.78 MeV gamma rays for 5 mins. These experiments were repeated using different degrees of source moderation (i.e., prethermalization), in the form of increasing thicknesses of polyethylene sheet. The first objective was to determine if a thermal neutron flux peak existed in the concrete and, if so, at what depth. As shown in Figure 28, a significant thermal peak does not occur. In fact, for moderator thicknesses greater than 0.5 in. (1.3 cm), the thermal neutron flux distribution follows the inverse square law with distance from the source. This, of course, implies negligible absorption of thermal neutrons in distances of the order of a few inches in dry concrete.

This type of experiment also yields information on moderator thicknesses for maximum thermal neutron flux from a ^{252}Cf source, using the "semi-infinite plane" type source-sample geometry required by this project. Note that, in the above experiment, the source-sample distance was held constant (to obtain unbiased flux gradients) and the thermal flux for a 2 in. (5 cm) moderator thickness is greater than that for a 1 in. (2.5 cm) thickness. However, if the source-to-detector distance is always made equal to the moderator thickness as it would be in a practical gauge, the maximum thermal flux in the sample occurs for a 1 in. (2.5 cm) moderator thickness. This maximum is approximately double that for the 1 in. (2.5 cm) thick moderator, shown in Figure 28, at all points on the curve.

*Available at grocery stores.

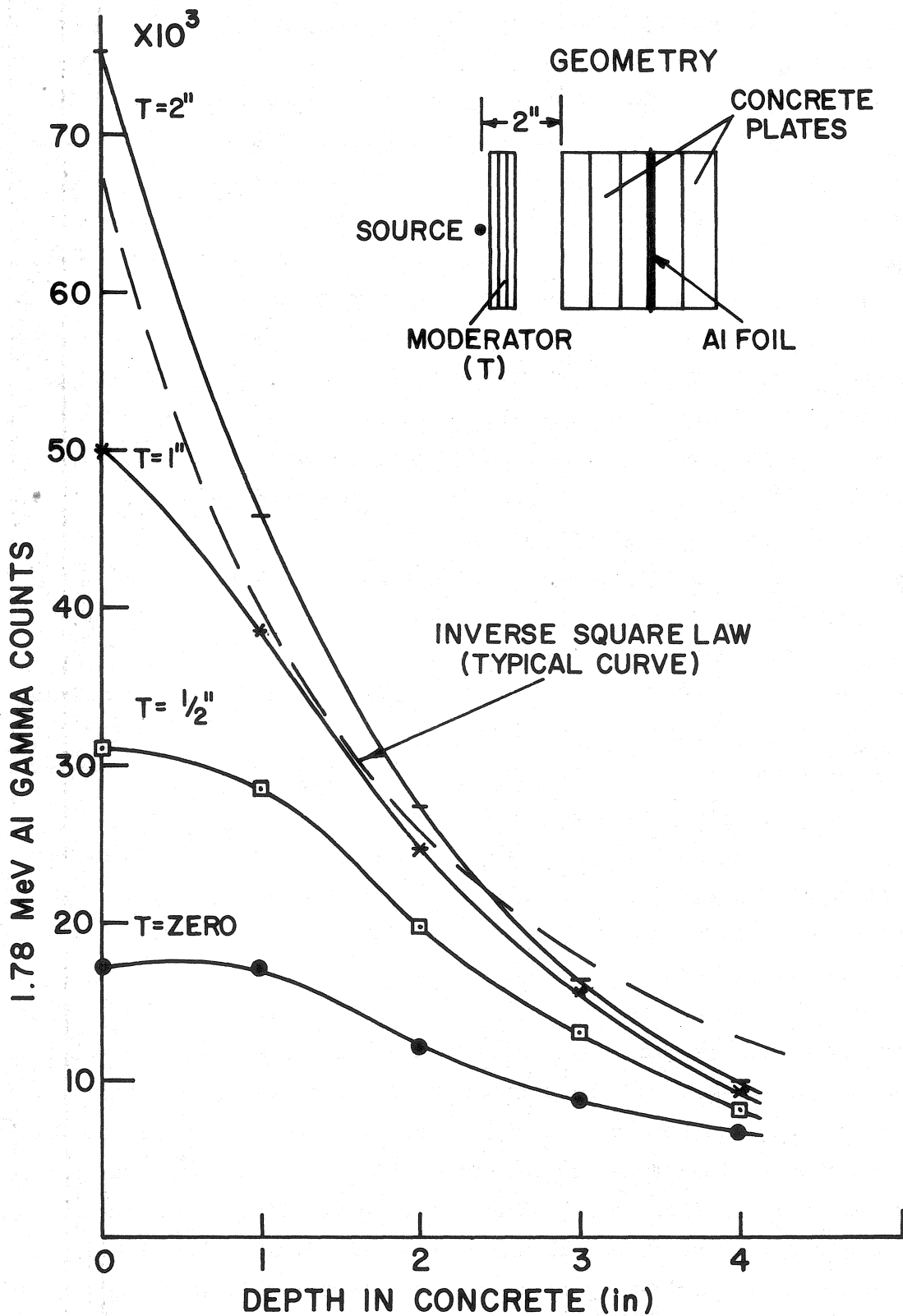


FIGURE 28. THERMAL NEUTRON FLUX GRADIENT IN CONCRETE AS A FUNCTION OF MODERATOR THICKNESS FOR ^{252}Cf SOURCE (1" = 2.54 cm)

As a result of this experiment, we decided to abandon the idea of using neutron spectrum tailoring to provide depth distribution information and to concentrate on maximizing the available thermal neutron flux. This alleviates a potential problem of interference from variations in moisture content of the concrete. Since water affects the rate of thermalization, both the location and intensity of any thermal flux peak in the sample would be a function of moisture content. If fully thermalized neutrons are used, the potential interference of water on the chloride determination is reduced considerably. The second result is to provide a preliminary optimization of thermal flux output. The 1 in. (2.5 cm) moderator thickness was used in all the feasibility tests reported herein. Further optimization is possible, including incorporation of neutron reflectors. This will be done at the instrument design phase.

5.4.2 Detector Collimation

Collimation is a means of defining a specific volume of sample to be irradiated (source collimation) and/or "seen" by the detector (detector collimation). This is done at the price of considerable loss of signal and we know from the results of Section 5.3 that the neutron-gamma methods are barely sensitive enough without any such losses. Since thermal neutrons are transported through the sample by diffusion, collimation of the source would be pointless.

The gradient of the induced chlorine signal, both for prompt and activation gamma rays, is precisely equal to that of the thermal neutron flux, which we have just seen follows the inverse square law for a point isotropic source.

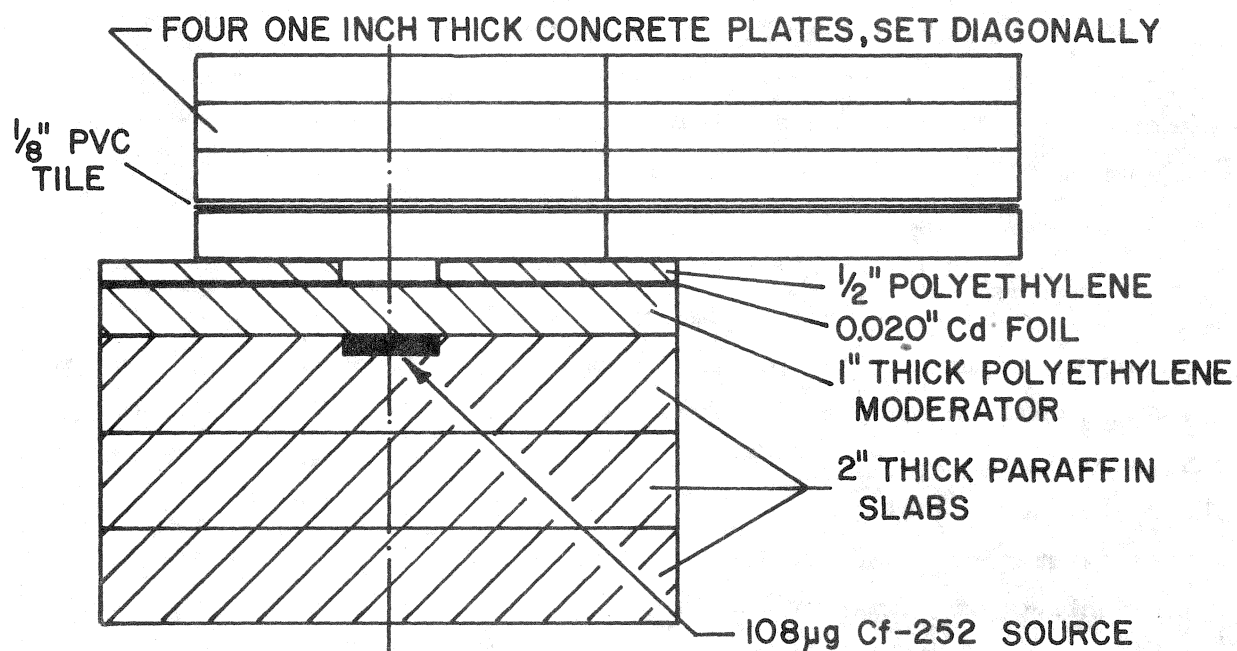
The objectives of detector collimation are 1) to discriminate against chlorine gammas from the surface layers of sample (say the first inch) and 2) to maximize the detector response to the depth increment 1 to 3 inches where the reinforcing mat is likely to be. According to Clear,⁽⁷⁾ the chloride concentration falls off at the rate of a factor of about 4 per inch (1.5 per cm) (see Table 5), with the possibility of surface washout reducing the concentration to near zero in the first 1/4 inch (0.6 cm) or so. Thus the discriminating power of the detector collimator against either high or low surface chloride concentrations must be at least an order of

magnitude. If this is achieved, then a single measurement could be made yielding chloride content in some specified depth range (e.g., 1.5 to 2.5 inches (3.8 to 6.4 cm)), depending on the depth response of the instrument.

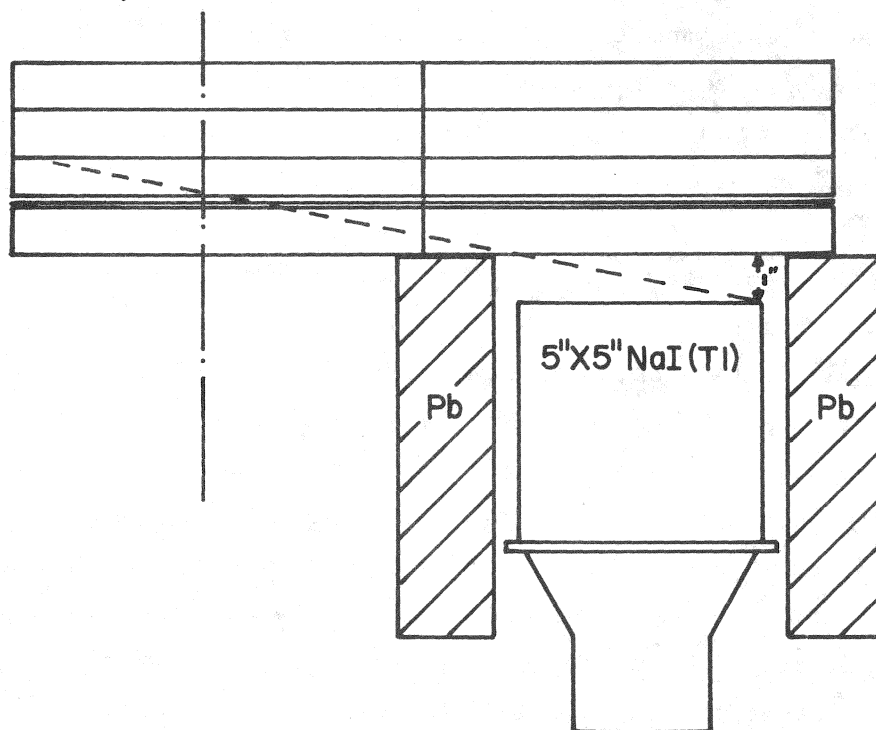
Using the irradiation and counting configurations sketched in Figure 29, thermal neutron activation data were obtained from 1/8 in. (3 mm) thick x 1 ft. (30.5 cm) square PVC tiles placed between the concrete plates. One PVC tile contains 265 mg/cm² Cl, which is equivalent to 44170 ppm Cl in a 1 in. (2.5 cm) thick concrete specimen. The tiles were placed at assigned positions for irradiation and then transferred to the corresponding positions in the counting stack. The concrete plates were not moved. Thus, strong chlorine signals could be obtained without the need to measure correction factors due to the long-lived sodium and manganese. The distance of the detector from the sample surface was varied, as was the distance between the axis of the detector and sample area directly above the source. Also data was obtained with and without the cadmium foil thermal neutron absorber in place. The purpose of the cadmium foil was to limit the surface area irradiated and so enhance the discrimination power of the configuration.

A number of combinations of the above parameters were tried. In no case were we able to obtain enough discrimination against the surface chloride without losing too much signal. Typical results using the 108 µg ²⁵²Cf source; 20 min. irradiation, 0.5 min. delay and 500 sec. count times; and integrating both the 1.64 and 2.17 MeV gamma rays, were as follows: For a detector distance of 9 in. (23 cm) from the point of irradiation and 1 in. (2.5 cm) from the sample surface, the counts for a PVC tile on the sample surface and one 2 in. (5 cm) deep were approximately equal, the values being 1500 with a statistical counting error of 100. This error represents 3000 ppm Cl. For the detector placed over the point of irradiation the total signal was 27000 ± 316 for the surface tile and 2300 ± 200 for the tile at 2 in. (5 cm) depth.

A limited number of similar experiments were performed to test the prompt gamma method, with similar negative results. The source-sample-detector configuration used was similar to that shown in Figure 37.



a) IRRADIATION GEOMETRY



b) COUNTING GEOMETRY

FIGURE 29. SKETCH OF IRRADIATION AND COUNTING GEOMETRIES USED FOR DETECTOR COLLIMATION STUDIES
(1" = 2.54 cm)

5.4.3 Detector Collimation with Coincidence Counting

Chlorine 38 emits its two gamma energies, 1.64 and 2.17 MeV, in coincidence, with equal intensities. A study of the prompt gamma emissions from ^{35}Cl and ^{37}Cl showed that ^{35}Cl emits several possible coincident gamma-ray pairs.

Coincidence counting of such gamma-ray pairs using two detectors collimated to view a common volume of sample (see Figure 30) offers the possibility of depth discrimination together with suppression of background as well as interfering gamma-ray peaks. A block diagram of the electronics used for the experiments described below is shown in Figure 31. The multichannel analyzer is not necessary in the final instrument, and so the electronics required for coincidence counting can be simpler than that required for gamma-ray spectrometry.

In operation one detector is set with its energy window bracketing one of the gamma rays while the second detector brackets the other. The slow coincidence module only allows a count to be recorded if pulses arrive from each detector within a certain time interval (of the order of one millisecond). This interval can be preset at the maximum value above which the accidental coincidence rate contributes an unacceptable background. If the detectors are collimated to view a common volume of sample, the signal is also restricted to those coincident gamma rays arriving from that volume. Figure 32 shows the gamma-ray spectrum from one of the detectors when it is "gated" in coincidence with the 2.17 MeV gamma-ray window of the second detector. The samples were either a single 2550 ppm Cl concrete plate or a 0 ppm plate, and were counted for 15 min. after a 15 min. irradiation, 1 min. delay sequence, using the 108 μg ^{252}Cf source with moderator. The geometry for this measurement was not that of Figure 30, but the samples were sandwiched between the two detectors placed face to face. Comparison with an ungated spectrum (see, for example, Figures 15 and 18) shows that the intense 1.78 MeV gamma peak and its associated Compton background are eliminated, together with most of the other interfering radiation. The 2.17 MeV chlorine gamma ray does not appear because it cannot be in coincidence with itself. The 1.64 MeV chlorine gamma ray is cleanly resolved. A peak appears at 0.85 MeV because the 0.85 and

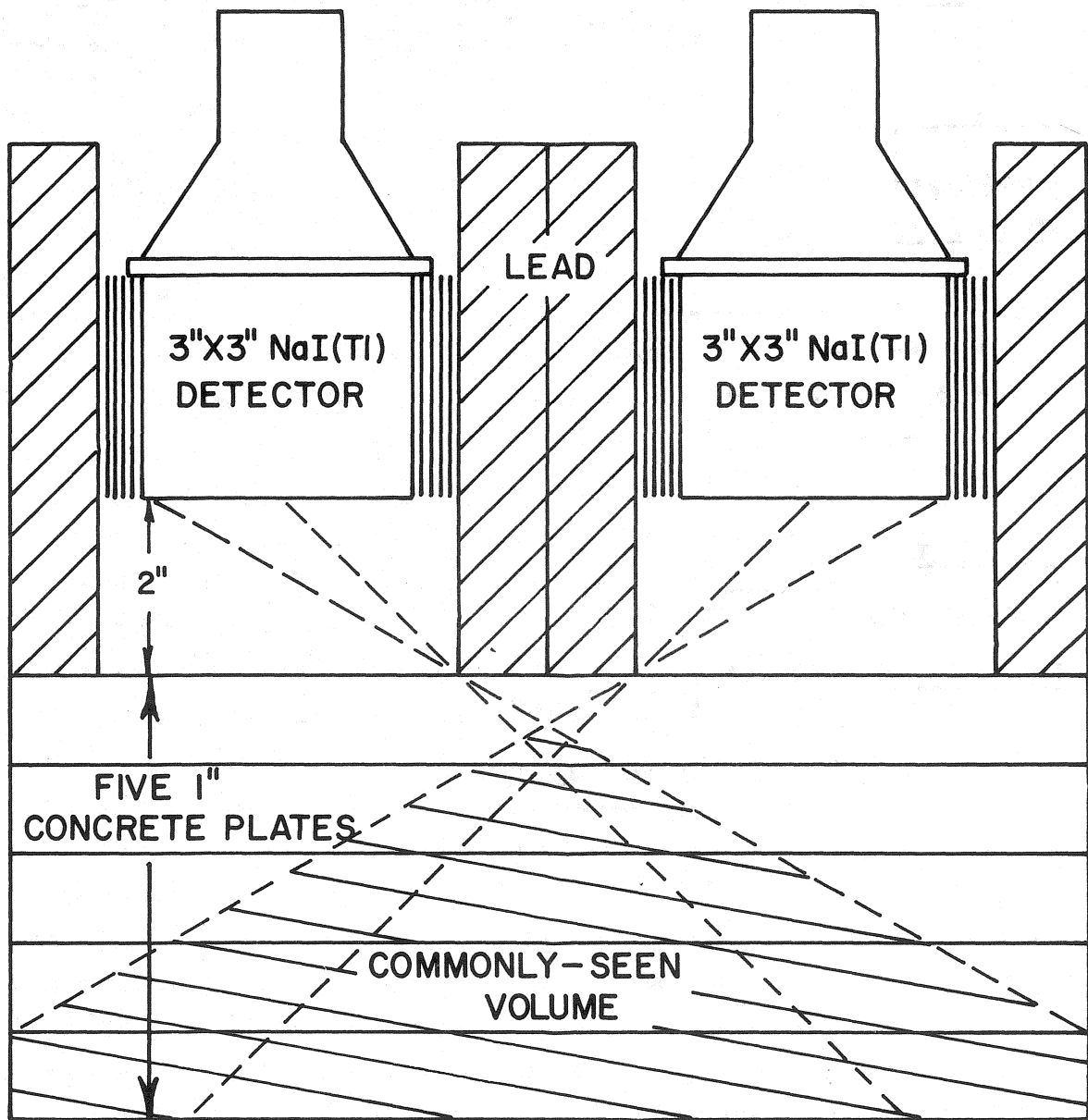


FIGURE 30. SKETCH OF TWO-DETECTOR GEOMETRY USED FOR COINCIDENCE COUNTING MEASUREMENTS
(1" = 2.54 cm)

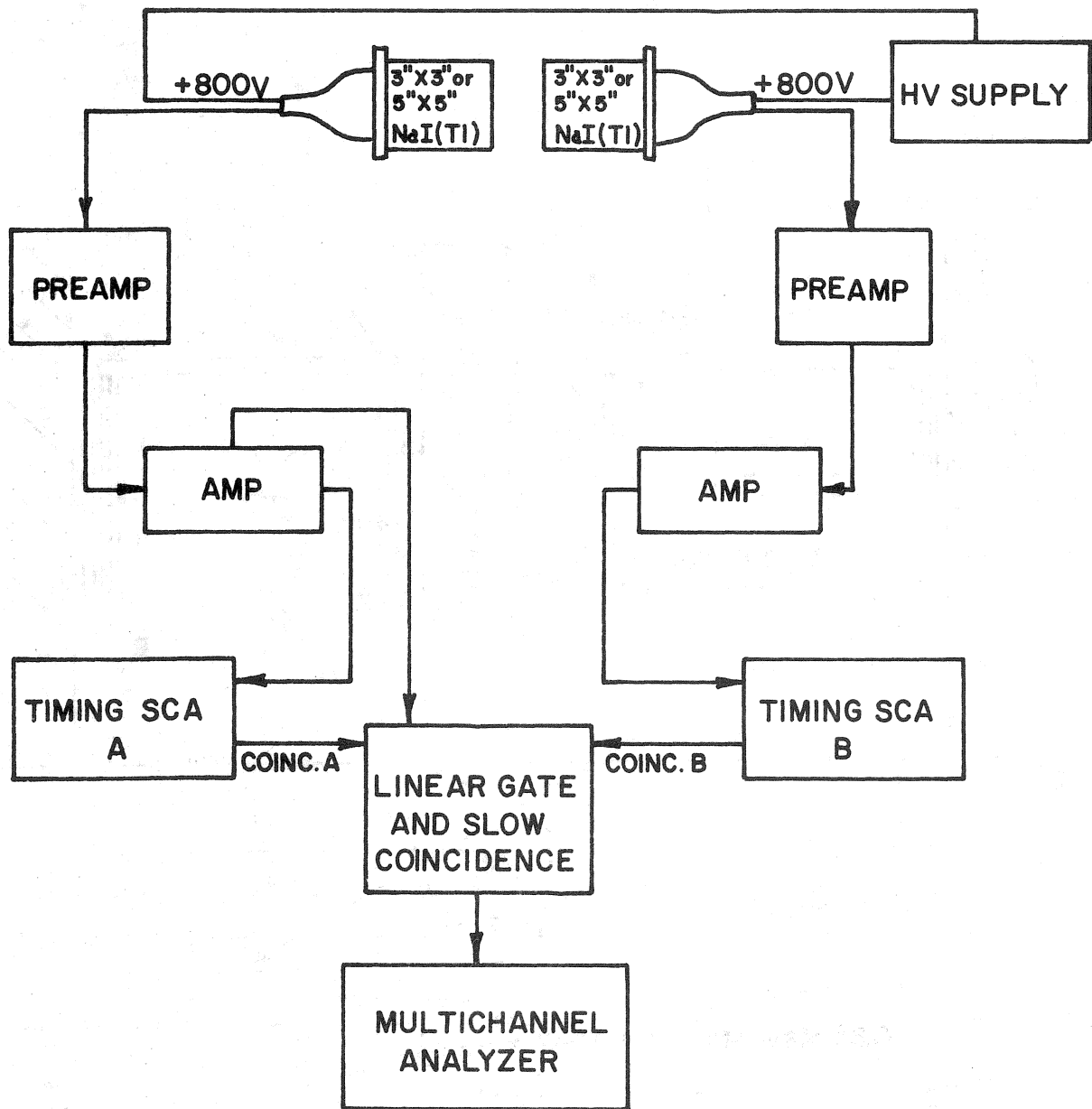


FIGURE 31. COINCIDENCE COUNTING SYSTEM - ELECTRONIC SCHEMATIC
(1" = 2.54 cm)

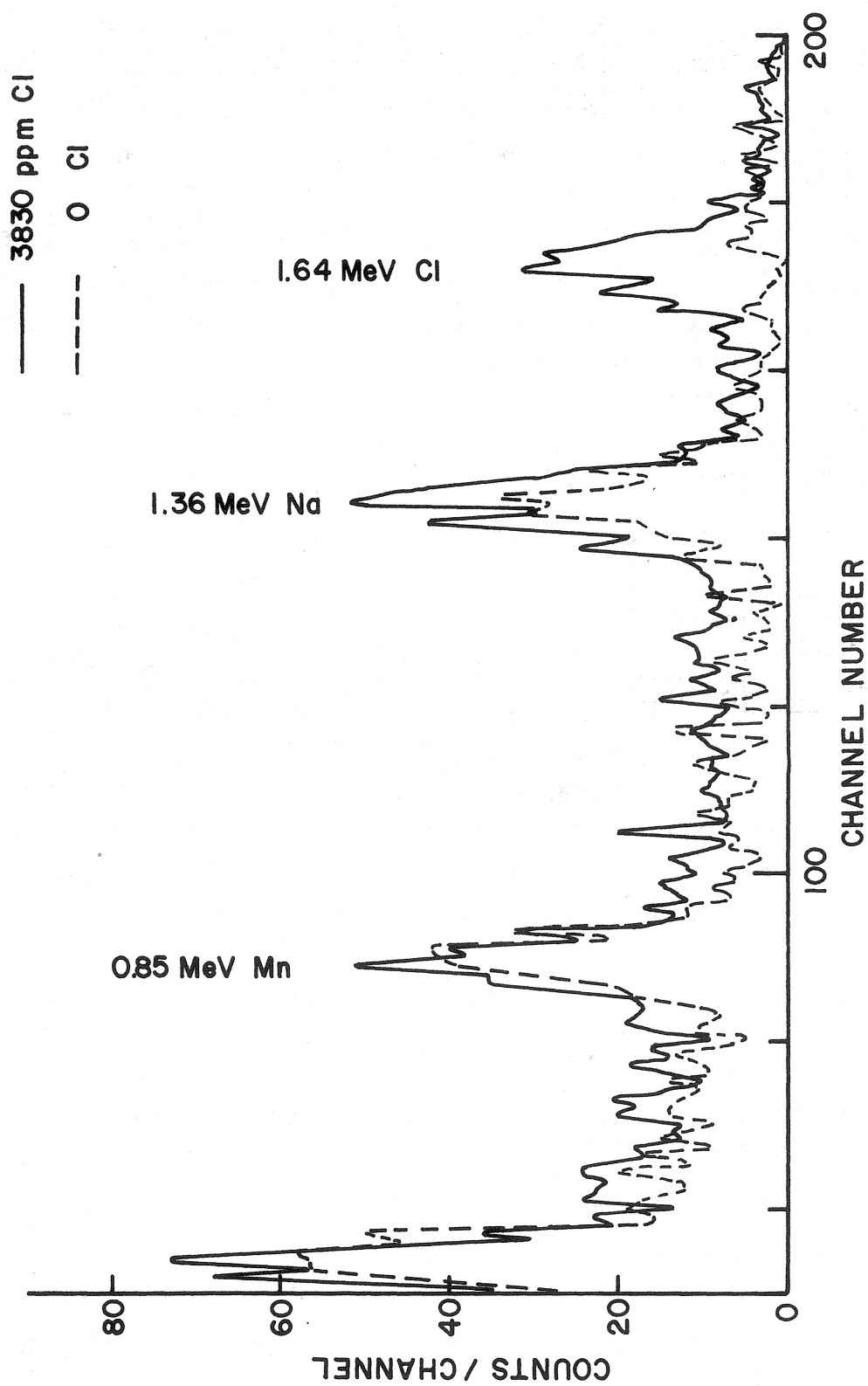


FIGURE 32. COINCIDENCE SPECTRA FROM A SINGLE PLATE, GATED ON 2.17 MeV

2.12 MeV manganese peaks are in coincidence with each other and the 2.12 MeV peak is not resolved from the 2.17 MeV chlorine peak and so is included in the coincidence gating energy window. Similarly, the 1.36 and 2.75 MeV sodium peaks are in coincidence with each other and with the 2.24 MeV first escape peak, which is not resolved from the 2.17 MeV chlorine gamma.

The total efficiency for coincidence counting is the product of the efficiencies of the two detectors. The efficiency of each detector is the product of the total absorption efficiency (the integral of the solid angle from the sample to the detector times the detector absorption efficiency) and the peak to total ratio (the fraction of the absorbed gamma energy that appears in the peak). This can be calculated from tables.⁽⁸⁵⁾ The total efficiency for each 3 in. (7.6 cm) dia. x 3 in. (7.6 cm) thick NaI(Tl) detector used and the detector-sample configuration of Figure 30 is 0.0036. The coincidence efficiency is therefore 1.3×10^{-5} .

The coincidence count of 1.64 MeV chlorine gamma rays obtained from a 2 to 3 in. (5 to 7.6 cm) depth increment using the configuration shown in Figure 30 was 37 ± 20 for a 3830 ppm specimen. The irradiation, delay and count sequence was 75, 1 and 75 mins., respectively, and the source used was the thermalized 108 μg ^{252}Cf source. In order to achieve the required sensitivity in a practical time (say 10 min. irradiate, 1 min. delay, 10 min. count) the count rate would have to be increased by a factor of 8000 which is clearly beyond the reach of any reasonable increase in source and detector sizes.

Since the overall sensitivity for the prompt-gamma method is very similar to that for the activation gamma method (see Table 4), any chance of using coincidence counting of prompt gammas is also ruled out by this result.

5.5 Chloride Gradient in a Dual Measurement

In the previous section it was shown that a single measurement will not provide the required information on chloride concentration gradient. We therefore decided to consider the chlorine signal as two variables, "surface" chloride concentration (x) and "depth" concentration (y), and to investigate the possibility of making two independent

measurements I_1 and I_2 which are each functions of the two variables, viz, $I_1 = f_1(x,y)$ and $I_2 = f_2(x,y)$.

The simplest model is to assume that the signal, I , is a linear combination of the "surface" and "depth" concentrations.

$$I_1 = C_{1x} x + C_{1y} y \quad (4)$$

$$I_2 = C_{2x} x + C_{2y} y \quad (5)$$

where the C 's are calibration constants.

Thus

$$x = \frac{I_1 C_{2y} - I_2 C_{1y}}{D} \quad (6)$$

$$\text{and } y = \frac{I_1 C_{2x} - I_2 C_{1x}}{-D} \quad (7)$$

where $D = C_{1x} C_{2y} - C_{2x} C_{1y}$.

The samples and methods used for calibration would determine the values of the calibration constants and what is meant by "surface" and "depth" concentration.

If errors in the C 's are negligible (this can be insured by proper calibration) and if I_1 and I_2 are uncorrelated (which is the case if statistical counting errors predominate, which they usually do), then the error on y is given by

$$\delta y = \left| \frac{1}{D} \right| \sqrt{\delta I_1^2 \cdot C_{2x}^2 + \delta I_2^2 \cdot C_{1x}^2} \quad (8)$$

and on x

$$\delta x = \left| \frac{1}{D} \right| \sqrt{\delta I_1^2 \cdot C_{2y}^2 + \delta I_2^2 \cdot C_{1y}^2} \quad (9)$$

where δI_1 , δI_2 are the statistical errors on I_1 and I_2 .

Note that these errors are minimized by making (D) large, which is the same as saying that the contrast in depth response to

chloride between the two measurements should be large. Ideally one measurement would be sensitive only to surface chloride, say in the first inch, while the second would be sensitive to chloride down to a depth of three inches.

5.5.1 Calculations of Depth Response

Since the mean free path of thermal neutrons in the sample is not affected by instrument design, and the mass absorption coefficient of the sample is approximately the same for all the chlorine gamma-ray energies, the only design parameters that can control the depth response are geometrical ones. Calculations of depth response as a function of source-detector separation (d) were made using the following model: point isotropic neutron source (this is a good assumption in view of the results described in Section 5.4.1); point detector; source and detector each on the surface of the sample which is a semi-infinite plane (see Figure 29).

The number of counts per second, I, is then given by

$$I = \int C(Z) \cdot I_0 \cdot \sigma \cdot \eta \cdot \frac{e^{-\mu_n \vec{r}}}{r^2} \cdot \frac{e^{-\mu_\gamma \cdot |\vec{r}_d - \vec{r}|}}{|\vec{r}_d - \vec{r}|^2} dv \quad (10)$$

where $C(Z)$ is the chloride concentration gradient [cm^{-1}]

I_0 is the source strength [n/sec]

σ is the cross section for production of chlorine gamma rays by neutrons [$\gamma \cdot \text{n}^{-1} \cdot \text{cm}^2$]

η is the detector efficiency [counts $\cdot \gamma^{-1}$]

μ_n is the effective absorption coefficient* for thermal neutrons in the sample [cm^{-1}]

μ_γ is the linear absorption coefficient for chlorine gamma rays in the sample [cm^{-1}]

\vec{r} is the source to volume element vector [cm]

$\vec{r}_d - \vec{r}$ is the detector to volume element vector [cm]

dv is the sample volume element [cm^3]

* $\frac{1}{\mu_n}$ is called the "migration length".

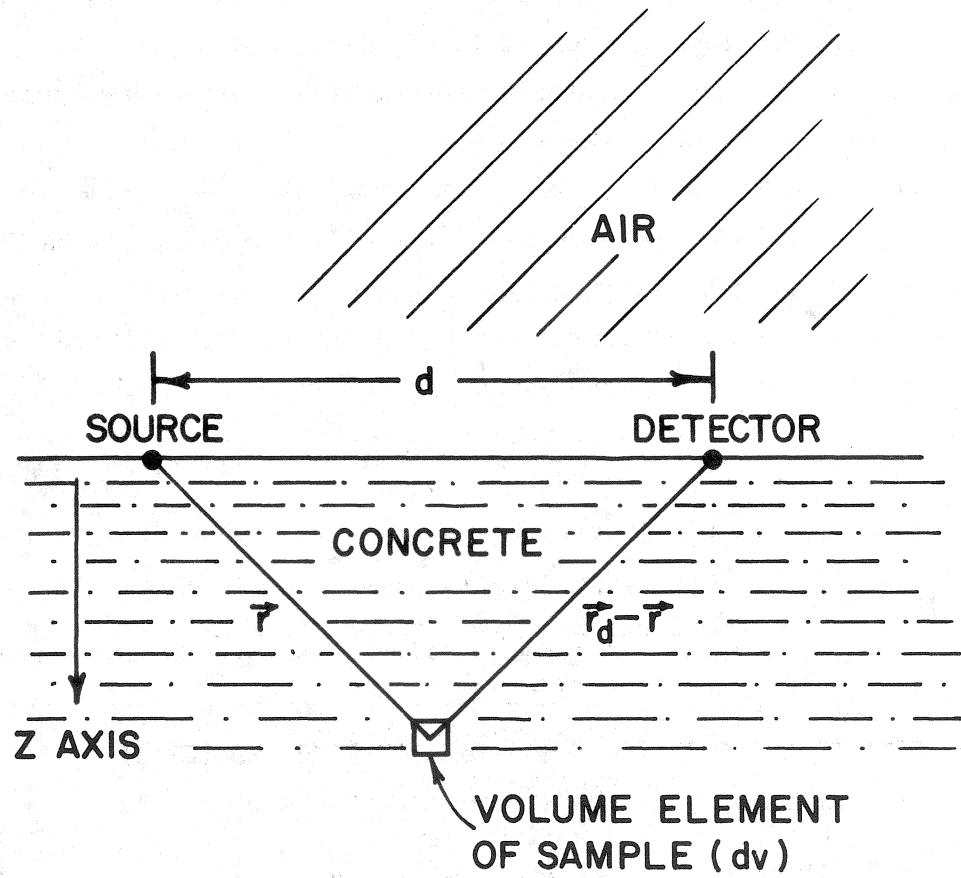


FIGURE 33. SCHEMATIC OF MODEL FOR DEPTH RESPONSE CALCULATIONS

Note that this equation does not include the time variation of induced activity (see Equation 3) and therefore is strictly true only for the prompt gamma method. Inclusion of the extra terms for activation is not necessary in the present context and would only change σ to $\sigma(t)$.

Equation 10 can be expressed as the product of the depth response function of the instrument, $R(Z)$, and the chloride concentration gradient:

$$I = \int \frac{dI}{dZ} \cdot dZ = \int R(Z) \cdot C(Z) \cdot dZ \quad (11)$$

The depth response function was calculated by numerical integration for the following cases: (1) $d = 0$; $\mu_n = 0.03 \text{ cm}^{-1*}$, $\mu_\gamma = 0.08 \text{ cm}^{-1+}$ and (2) $d = 10, 20$ and 45 cm ; $\mu_n = \mu_\gamma = 0$. The results are shown in Figure 34. It is very difficult to integrate $R(Z)$ when both d and μ are non-zero. However, the results obtained yield the required information. They show that the greatest contrast between depth responses is obtained for a small and a large value of source-detector distance. Neutron and gamma attenuation just increases the slopes of all the curves. Note that the relatively flat response for $d = 45 \text{ cm}$, compared with that for $d = 0 \text{ cm}$, is obtained at the expense of one to two orders of magnitude of signal.

Figure 35 shows curves of dI/dZ obtained by folding the depth response $R(Z)$ into Clear's chloride depth distribution, $C(Z)$ (see Figure 5). This just illustrates what a small fraction of the total signal originates from depths greater than about 2 in. (5 cm).

5.5.2 Neutron Activation Experiments

Using activation and counting arrangements similar to those shown in Figure 29, depth response curves for different source-detector distances were obtained by irradiating and counting 1/8 in. (3 mm) thick PVC tiles as in Section 5.4.2. At the same time data from pairs of source-detector distances were tested by substituting in Equations 6 to 9.

*Based on estimated migration length of thermal neutrons in concrete of about 30 cm.

+Approximate value based on average narrow beam attenuation coefficient in gamma energy range 2 to 6 MeV.

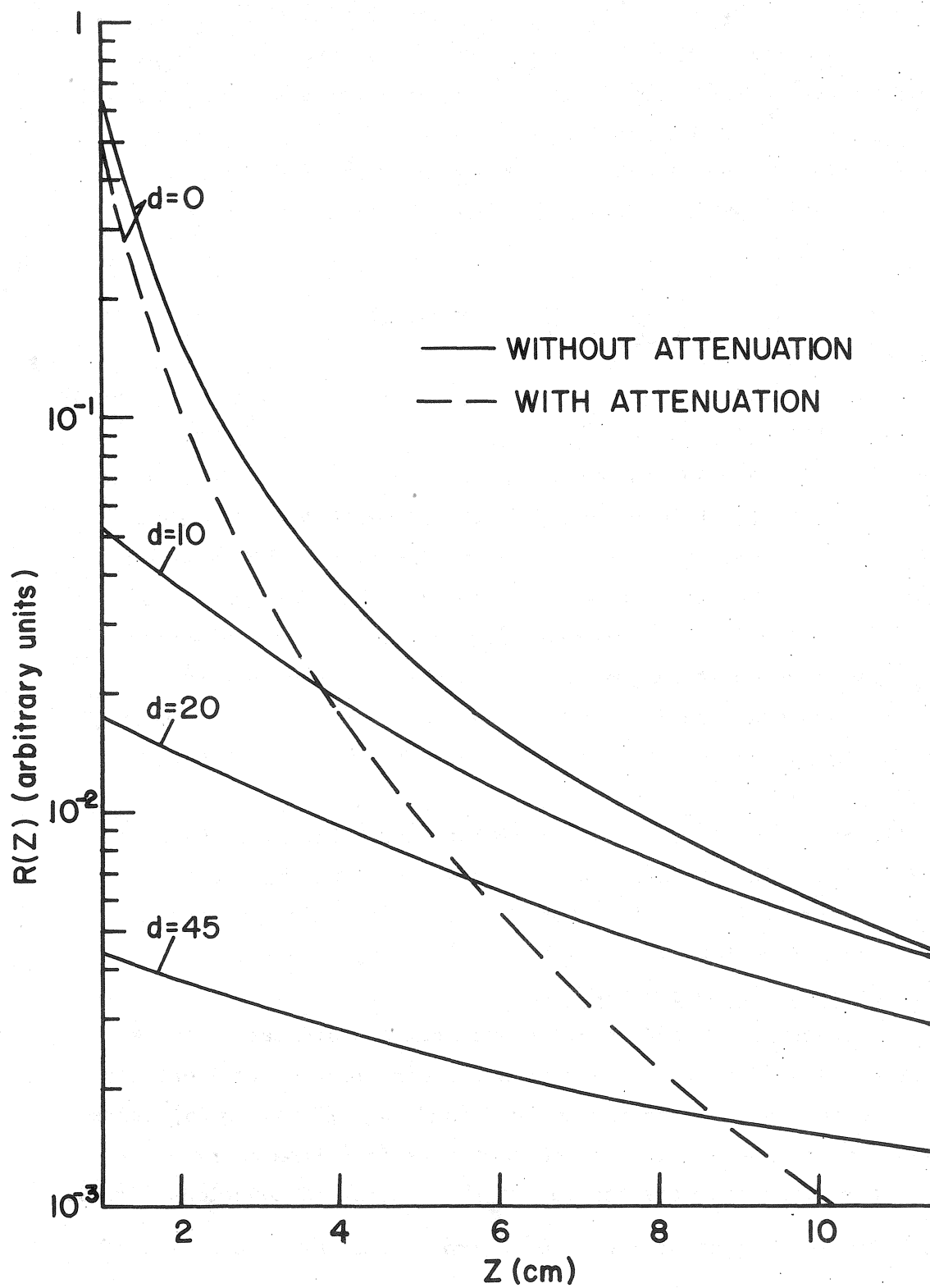


FIGURE 34. CALCULATED RESPONSE FUNCTIONS $R(Z)$

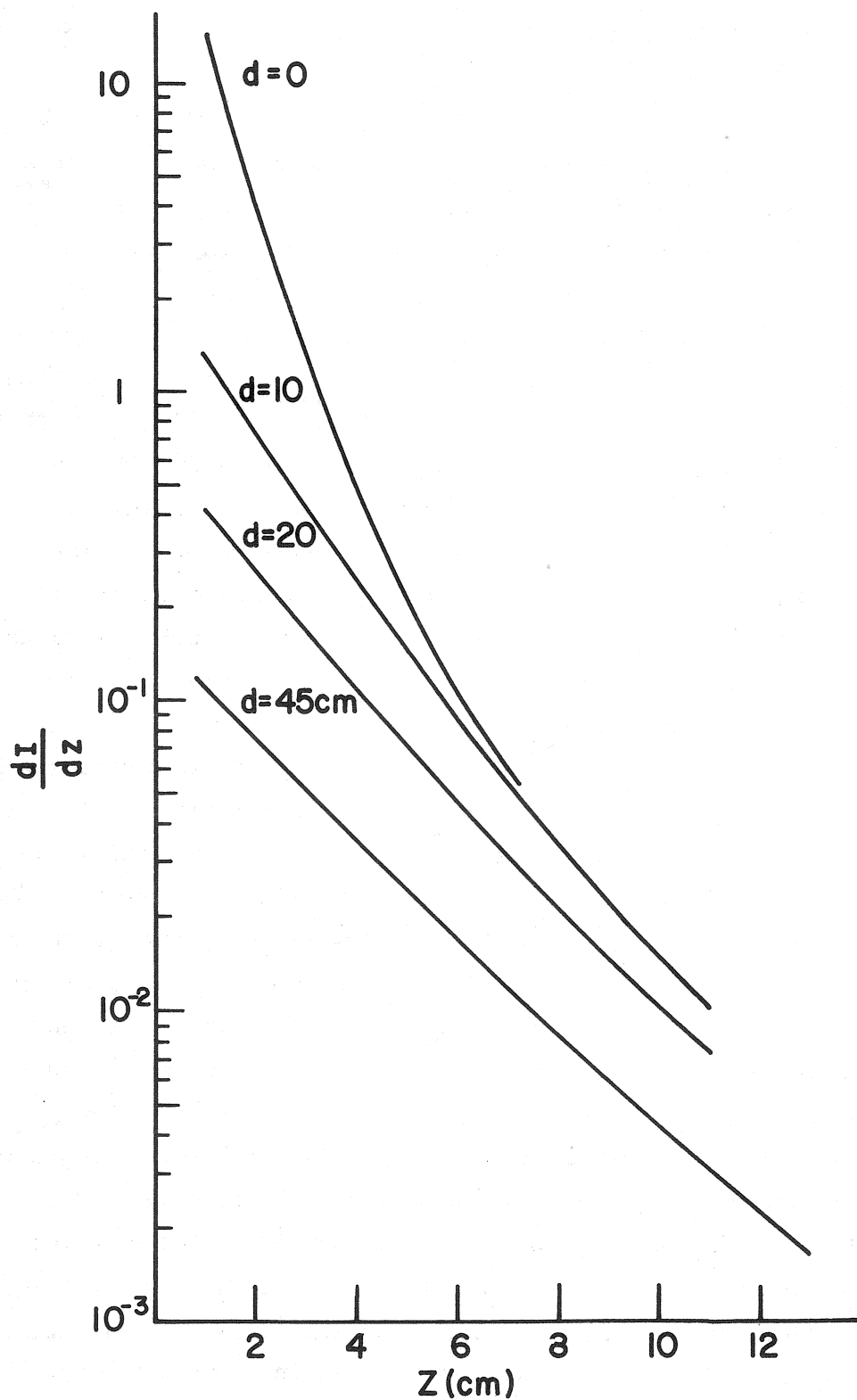


FIGURE 35. CALCULATED CURVES OF $\frac{dI}{dz}$ VS DEPTH (Z), FOR AN EXPONENTIAL CONCENTRATION GRADIENT $C(Z)$

It was found that, for "horizontal" source-detector separations (both source and detector positions close to the sample surface), sufficient contrast between a pair of configurations could not be obtained until one of the distances was so great (over 30 cm) that the statistical errors on the residual chlorine signals were unacceptably large. It was also found that the best results were obtained when one member of a pair of configurations was always $d = 0$. Further tests using "vertical" separation of irradiation and counting positions were made. The source was always close to the sample but detector distances up to 30 cm vertically away from the irradiation point were tested. Figure 36 shows the depth responses for $d = 0$ and 25 cm (vertically away). Also shown on the same scale are the calculated responses for $d = 0$, with and without attenuation, and normalized at 1 in. (2.5 cm) for the no attenuation case. The experimental data falls closer to the calculated curve without attenuation than to that with attenuation. Even though the attenuation model is crude and the coefficients very approximate, it is clear that geometry, rather than absorption, has the predominant effect on depth response.

The best compromise between signal strength and contrast was found to be for $d = 0$ and 6 in. (15 cm). Using these values, simulated concrete slabs consisting of stacks of five 1 in. (2.5 cm) thick plates were irradiated and counted using the 108 μg ^{252}Cf source and the following sequence: irradiate for 30 min., delay 10 min., count at 6 in. (15 cm) detector position for 1000 sec., count at 0 detector position for 1000 sec. The 2.17 MeV chlorine gamma peak was integrated, and spectral background and interferences from sodium and manganese subtracted, as described in Section 5.2.3.

Stacks containing the following plates were treated as calibration samples: 1) 3830* (nearest the source), 0, 128, 255, 383; 2) 0, 3830, 128, 255, 383 and 3) 0, 0, 128, 255, 383. The chlorine signals from stack 1 minus the blank (stack 3) give C_{1x} and C_{2x} . Those for stack 2 minus stack 3 give C_{1y} and C_{2y} . The "surface" chloride concentration is thus defined as that in the first inch and the "depth"

*The numbers refer to ppm Cl in the 1 in. (2.5 cm) plate, i.e., "ppm-in." of Cl.

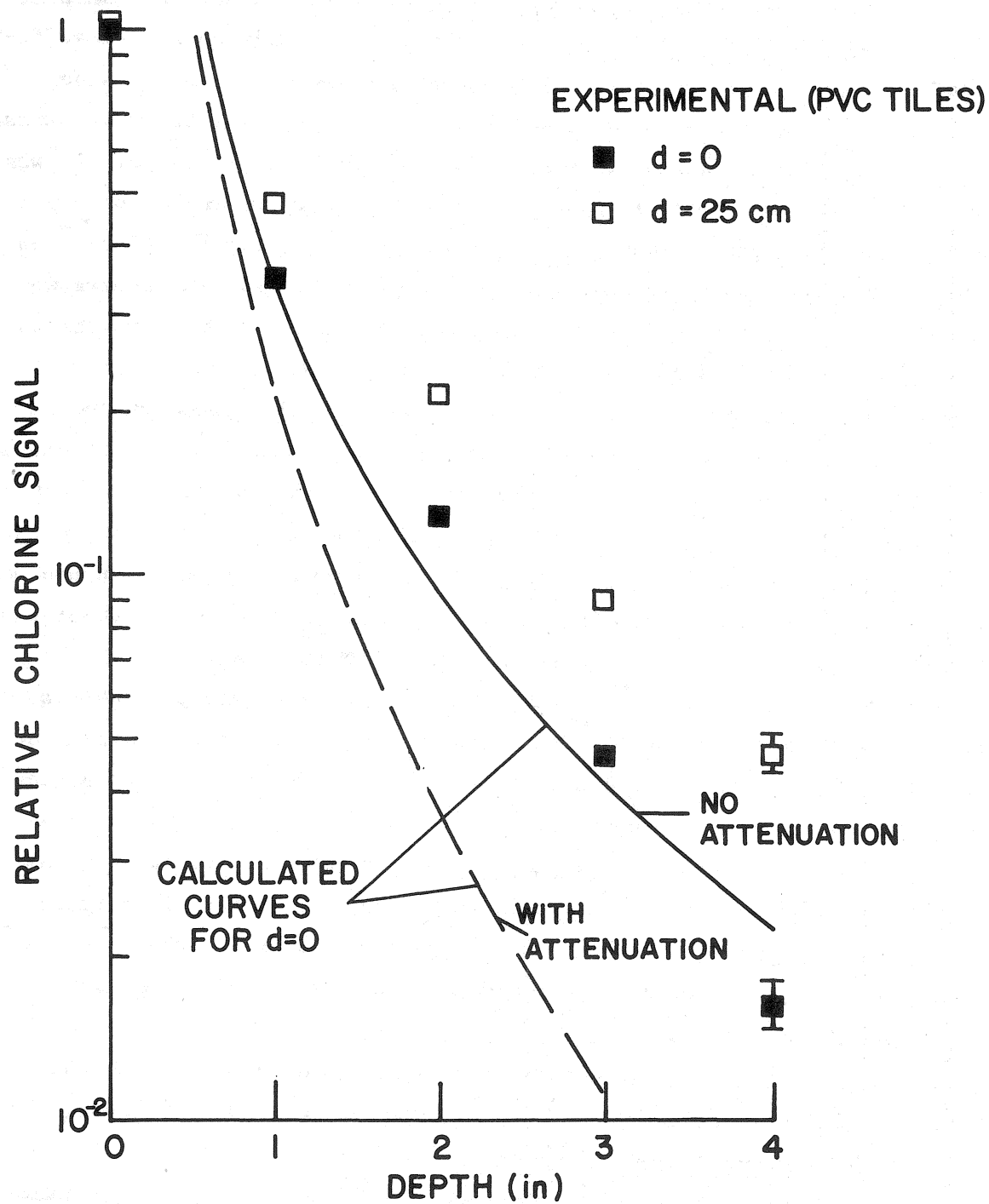


FIGURE 36. DEPTH RESPONSE CURVES, NEUTRON ACTIVATION METHOD
(1 in. = 2.54 cm)

concentration as that in the second inch. Deeper plates are assumed to contribute no signal. Table 6 gives the values obtained for the net chloride signals and for the calibration factors.

The following stacks of plates were then measured with the same irradiate-delay-count sequence and treated as unknowns: 4) 3830, 3830, 128, 255, 383; 5) 2550, 1280, 255, 383, 510; 6) 0, 2550, 255, 383, 510; 7) 1910, 893, 510, 638, 765 and 8) 2550, 1280, 510, 638, 765. The blank signals (from stack 3) were subtracted in each case and the values of x , y , δx and δy calculated using Equations 6 to 9. They are shown in Table 7.

Some of the plates in the second or third positions down had reinforcing bars. A slight increase in Mn signal was observed in these cases but since Mn is monitored anyway, this caused no problem.

It is seen that depth chloride measurements can be made using the dual measurement method; however, the statistical errors are relatively large. These errors can be reduced by increasing the signal as follows. Use of the largest practicable source (1 mg) and the largest practicable detector (an 8 in. (20 cm) dia. x 4 in. (10 cm) thick NaI(Tl) crystal) would increase the signal plus background by factors of 10 and 2.56, respectively. Measurement of the 1.64 MeV chlorine gamma peak would increase the signal by a factor of two and the background by a somewhat greater factor. The resulting statistical error would be reduced by $\sqrt{10 \times 2.5 \times 2} = 7$, at best, yielding errors of ~ 70 ppm for "surface" chloride content and ~ 200 ppm for "depth" chloride content in a total measurement time of about half an hour (note that one location can be counted while a new location is being irradiated, so saving time). Since both signals fall off so rapidly with depth very little information can be obtained from depths below 2 in. (5 cm).

5.5.3 Prompt-Gamma Experiments

The existing source-detector configuration used for the preliminary prompt-gamma ray experiments (Figure 22) was never intended for measurement of extended surfaces. Experiments were performed using various shielding materials and source-shield-detector arrangements with the objective of optimizing the signal-to-background ratio for such

TABLE 6. CALIBRATION DATA FOR DUAL NEUTRON ACTIVATION
CHLORIDE CONCENTRATION GRADIENT MEASUREMENTS

| Stack Number, ppm-in. Chloride Values | Net 2.17 MeV Chlorine Gamma Signal | |
|--|------------------------------------|--------------------------------|
| | Method 1 Zero Spacing | Method 2 6" (15 cm) Spacing |
| 1. 3830, 0, 128, 255, 383 | 20239 | 4036 |
| 2. 0, 3830, 128, 255, 383 | 8468 | 1761 |
| 3. 0, 0, 128, 255, 383 | 3503 | -517 |

Calibration Factors

$$C_{1x} = 16736$$

$$C_{2x} = 4553$$

$$C_{1y} = 4965$$

$$C_{2y} = 2278$$

TABLE 7. RESULTS OF DUAL NEUTRON ACTIVATION MEASUREMENTS
OF CHLORIDE CONCENTRATION GRADIENT

| Stack No., Actual Values for x, y | Measured Values for x, y (ppm-in. Cl) | |
|--------------------------------------|---------------------------------------|------------------|
| | $x \pm \delta x$ | $y \pm \delta y$ |
| 4. 3830, 3830 | 2470 ± 523 | 3462 ± 1457 |
| 5. 2550, 1280 | 1908 ± 496 | 978 ± 1402 |
| 6. 0, 2550 | -1187 ± 471 | 5885 ± 1340 |
| 7. 1910, 893 | 2144 ± 475 | 536 ± 1353 |
| 8. 2550, 1280 ^{a)} | 3379 ± 481 | 2049 ± 1369 |

a) Has higher chloride contents in the 3rd-5th plates than does Stack 5.

measurements. The use of active shielding (anticoincidence detectors) was carefully considered and rejected as unnecessarily complicated at this stage. Figure 37 shows a sketch of the best configuration obtained. This was used for all the prompt gamma-ray studies reported herein (except the preliminary ones described in Section 5.2.3). Further refinements of this design might yield an increase of up to a factor of two in signal-to-background ratio. This would be done at the instrument design stage.

Depth response data were obtained using this instrument configuration and integrating the two main chlorine prompt gamma peaks (5.60 and 6.11 MeV). PVC tiles were placed at increasing depths in a stack of concrete plates containing zero chloride. Response curves were obtained for different detector distances both "horizontally", away from the source and "vertically" away from the sample surface. The closest source to detector distance allowed by the shielding is 18 in. (46 cm), as shown in Figure 37. The response for this distance is shown in Figure 38, along with the corresponding calculated curve (from Figure 34) and data from concrete plates. The latter were obtained by moving a pair of 2550 ppm plates through the stack.

Note that the depth response of the prompt-gamma method is much flatter than those obtained by neutron activation (Figure 36). Also the response profiles obtained for different detector distances were very similar to each other. Both these results are expected from the geometrical calculations (Section 5.5.1).

Since two contrasting depth responses cannot be produced by the prompt gamma method, the method cannot be used alone to measure chloride concentration gradient. However, the contrast between the prompt gamma response (Figure 38) and the neutron activation response at zero distance (Figure 36) is very good and a combined activation-prompt gamma measurement is indicated.

5.5.4 Combined Neutron Activation-Prompt Gamma Measurements

A dual measurement combining prompt gamma and neutron activation can be made as follows. Irradiate at a certain location on the sample surface during which time prompt gamma data is being accumulated.

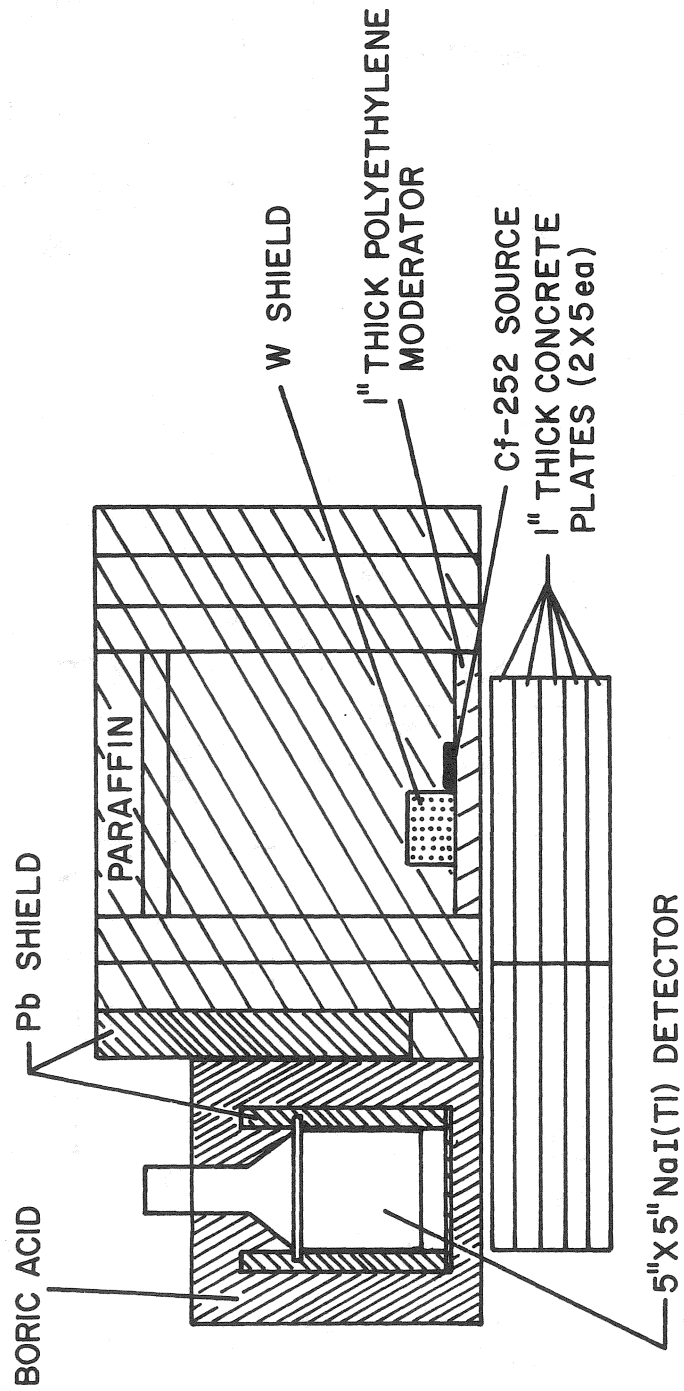


FIGURE 37. SOURCE-SHIELD-DETECTOR-SAMPLE CONFIGURATION
 USED FOR PROMPT GAMMA-RAY MEASUREMENTS
 (1" = 2.54 cm)

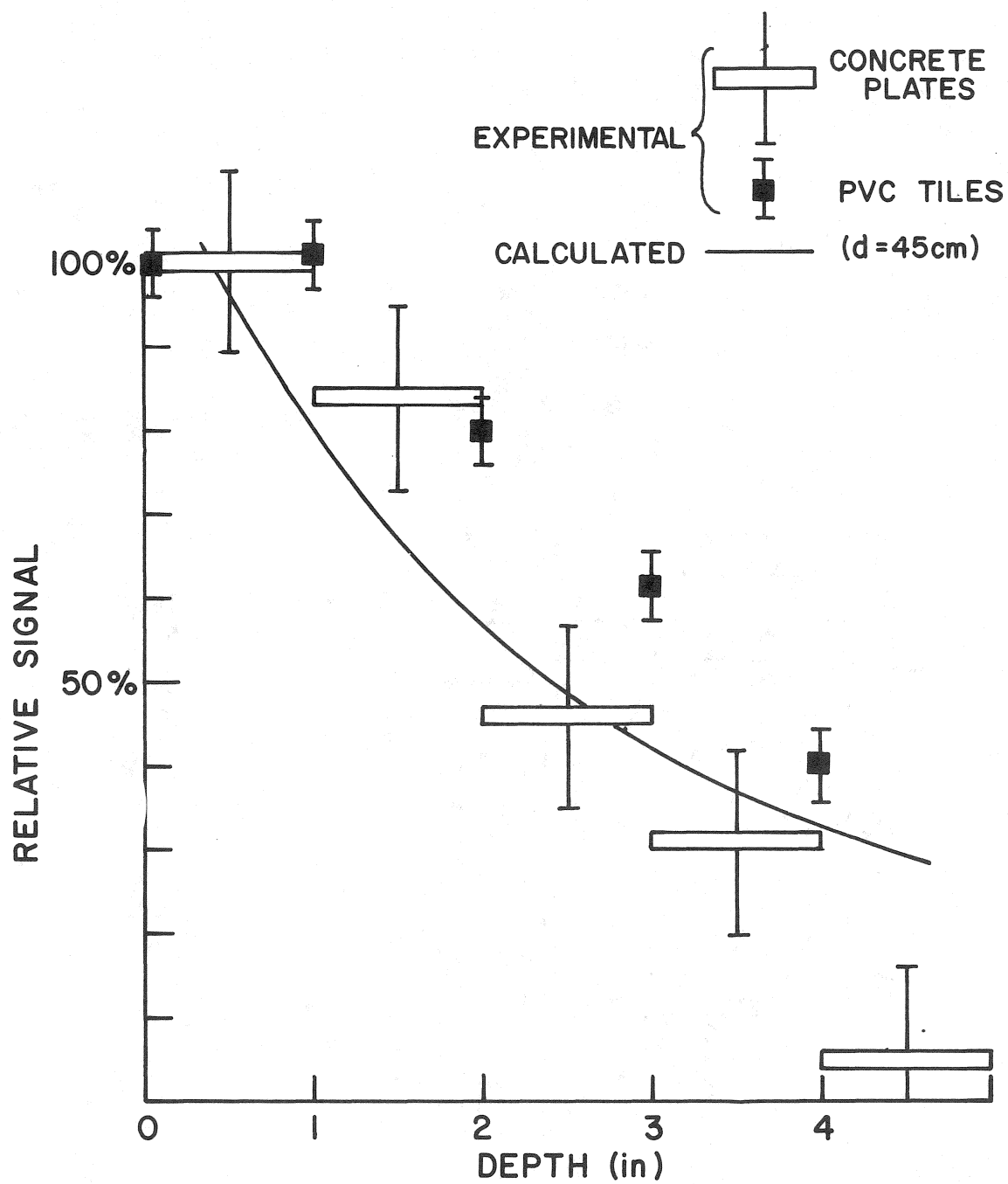


FIGURE 38. DEPTH RESPONSE CURVES, PROMPT GAMMA METHOD
(1 in. = 2.54 cm)

Move the irradiation-prompt gamma assembly away (to irradiate a new location, say) and move the activation gamma detector over the irradiated spot. After the proper delay period accumulate the activation gamma data.

In order to test this approach the concrete plate stacks previously measured by neutron activation (Section 5.5.2) were remeasured, then set up in duplicate for prompt gamma tests using the setup shown in Figure 37. Table 8 shows the calibration data obtained with the 3830 ppm plates in the 0 to 1 in. (2.5 cm) and 1 to 2 in. (2.5 to 5 cm) positions as before, to define "surface" and "depth" chloride content.

Table 9 shows the results obtained for the "unknowns", samples 4 to 8. The most important result is the reduction of statistical error compared to the dual neutron activation method. The error is reduced by a factor of three for the "depth" measurement and by a factor of two for the "surface" measurement. Secondly, the total measurement time is also reduced, since one of the measurements is now taken during the irradiation period. The effective measurement time for this data was 20 minutes, assuming that a second location is being irradiated while the activation data from the first is being accumulated. Thirdly, due to the increased depth response of the prompt gamma method, it is possible to obtain useful data down to at least 4 in. (10 cm). Fourthly, and not least, the measured values for the "surface" and "depth" chloride concentrations agree to within about one standard deviation (due to counting statistics) with the actual values. This indicates that the main errors are due to counting statistics and, at this level of accuracy, there are no significant systematic errors.

5.5.5 Discussion of Dual Measurement Technique

An analysis of errors for the dual measurement method was done. It showed the error contribution from each method to be approximately equal. Also, it was found that, although the statistical errors predominated, they can not be reduced by more than a factor of about two in the prompt gamma measurement and about 3.2 in the activation measurement before other problems such as instrumental drift and "dead" time become important. Such reductions in statistical errors can be accomplished by increasing the source size to 400 μ g and the neutron activation detector

TABLE 8. CALIBRATION DATA FOR COMBINED NEUTRON
ACTIVATION-PROMPT GAMMA MEASUREMENTS

| Sample | Neutron Activation Zero Spacing Net 2.17 MeV Signal ^{a)} | Prompt Gamma 18" (45 cm) Spacing Net 5.60 + 6.11 MeV Signals ^{a)} |
|------------------------|---|--|
| 3830, 0, 128, 255, 383 | 12262 (C_{1x}) | 21466 (C_{2x}) |
| 0, 3830, 128, 255, 383 | 4134 (C_{1y}) | 20223 (C_{2y}) |

a) Counts less blank.

TABLE 9. RESULTS OF COMBINED NEUTRON ACTIVATION-PROMPT GAMMA MEASUREMENTS OF CHLORIDE CONCENTRATION GRADIENT

| Stack No., Actual Values for x and y | Measured Values for x, y (ppm-in. Cl) | |
|--------------------------------------|---------------------------------------|------|
| | x | y |
| 4. 3830, 3830 | 4126 | 3768 |
| 5. 2550, 1280 | 2984 | 702 |
| 6. 0, 2550 | 584 | 2280 |
| 7. 1910, 893 | 1853 | 1040 |
| 8. 2550, 1280 ^{a)} | 2460 | 1880 |

Average Statistical Errors $\delta x = 240$ ppm-in. Cl

$\delta y = 490$ ppm-in. Cl

a) Higher values of Cl in 3rd-5th plates than Stack No. 5, see text.

size to 8 in. (20 cm) dia. x 4 in. (10 cm) thick. These improvements are desirable in any case, to increase the sensitivity of the drill hole sample and total chloride analysis methods (Section 5.3). The effect of these improvements on the precision of the dual measurement method would be to decrease the errors, δx and δy , to 64 ppm-in. Cl and 135 ppm-in. Cl respectively, for the same measurement time. Further improvements in sensitivity, or reductions in measurement time, must come from increases in signal/background (S/N) ratio. We have already stated that the prompt gamma S/N ratio can possibly be improved by up to a factor of 10 by using spectrum fitting techniques. Also we expect an improvement of up to a factor of two from better shielding design of the irradiation-counting geometry. Spectrum fitting techniques would also improve the neutron activation method by allowing the use of the 1.64 MeV Cl gamma ray, thus doubling the signal. An increase of a factor of 10 in prompt gamma S/N ratio and a factor of two in neutron activation S/N ratio could decrease the errors in "depth" chloride measurement to below 100 ppm-in. Cl and decrease the measurement time to less than 10 minutes. This would require a 400 μg ^{252}Cf source, an 8 in. (20 cm) dia. x 4 in. (10 cm) thick NaI(Tl) crystal for the neutron activation measurement, and a 5 in. (13 cm) dia. x 4 in. (10 cm) thick NaI(Tl) crystal for the prompt gamma measurement.

Preliminary theoretical studies of an exponential concentration gradient model were also undertaken to find out if this model could facilitate calibration and improve the accuracy of "depth" chloride measurements. They showed that, in principle, a simple field calibration procedure is possible involving measurements on the bridge deck with and without a sheet containing a known concentration of chlorine. They also showed that it is possible, in principle, to measure either the total chloride below a certain depth or the chloride content in a given depth increment.

6. RECOMMENDATIONS

6.1 Recommendations

1. The instrument configuration recommended for development and field testing in Phase II of this project is the Combination Neutron Activation-Prompt Gamma Instrument. We have shown that this combination can yield nondestructive chloride depth measurements down to 3 or 4 in. (7 to 10 cm), independent of the chloride content in the surface layers. It has the potential of performing several measurements per hour with a sensitivity of better than 100 ppm-in. Cl for nondestructive depth measurements. Figure 39 shows a schematic of the proposed prototype instrumentation. The ^{252}Cf source could be made available on loan. The instrument would be field portable but heavy, its transportation shielding weighing at least 1000 Kg. The measuring heads of the prototype would weigh several 100 Kg and could directly monitor the road surface but not, at first, pilings or the undersides of decks. The latter measurements are not ruled out, however, since it is possible to conceive of a suitable mechanism for hoisting and positioning the instrumentation in accessible places.

The same instrument operated in the prompt gamma or activation mode can yield nondestructive, rapid total chloride data with adequate sensitivity, assuming the chloride concentration gradient to be constant, known or not important. Finally, the same instrument operated in the activation mode can perform in situ analysis of drill hole samples in those cases (asphalt overlay, pilings, etc.) where access to the surface to be monitored is not possible.

2. A low cost, portable X-ray fluorescence analyzer, using an ^{55}Fe radioisotope source, X-ray filters and a proportional counter, is feasible for in situ analysis of pulverized, briquetted drill hole samples. The development effort required to perfect this instrument would be greater than that required for recommendation No. 1. Furthermore, a

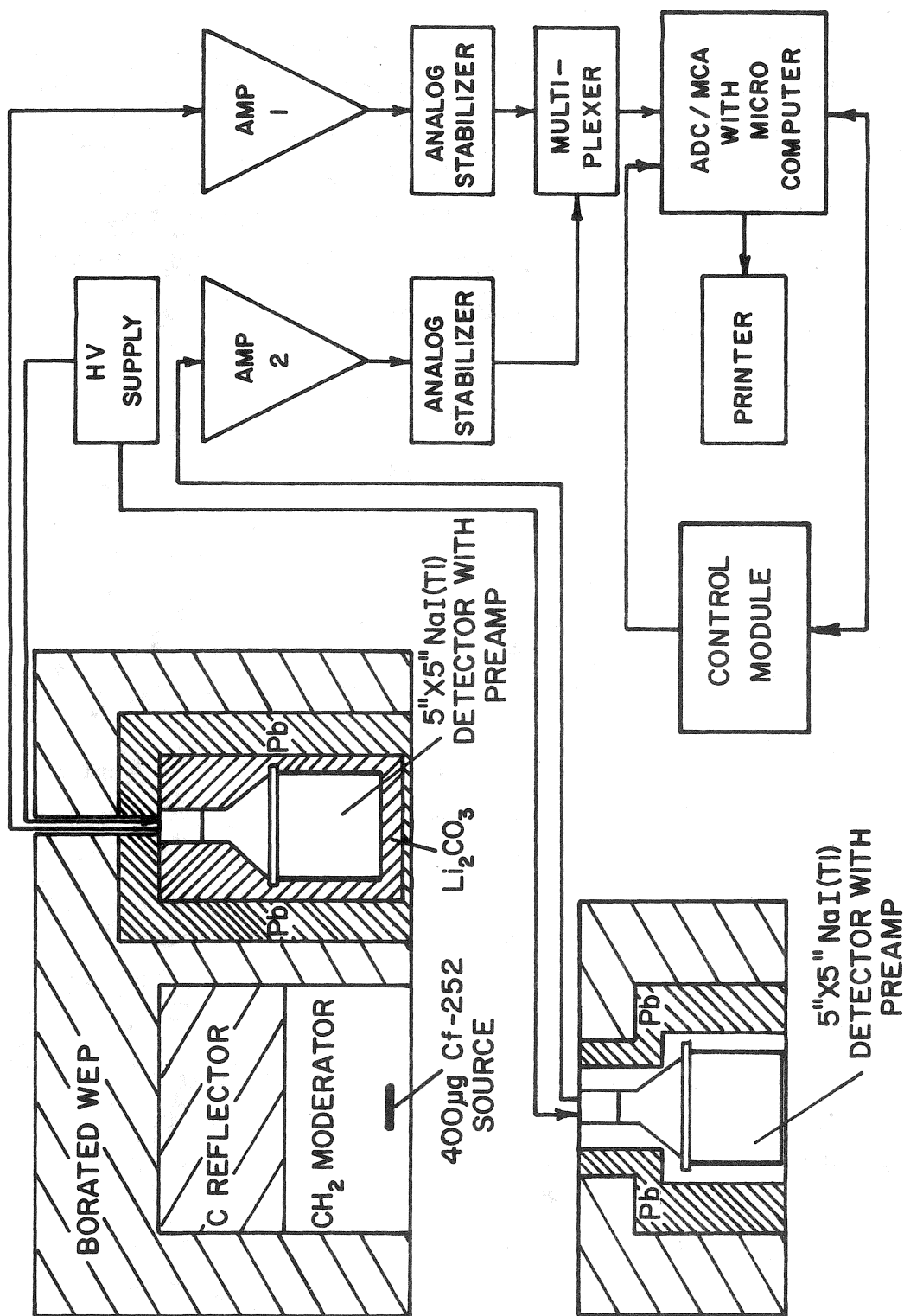


FIGURE 39. SCHEMATIC OF COMBINATION NEUTRON
ACTIVATION-PROMPT GAMMA CHLORIDE ANALYZER
(1" = 2.54 cm)

precision better than ± 200 ppm Cl cannot at this point be guaranteed because of heterogeneity and reproducibility errors.

3. Energy dispersive X-ray fluorescence, using a Si(Li) spectrometer and an ^{55}Fe source together with an automatic sample changer, is a satisfactory method for rapid analysis of pulverized, briquetted drill hole samples. The method and instrumentation are already developed and have been used routinely in this project. The instrumentation can be used in the laboratory or mounted in a truck. It is, however, more expensive than both previously-mentioned instruments. No further development work is required on this.

7. BIBLIOGRAPHY

1. Clear, K. C., "Evaluation of Portland Cement Concrete for Permanent Bridge Deck Repair", FHWA-RD-74-5, 1974, 49 p.
2. Berman, Horace A., "Determination of Chloride in Hardened Portland Cement Paste, Mortar, and Concrete", FHWA-RD-72-12, 1972, 24 p.; J. Mater. 7, 1972, p. 330-5; and J. Test. Eval. 3, 1975, p. 208-10.
3. Morrison, Garrett L. et al., "Rapid In-Situ Determination of Chloride Ion in Portland Cement Concrete Bridge Decks", F.C.P. Review, Penn State University, September 1976 (to be published).
4. Mozer, J. D. Bianchini, A. C. and Kesler, C. E., "Corrosion of Reinforcing Bars in Concrete", J. Am. Concrete Inst., Proceedings 62, August 1965, p. 909.
5. Stratfull, R. F., "How Chlorides Affect Concrete Used with Reinforcing Steel", Mater. Protection 7, 1968, pp. 29-34.
6. Szilard, R., "Corrosion and Corrosion Protection of Tendons in Prestressed Concrete Bridges", ACI Journal 66, 42, January 1969.
7. Clear, K. C., "Time to Corrosion of Reinforcing Steel in Concrete Slabs - Volume 3: Performance after 830 Daily Salt Applications", Interim Report, FHWA-RD-76-70, Federal Highway Administration, April 1976.
8. Clear, K. C. and Hay, R. E., "Time to Corrosion of Reinforcing Steel in Concrete Slabs - Volume I: Effect of Mix Design and Construction Parameters", Interim Report FHWA-RD-73-32, April 1973.
9. Smoak, W. Glenn, "Surface Impregnation of New Concrete Bridge Decks", Public Roads Magazine, Vol. 40, No. 1, June 1976, pp. 1-5.
10. Clear, K. C. and Ormsby, W. C., "Concept of Internally Sealed Concrete", Federal Highway Administration, Report FHWA-RD-72-21, January 1975.

11. Jenkins, J. C., Beecroft, G. W., and Quinn, W. J., "Polymer Concrete Overlay Test Program", Oregon State Highway Division for the Federal Highway Administration, Interim Report FHWA-RD-75-501, November 1974.
12. Morrison, Garrett L. and others, "Chloride Removal and Monomer Impregnation of Bridge Deck Concrete by Electro-Osmosis", Kansas Department of Transportation, Report No. FHWA-Ks-RD-74-1, April 1976.
13. Li, Shu-t'ien, Ramakrishnan, Y., Russell, J. E., "Advances in Non-destructive Testing of Concrete", Highway Research Record 378, 1972, pp. 1-11.
14. Maerker, R. E., Muckenthaler, F. J., "Gamma-Ray Spectra Arising from Thermal-Neutron Capture in Elements Found in Soils, Concretes, and Structural Materials", ORNL-4382, 1969, 267 p.
15. Parry, William T., Chachas, Catherine, Sorbe, Victor K., "Utilization of the Electron Probe Microanalyzer in Highway Materials Analysis -- Feasibility Study", UTAH-RR-500, 922, 1973, 30 p.
16. Spellman, D. L., Stratfull, R. F., "Chlorides and Bridge Deck Deterioration", Highway Research Record 328, 1970, pp. 38-39.
17. Browne, F. P., Bolling, N. B., "New Technique for Analysis of Chlorides in Mortar", J. Mater. 6, 1971, pp. 524-31.
18. Stratfull, R. P., Jurkovich, W. J., Spellman, D. L., "Corrosion Testing of Bridge Decks", Transp. Res. Rec. 539, 1975, pp. 50-59.
19. Wolhufer, C. W., Turkstra, J., Morris, R. M., "Application of Quantitative Neutron Activation Analysis to the Study of the Cement-Chloride Reaction", Mater. Constr., Mater. Struct. 7, 1974, pp. 201-206.
20. Figg, J. W., Lees, T. P., "Field Testing the Chloride Content of Sea Dredged Aggregates", Concrete (Land) 9, 1975, pp. 38-40 (wet chemistry methods).
21. Ost, B., Monfore, G. E., "Penetration of Chlorides into Concrete", Mater. Performance 13, 1974 pp. 21-24.
22. Colleparki, M., Marcialis, A., Turriziani, R., "Penetration of Chloride Ions into Cement Pastes and Concretes", J. Amer. Ceramic Soc. 55, 1972, pp. 534-5 (chemical analysis).

23. Krastavcevic', M., Ducic', V., "Allowable Chloride Contents in Cement from the Standpoint of their Effect on Reinforcements in Concrete", *Cement (Zagreb)* 16, 1972, pp. 78-80.
24. Gould, R. W., Healey, J. T., "X-Ray Spectrometric Analysis of Chlorine in Concrete by Borate Fusion", *X-Ray Spectrometry* 3, 1974, pp. 170-171.
25. Hausmann, D. A., "Criteria for Cathodic Protection of Steel in Concrete Structures", *Mater. Protection* 8, 1969, pp. 23-25.
26. Atimtay, E., Ferguson, P. M., "Early Chloride Corrosion of Reinforced Concrete", *J. Am. Concrete Inst.* 70, 1973, pp. 606-611.
27. Berman, H. A., Chaiken, B., "Techniques for Retarding the Penetration of Deicers into Cement", *Public Roads* 38, No. 1, June 1974, pp. 9-18.
28. Ramachandran, V. S., "Calcium Chloride in Concrete", *Precast. Concr.* 6, No. 3, March 1975, pp. 149-151.
29. Clifton, J. R., Beeghly, H. F., Mathley, R. G., "Nonmetallic Coatings for Concrete Reinforcing Bars", *Nat. Bur. Stand. Build. Sci. Ser. No. 65*, August 1975, 34 p.
30. Chan, F. L., Jones, W. B., "Quantitative Determination of Sulfur, Chlorine, Potassium, Calcium, Scandium and Titanium in Aqueous Solutions by Radioisotopic Excited Fluorescent Spectrometer and by Conventional X-Ray Spectrometer", *Advances in X-Ray Analysis* 14, 1971, pp. 102-126.
31. Rhodes, J. R., Furuta, T., Berry, P. F., "Radioisotope X-Ray Fluorescence Drill Hole Probe", *Nuclear Techniques and Mineral Resources*, IAEA, 1970, pp. 353-363.
32. Fabbi, B. P., Espos, L. F., "X-Ray Fluorescence Determination of Chlorine in Standard Silicate Rocks", *Applied Spectroscopy* 26, 1972, pp. 293-295.
33. Wickert, H., "Contribution to the Analysis of Raw Meal and of Clays, Marls and Similar Cement Raw Materials", *Cement Technology* 5, 1974, pp. 465-468.
34. Tanemura, T., Suita, H., "Radioisotope X-Ray Fluorescence Analyzer for On-Line Process Control", *Appl. Low Energy X- and Gamma Rays*, 1971, pp. 69-80.

35. Rio, A., Saini, A., "X-Ray Fluorescence Spectrometry of Cement Materials", *Cemento* 69, 1972, p. 31-42.
36. Anderson, C. H., Mander, J. E., Lietner, J. W., "X-Ray Fluorescence Analysis of Portland Cement Through the Use of Experimentally Determined Correction Factors", *Advances in X-Ray Analysis* 17, 1974, pp. 214-224.
37. Rhodes, J. R., "Design and Application of X-Ray Emission Analyzers Using X-Ray and Gamma-Ray Sources", *ASTM Special Technical Publication* 485, 1971, pp. 243-285.
38. Rhodes, J. R., Taylor, M. C., "Rapid Major Element Mine Dust Analyzer", Final Report, U. S. Bureau of Mines Contract H0110985, 1972.
39. Araki, S., "Gas Chromatography of Reactive Inorganic Gases", *Bunseki Kagaku* 12, 1963, pp. 450-457.
40. Paciorek, K. L. et al., "Coal Mine Combustion Products: Identification and Analysis", Annual Report, U. S. Bureau of Mines Contract H0133004, 1973.
41. Taylor, M. C., "A New Method for Field Analysis of Plastic Concrete-Feasibility Study", *CERL-TR-M-64*, 1973, 58 p.
42. McGee, T. D., "Properties of Ceramic Materials", *ARL-TR-75-0003*, 1975, 17 p.
43. Howdysshell, P. A., "Rapid Testing of Fresh Concrete", *CERL-CP-M-128*, 1975, 153 p.
44. Lutz, G. J., "14 MeV Neutron Generators in Activation Analysis: A Bibliography", *NBS-TN-533*, 1970, 94 p.
45. Maerker, R. E., Muckenthaler, F. J., "Gamma-Ray Spectra Arising from Fast-Neutron Interactions in Elements Found in Soils, Concretes and Structural Materials", *ORNL-4475*, 1970, 238 p.; *Nucl. Sci. Eng.* 42, 1970, pp. 335-351.
46. Iddings, F. A., et al., "Determination of Cement in Concrete by Activation Analysis with Cf-252", *Trans. Res. Rec.* 538, 1975, pp. 20-26.
47. Tajima, E. Akaiwa, H., "Simultaneous Determination of Chlorine, Bromine and Iodine in Sedimentary Rocks by Neutron Activation", *Radioisotopes* 20, 1971, pp. 165-170.

48. Ishaq., A. F. M., Kenneth, T. J., "Thermal Neutron Capture in Chlorine", Can. J. Phys. 50, 1972, pp. 3090-3099.
49. Tyalor, M. C., Rhodes, J. R., "Analyzing Process Streams by Neutron Activation. A Dual Source Technique", Instrum. Technol. 21, 1974, pp. 32-35.
50. Barrett, M. J., Waldman, J., "Experimental Gamma-Ray Backscattering by Various Materials", TO-B-64-68, 1964, 38 p.
51. Mitchell, T. M., "A Radioisotope Backscatter Gauge for Measuring the Cement Content of Plastic Concrete", FHWA-RD-73-78, 1973, 55 p.
52. El-Kady, A. A., Hamoceda, I., "Evaluation of Thermal Neutron Gamma-Ray Techniques for Nondestructive Analysis of Geological Samples. I", Atomic Energy Establishment of Egypt Report No. AREAEE-187, 1973, 26 p.
53. Berry, P. F., Radioisotope X- and Gamma-Ray Methods for Field Analysis of Wet Concrete Quality. Phase II. Instrument Design and Operation", ORO-3842-2, 1970, 98 p.
54. Fubini, A., et al., "Method for Analysis of Neutron Capture Gamma-Ray Spectra", Com. Naz. Energ. Nucl. (Italy), Report RT/FI 47, 1970, 25 p.
55. Duffey, D. et al., "Concrete Analysis by Neutron-Capture Gamma-Ray Using Cf-252", Highway Research Record 412, 1972, pp. 13-24.
56. Duffey, D., El-Kady, A., Senftle, F. E., "Analytical Sensitivities of Thermal-Neutron-Capture Gamma-Rays", Nucl. Inst. and Meth. 80, 1970, p. 149.
57. Bickle, L. W., Smiel, A. J., "Applicability of Acoustic-Emission Techniques to Civil Engineering Research", AFWL-TR-74-299, 1974, 102 p.
58. DiCocco, J. B., Nuzzo, W. W., "Sonic and Conventional Measurement of Rigid Pavement Thicknesses", New York Dept. of Trans. Dept. RR-69-12, 1970, 22 p.
59. Furr, H. L. et al., "Bridge Deck Deterioration, A Summary of Reports", Texas Trans. Inst., Report No. TTI-2-18-68-130-11F, 1972, 106 p.

60. Swift, G., Moore, W. M., "Investigation of Applicability of Acoustic Pulse Velocity Measurements to Evaluation of Quality of Concrete in Bridge Decks", Highway Research Record 378, 1972, pp. 29-39.
61. Instrumental Analysis of Chemical Pollutants Training Manual, Environmental Protection Agency, Washington, D. C., 1971, 294 p.
62. Sheets, T. J., Jackson, M. D., Phelps, L. D., "A Water Monitoring System for Pesticides in North Carolina", N. C. Water Resources Research Inst. Report No. 19, 1970, 109 p.
63. Lyons, E. T., Salman, H. A., "Development of Analytical Procedures for Determining Chlorinated Hydrocarbon Residues in Waters and Sediments from Storage Reservoirs", Colorado Bureau of Reclamation Report, REC-ERC-72-15, 1972, 13 p.
64. Salmon, L., "Instrumental Neutron Activation Analysis in Environmental Studies of Trace Elements", UKAEA Report. AERF-R-7859, 1975, 31 p.
65. Henkelmann, R., Born, H. J., "Analytical Use of Neutron Capture Gamma-Rays", AEC CONF - 721010-23, 1972, 10 p.
66. Hayes, D. W., Peterson, S. F., "Multi-Element Neutron Activation Analysis of Sediment Using a Cf-252 Source", Topical Meeting on the Applications of Cf-252, CONF - 720902-4, 1972, 5 p.
67. Berry, P. F., "Analyzing Cement Raw Mix via New Radioisotope Instruments", Rock Prod. 73, 1970, pp. 66-73.
68. Bhargava, J., "Application of Some Nuclear and Radiographic Methods on Concrete", Mater. Constr., Mater. Struct. 4, 1971, pp. 231-240.
69. Gluskoter, H. G., Ruch, R. R., "Chlorine and Sodium in Illinois Coals as Determined by Neutron Activation Analyses", Fuel 50, No. 1, 1971, pp. 65-76.
70. Tertian, R., "New Approach to the Study and Control of Interelement Effects in the X-Ray Fluorescence Analysis of Metal Alloys and Other Multicomponent Systems", X-Ray Spectrom. 2, 1973, pp. 95-109.
71. Cram, S. P. and Juvet, R. S., "Gas Chromatography", Analytical Chemistry 44, 213R (1972).

72. Burlingame et al., "Mass Spectrometry", Analytical Chemistry 44, 337R, 1972.
73. Wolf, C. J. et al., "Pyrolysis Gas Chromatography", Industrial Research 13, 49, January 1971.
74. Ost, B. and Monfore, G. E., "Penetration of Chloride into Concrete", Journal of the PCA Research and Development Laboratories 8, 1, January 1966, pp. 46-52.
75. Kukacka, L. E. et al., "Introduction to Concrete Polymer Materials", FHWA-RD-75-507, April 1975.
76. Rhodes, J. R., "Energy Dispersive X-Ray Spectrometry", American Laboratory 5, 7, July 1973, p. 57.
77. Stratton, F. W. and McCollum, B. F., "Repair of Hollow or Softened Areas in Bridge Decks by Rebonding with Injected Epoxy Resin or Other Polymers", Report No. K-F-72-5, State Highway Commission of Kansas, Topika, Kansas, July 1974.
78. Pradzynski, A. H. and Rhodes, J. R., "Development of Synthetic Standard Samples for Trace Analysis of Air Particulates" in ASTM Special Technical Publication 598, American Society for Testing Materials, 1976, pp. 320-336.
79. Rhodes, J. R. and Furuta, T., in Advances in X-Ray Analysis 11, 1968, pp. 249-274.
80. Stehn, J. R. et al., "Neutron Cross Sections", BNL 325, Second Edition, Supplement No. 2, Vols. I, IIA, IIB, IIC and III, Brookhaven National Laboratory, 1964-1965.
81. Lederer, C. M. et al., "Table of Isotopes", Sixth Edition, John Wiley & Sons Ltd., 1967.
82. Giarratano, J. C., "Prompt Gamma-Ray Analysis of Bone Using Californium-252", Ph.D. Dissertation, University of Texas, 1974.
83. "Californium-252", Proc. Symp. Sponsored by the American Nuclear Society, New York City, 1968, CONF-681032, 1969.
84. "Californium-252 Progress", a Quarterly Journal Published by USERDA, P. O. Box A, Aiken, S. C. 29801.
85. Marion, J. B., Nuclear Data Tables, Part 3, 1960, p. 59.

